



1977

The Autonomic Control of the Canine Left Ventricle

David B. Lippincott
Loyola University Chicago

Recommended Citation

Lippincott, David B., "The Autonomic Control of the Canine Left Ventricle" (1977). *Dissertations*. Paper 1601.
http://ecommons.luc.edu/luc_diss/1601

This Dissertation is brought to you for free and open access by the Theses and Dissertations at Loyola eCommons. It has been accepted for inclusion in Dissertations by an authorized administrator of Loyola eCommons. For more information, please contact ecommons@luc.edu.



This work is licensed under a [Creative Commons Attribution-Noncommercial-No Derivative Works 3.0 License](https://creativecommons.org/licenses/by-nc-nd/3.0/).
Copyright © 1977 David B. Lippincott

THE AUTONOMIC CONTROL OF THE
CANINE LEFT VENTRICLE

by

David B. Lippincott

A Dissertation Submitted to the Faculty of the Graduate
School of Loyola University in Partial Fulfillment
of the Requirements for the Degree of
Doctor of Philosophy

July

1976

ACKNOWLEDGEMENTS

I would like to express my thanks and appreciation to my advisor, Dr. Walter C. Randall, whose help, guidance and encouragement helped me over the difficult times and made the less difficult times a true experience.

Gratitude also goes to the members of the Department of Physiology, both students and faculty, for their help and encouragement throughout my stay there. Special thanks is extended to Jeanne Norris for her invaluable help and assistance with the statistics.

Finally, I have a deep-felt thank you and a great debt for my family who had faith in my ability to finish this undertaking even when I lost that faith.

BIOGRAPHY

David Bruce Lippincott was born May 16, 1947 in Philadelphia, Pa. He attended New Trier Township High School, Winnetka, Illinois and received a B.S. in chemistry from St. Lawrence University, Canton, New York in 1969. In September 1969 he enrolled in the Physiology Department of Loyola University. While there he worked under the direction of Dr. Walter C. Randall. In October 1973 he taught physiology part-time at Northern Illinois University. Beginning September 1974 until present he has been Assistant Professor of Biology at California State University, Long Beach.

TABLE OF CONTENTS

	Page
ACKNOWLEDGEMENTS	ii
BIOGRAPHY	iii
LIST OF TABLES	vi
LIST OF FIGURES	vii
CONTENTS OF APPENDIX	x
 Chapter	
I. INTRODUCTION	1
II. LITERATURE REVIEW	4
A. Anatomy of the Cervical Cardiac Autonomic Nerves	4
B. Functional Anatomy of the Cervical Cardiac Autonomic Nerves	6
C. Ventricular Activation	18
D. Sequence of Muscle Segment Contraction	29
III. METHODS	38
A. Surgical Procedure	38
B. Walton-Brodie Strain Gauge Arch	42
C. Analysis of the Data	
1. Analysis of Force Changes	47
2. Analysis of Time Intervals	
a. R-wave Reference	49
b. Left Ventricular Anterior Electrogram Reference	50
IV. RESULTS	55
A. Control Time Intervals	55
B. Heart Rate and Force Changes During Autonomic Stimulation	65
C. Time Interval Changes	95

1.	R-wave Reference--Autonomic Nerve Stimulation	95
2.	Electromechanical Coupling Interval-Calcium, Norepinephrine and Atrial Pace	109
3..	Electromechanical Coupling Interval-Autonomic Nerve Stimulation	123
V.	DISCUSSION	136
A.	Control Time Intervals	136
B.	Chronotropic and Inotropic Changes during Autonomic Cardiac Nerve Stimulation	143
C.	Time Interval Changes with Small Nerve Stimulation	166
D.	Cardiac Neuromuscular Junctions	177
E.	Synchrony Changes: Cellular Level	181
VI.	SUMMARY	191
A.	Control Time Intervals	191
B.	Force Alterations during Autonomic Nerve Stimulation	192
C.	Time Interval Changes	192
D.	Hypothesis	194
	BIBLIOGRAPHY	195
	APPENDIX	205

LIST OF TABLES

Table	Page
I. R-WAVE TO MECHANICAL TIME INTERVALS	57
II. ELECTRICAL-ELECTRICAL COUPLING INTERVALS	61
III. ELECTROMECHANICAL COUPLING INTERVALS	64
IV. CONTRACTILE FORCE CHANGES	75
V. CONTRACTILE FORCE CHANGES--AFTER ATROPINE	87
VI. STATISTICAL ANALYSIS OF THE ELECTROMECHANICAL COUPLING INTERVAL CHANGES CAUSED BY STELLATE STIMULATION, NOREPINEPHRINE, CALCIUM AND ATRIAL PACING	120

LIST OF FIGURES

Figure	Page
1. DRAWING OF THE LEFT VENTRICULAR ENDOCARDIUM	41
2. DRAWING OF THE THORACIC CARDIAC NERVES, LEFT SIDE	43
3. DRAWING OF THE THORACIC CARDIAC NERVES, RIGHT SIDE	44
4. MEASURED TIME INTERVALS	52
5. CONTROL R-WAVE TO MECHANICAL ONSET TIME INTERVALS	56
6. CONTROL ELECTRICAL-ELECTRICAL COUPLING INTERVALS	60
7. CONTROL ELECTROMECHANICAL COUPLING INTERVALS	63
8. HEART RATE: CONTROL AND STIMULATION	66
9. TYPICAL FORCE RECORDING, LEFT SIDE NERVE STIMULATIONS	70
10. TYPICAL FORCE RECORDING, RIGHT SIDE NERVE STIMULATIONS	71
11. TYPICAL FORCE RECORDINGS, PARASYMPATHETIC NERVES AFTER ATROPINE	73
12. FORCE COMPARISONS DURING LEFT STELLATE GANGLION STIMULATION	77
13. FORCE COMPARISONS DURING RIGHT STELLATE GANGLION STIMULATION	80
14. FORCE COMPARISONS DURING VENTROLATERAL CARDIAC NERVE STIMULATION	81

15.	FORCE COMPARISONS DURING RECURRENT CARDIAC NERVE STIMULATION	83
16.	FORCE COMPARISONS DURING INNOMINATE, CAUDAL VAGAL AND RIGHT THORACIC NERVE STIMULATIONS	84
17.	FORCE COMPARISONS DURING LEFT SIDE NERVE STIMULATIONS FOLLOWING ATROPINE	89
18.	FORCE COMPARISONS DURING RIGHT SIDE NERVE STIMULATION FOLLOWING ATROPINE	93
19.	FORCE COMPARISONS FOLLOWING ISOPROTERENOL INJECTION	96
20.	TYPICAL R-WAVE UPSTROKE TO MECHANICAL ONSET RECORDINGS, LEFT SIDE NERVES	97
21.	TYPICAL R-WAVE UPSTROKE TO MECHANICAL ONSET RECORDINGS, RIGHT SIDE NERVES	101
22.	R-WAVE TO MECHANICAL ONSET TIME INTERVAL CHANGES, LEFT SIDE NERVES	103
23.	R-WAVE TO MECHANICAL ONSET TIME INTERVAL CHANGES, RIGHT SIDE NERVES	105
24.	EFFECT OF STELLATE STIMULATION ON THE ELECTROMECHANICAL COUPLING INTERVAL	110
25.	EFFECT OF ATRIAL PACING ON THE ELECTROMECHANICAL COUPLING INTERVAL	113
26.	EFFECT OF CALCIUM AND NOREPINEPHRINE ON THE ELECTROMECHANICAL COUPLING INTERVAL	115
27.	EFFECT OF CALCIUM AND NOREPINEPHRINE ON THE ELECTROMECHANICAL COUPLING INTERVAL AFTER PROPRANOLOL	116
28.	ANALYSIS OF ELECTROMECHANICAL COUPLING INTERVAL CHANGES	118
29.	ELECTROMECHANICAL COUPLING INTERVAL CHANGES, LEFT SIDE CARDIAC NERVES	124
30.	ELECTROMECHANICAL COUPLING INTERVAL CHANGES, RIGHT SIDE CARDIAC NERVES	127

31.	STATISTICAL ANALYSIS OF ELECTROMECHANICAL COUPLING INTERVAL CHANGES, LEFT SIDE CARDIAC NERVES	130
32.	STATISTICAL ANALYSIS OF ELECTROMECHANICAL COUPLING INTERVAL CHANGES, RIGHT SIDE CARDIAC NERVES	132
33.	INNERVATION PATTERNS--POSITIVE INOTROPIC LEFT SIDE NERVES	148
34.	INNERVATION PATTERNS--POSITIVE INOTROPIC RIGHT SIDE NERVES	153
35.	INNERVATION PATTERNS--NEGATIVE INOTROPIC NERVES	157
36.	INNERVATION PATTERNS--LEFT SIDE NERVES AFTER ATROPINE	160
37.	INNERVATION PATTERNS--RIGHT SIDE NERVES AFTER ATROPINE	164
38.	MYOCARDIAL CELLULAR STRUCTURE	184

CONTENTS OF APPENDIX

Table	Page
A-1. HEART RATE--BEFORE ATROPINE	206
A-2. HEART RATE--AFTER ATROPINE	207
A-3. LEFT VENTRICULAR ANTERIOR R-WAVE	209
A-4. LEFT VENTRICULAR LATERAL APEX R-WAVE	210
A-5. LEFT VENTRICULAR LATERAL BASE R-WAVE	211
A-6. LEFT VENTRICULAR POSTERIOR R-WAVE	212
A-7. FREE WALL APEX R-WAVE	213
A-8. FREE WALL BASE R-WAVE	214
A-9. SEPTAL APEX R-WAVE	215
A-10. SEPTAL BASE R-WAVE	216
A-11. ELECTROMECHANICAL COUPLING--ANTERIOR	217
A-12. ELECTROMECHANICAL COUPLING--POSTERIOR	218
A-13. ELECTROMECHANICAL COUPLING--LATERAL APEX	219
A-14. ELECTROMECHANICAL COUPLING--LATERAL BASE	220
A-15. ELECTROMECHANICAL COUPLING--FREE WALL APEX	221
A-16. ELECTROMECHANICAL COUPLING--FREE WALL BASE	222
A-17. ELECTROMECHANICAL COUPLING--SEPTAL APEX	223
A-18. ELECTROMECHANICAL COUPLING--SEPTAL BASE	224
A-19. ANALYSES OF VARIANCE, R-WAVE LEFT SIDE NERVES	225

A-20.	ANALYSES OF VARIANCE, R-WAVE RIGHT SIDE NERVES	226
A-21.	ANALYSES OF VARIANCE, ELECTROMECHANICAL COUPLING--LEFT SIDE NERVES	228
A-22.	ANALYSES OF VARIANCE, ELECTROMECHANICAL COUPLING--RIGHT SIDE NERVES	229

CHAPTER I

INTRODUCTION

The sequence of electrical activation of the heart is well established, Sir Thomas Lewis (38) having first described the activation pattern. Since then there have been many reports dealing with the spread of the action potential through the myocardium (26, 50, 69, 78, 79). The most recent report was by Myerburg et al. (43), using microelectrodes to fully map the activation sequence of the Purkinje network and the endocardial muscle. In contrast to a large amount of data concerning the electrical activation of the heart, few data have been presented dealing with the contraction sequences of the ventricles.

Wiggers in 1927 (91) used the term "Fractionate contraction" to define the asynchronous contraction of the ventricles. His conclusion that different areas of the heart contracted at different times was based on electrical, not mechanical, recordings. Several studies by Rushmer (71, 73) described the contraction sequences of major portions of the ventricles but did not deal with the localized muscle segments. Several reports (3, 6, 46) from the laboratory of W. C. Randall have given Q-wave to onset of selected segment contraction time intervals.

These reports deal with only a small number of left ventricular muscle segments.

In 1972, Randall, Armour, Geis and Lippincott (62) published a paper describing the distribution of the sympathetic innervation of the heart. They described the innervation patterns of the small thoracic cardiac nerves using force changes as the indicator of innervation. The patterns described included the epicardium of both ventricles, all the papillary muscles and both sides of the interventricular septum. The innervation to the free wall endocardium was not studied. The innervation patterns of the interventricular septum have only been presented in one other paper by Armour, Lippincott and Randall. In this paper only left and right stellate ganglion innervation patterns were reported (3).

Several reports (3, 46, 49, 55, 76) dealing with changes in time intervals, either Q-wave to onset of pressure rise or Q-wave to onset of contraction have indicated that these time intervals change with stimulation of the autonomic nervous system.

The purpose of the present experiments is to describe (1) the control sequence of the contraction in the left ventricle; (2) the innervation patterns of the small thoracic cardiac nerves in the left side of the interventricular septum and free wall endocardium; and (3) the time changes elicited by stimulation of the

thoracic cardiac nerves.

CHAPTER II

LITERATURE REVIEW

A. Anatomy of the Cervical Cardiac Autonomic Nerves

In 1886 Gaskell (19) described the structure and function of the autonomic nervous system. He showed that the sympathetic cardiac fibers leave the spinal cord in the thoracic region and synapse in the lateral chain. Then they "pass from below upwards into the ganglion stellatum" where the fibers travel either directly to the heart or by way of the inferior cervical ganglion. He also observed that the vagus nerve in the frog was in fact the vago-sympathetic nerve which had both an inhibitory and an excitatory effect on the heart. He observed that the sympathetic component was responsible for the acceleration of rate and augmentation of contractile force. The inhibitory effect on the heart of the vagus was due to a distinctly different group of fibers from those that caused excitation.

In 1926 H. H. Woollard (93) using a methylene blue staining technique, confirmed and extended earlier observations on the terminal innervation of the myocardium. He described a "robust plexus of nerves" located both throughout the epicardium and the endocardium. These nerves reached the endocardium by penetrating the myocardium along

with the blood vessels. He concluded on the basis of both normal dogs and dogs with both stellate ganglia removed that most of the nerve fibers in both epicardial and endocardial plexi in the ventricles were sympathetic in nature. With respect to the terminal innervation Woollard thought the fibers from the subcardial plexus ultimately penetrated the individual cells. In cross-section a nerve cell was completely surrounded by the muscle cell. He also observed that the nerve fiber crossed the "protoplasmic bridges" connecting the muscle fibers.

One of the first comprehensive descriptions of the thoracic cardiac nerves was given by Nonidez (45) in 1939. Using a silver stain Nonidez was able to distinguish between the dark-staining parasympathetic and the light-staining sympathetic postganglionic fibers. He described and named the nerves originating from the sympathetic chain. He described three major sympathetic nerves on each side, superior, middle and inferior. He found that both the left and right vagus nerves give off few fibers that innervate the heart. Most of these fibers end in the intrinsic ganglia in the atrium. In following the parasympathetic fibers Nonidez found that there were scattered thickenings along the neurons. These fibers did not enter the muscle cells but were found in the spaces between the cells. Finally, both parasympathetic and sympathetic neurons were contained in a single nerve.

As a partial fulfillment of the requirements for his Ph.D., N. Mizeres completely described the anatomy of the autonomic nervous system of the dog (40). In so doing he introduced new terminology describing the various cardiac nerves. The names given to the nerves by Mizeres are the names that are used in this dissertation. Nonidez's (45) names for the nerves indicated where the nerve originated and terminated, i.e. the left middle cardiosympathetic nerve. But as Nonidez himself pointed out, many of the nerves contained both sympathetic and parasympathetic fibers. Mizeres used names that described only the anatomical location of the nerve. For example Nonidez's left middle cardiosympathetic nerve was called the ventrolateral cervical cardiac nerve under the Mizeres system. Most of the cervical cardiac nerves from both left and right side entered the pretracheal plexus before entering the heart. Some of the nerves, the caudovagal, ventrolateral cervical cardiac and left and right stellate cardiac nerves all innervated the heart directly without passing through a plexus. The left innominate nerve passed into the walls of the large arteries.

B. Functional Anatomy of the Cervical Cardiac

Autonomic Nerves

As early as 1899 studies were conducted on the tonic activity of the autonomic nerves (32). Reid Hunt found the accelerator nerves were tonically active. He cut

the accelerator nerves and heart rate decreased with little or no decrease in blood pressure. Section of the right side nerves usually resulted in a greater decrease than the section of the left side nerves. Also Hunt found the duration of both systole and diastole were prolonged with section of the accelerator nerves, with the systolic time interval prolonging relatively more than diastole. In a second series of experiments Hunt demonstrated that the activity of the accelerators and vagi can be changed by stimulation of the saphenous nerve in the leg. Hunt did not find much alteration in blood pressure with section of the nerves. Nor did he find that the force of the heart-beat increased when heart rate was increased during stimulation of the accelerator nerves. Stimulation of the left side accelerators, however, which usually did not increase heart rate, did lead to an increase in blood pressure.

In 1944 and 1945 Donald Gregg and Robert Shipley published two papers (23, 81) on the effect of autonomic nerve stimulation on both left and right coronary artery blood flow. Stimulation of either left or right stellate ganglion caused coronary blood flow to increase. This occurred whether blood pressure was controlled or allowed to change. During the recording of blood flow the authors noticed that the vigor of contraction seemed to increase with stimulation of the nerves.

In the second paper (81) Shipley and Gregg found that stimulation of the cardiac nerves led to an increase in cardiac output and an unchanged or increased blood pressure. From this the authors concluded that the work of both the left and right ventricle was increased. In association with this the O_2 consumption also increased.

Exactly how nerve stimulation increased the vigor of contraction the authors did not know. They discounted adrenal involvement by clamping off the adrenals. The response to stimulation was identical before and after the clamping. They speculated that some "myocardial stimulating substance" was released from the nerve endings. Shipley and Gregg (81) concluded that coronary flow increased due to the increased metabolic demand of the cardiac cells. They also concluded the cardiac nerves were involved in adapting the work output of the heart to the demands of the entire organism.

In 1955 Anzola and Rushmer (2) reported on the changes in ventricular pressures and dimensions during sympathetic stimulation. Left stellate stimulation caused LV circumference and RV wall thickness to decrease. In association, LV systolic pressure increased while diastolic pressure fluctuated in an "unpredictable fashion." When the stimulation was turned off, all the measured parameters returned to normal within 2 minutes. Isolation of the left stellate ganglion from the rest of the nervous system

did not change the response to stimulation. In another series of experiments the authors tried to eliminate the possibility that neurohormones released in the heart circulated to the resistance vessels resulting in the large ventricular systolic pressure increase. They cross-clamped the aorta and then stimulated the ansa subclavia. With the aorta cross-clamped no blood could leave the heart. With stimulation ventricular pressure increased. Similar responses were seen in unanesthetized, intact dogs. The authors concluded that the stimulation led to an increase in the contractility of the muscle fibers. Also they concluded that "neural controls play an important role in the regulation of cardiac function."

Less than a year later, Randall and Rohse (66) described the results of stimulation of the stellate ganglia on pressure and heart rate. They found that stimulation of each stellate ganglion resulted in both increased pressure and increased rate. However, the magnitude of response was different. Right stellate stimulation (RSS) primarily caused an increase in rate with some augmentation of pressure. Left stellate stimulation (LSS) had little or no effect on heart rate but did cause marked augmentation of pressure. The authors also stimulated the interganglionic segments of the sympathetic chain from T2 (caudal pole of the stellate ganglion) down to T10 or T11. The stimulation at T2 resulted in a prompt

response that was primarily systolic. From T2 to T5 the responses were progressively smaller with little or no response at T5. Below T5, the responses to stimulation were pressor with equal rises in both systolic and diastolic pressures indicative of splanchnic vasoconstriction. During later experiments they isolated the sympathetic efferents by sectioning the ganglionic chain below T5 and sectioning of the vagi above the caudal cervical ganglion.

In 1960 Sarnoff and co-workers (39, 76) demonstrated that ventricular contractility could be altered by stimulation of the sympathetic nerves or by infusion of norepinephrine. Both left ventricular diastolic pressure and myocardial segment length were measured and pressure-length curves were plotted. Left stellate ganglion stimulation caused both diastolic pressure and segment length to decrease (39). Along with the above, systole was shortened and diastole was lengthened. This allowed more time for complete filling following the increased peak of contraction. Initially Sarnoff and co-workers thought that the sympathetics increased and the parasympathetics decreased the extensibility of the myocardium. This would allow the length to change, creating the change in force of contraction. They found however, that myocardial extensibility was not altered by either division of the autonomic nervous system. The shorter systole and longer diastole (than normal) allowed the

heart to maintain nearly normal pressure-length relationships at high heart rates. The authors concluded that the myocardium contracted more forcefully during stellate stimulation from a given diastolic pressure with no length change.

In a second series of experiments (76) Sarnoff and co-workers expanded upon the above conclusions. They found a series of pressure-length curves that were dependant upon the level of catecholamine present. The curves shifted up and to the left as the catechol levels increased either by infusion or stellate stimulation. This relationship held for both the atria and ventricles. The authors proposed the following concerning the control of myocardial contractility. Stimulation of the stellates increased force of atrial contraction causing more blood to enter the ventricles. This increased end-diastolic volume led to an increase of fiber length resulting in a more forceful contraction. Along with this the stellate stimulation also increased the force of contraction of the ventricles at whatever the end-diastolic fiber length was. This caused more complete systolic emptying which lowered diastolic impedance to ventricular inflow. Sarnoff also felt that part of the increase in ventricular contractility with stellate stimulation was the result of a greater synchrony between the contracting cardiac cells.

In 1963, W. C. Randall, D. V. Priola and R. H.

Ulmer (58) showed that chronic removal of one stellate ganglion with stimulation of the opposite stellate resulted in augmentation of pressure in only two or three chambers with no change or a decrease in the rest. If the left stellate was removed, and the right stellate stimulated, heart rate and atrial force increased immediately while the ventricular force increase was delayed. Left stellate stimulation following right stellectomy produced a much smaller acceleration in most animals. Occasionally heart rate was markedly increased indicating that the left stellate innervates the SA node in only a small number of animals. Force response was seen in both left side chambers and right ventricle.

Matthew Levy and co-workers (36) confirmed the above observations that right stellate stimulation primarily caused an increase in heart rate and left stellate stimulation primarily caused a pressure increase in the left ventricle. They also found that when the stellates were stimulated simultaneously the response was slightly less than the sum of the responses of the individual stimulations. This indicated some overlap between the left and right stellate innervation. In this study the authors also noted the relationship between two potent cardiovascular reflexes and cardiac sympathetic tone. The two reflexes studied were the carotid baroreceptor and cerebral ischemic reflexes. They found that the cardiac

response during both of these forms of stimulation could be significantly attenuated by decentralization of the stellate ganglia.

While studying the cervical vagosympathetic trunks Randall, Priola, Pace and Wechsler (57) again showed that stimulation of augmentor fibers did not result in equal response in all four chambers. The authors utilized modified Walton strain gauge arches to measure changes in contractile force of various areas of the atria and ventricles. Following the injection of atropine stimulation of the left or right cervical vagosympathetic trunk caused augmentation in heart rate and contractile force in some but usually not all the muscle segments. The augmentation of contractile force was seen primarily in the atria and in the right ventricle.

The above report was followed shortly by a paper authored by Szentivanyi, Pace, Wechsler and Randall (84). Using strain gauge arches sutured to various muscle segments on both ventricles, they stimulated the small nerves distal to the stellate and caudal cervical ganglia. Stimulation of the ganglia resulted in a generalized increase in contractile force in all areas. As smaller and more distal portions of the nerves were stimulated fewer muscle segments responded. In some instances only one muscle segment would respond to stimulation of a thoracic branch. To eliminate heart rate decreases due to

stimulation of parasympathetic fibers in the nerve branches atropine was given before the stimulations were started. Further evidence for specific innervation of a muscle segment by a nerve was obtained by stripping a small portion of the right ventricular epicardium.

Following this procedure and stimulation of the right anterior ansa subclavia, the response of the right ventricle was diminished indicating that some fibers to the RV muscle segment had been destroyed while the fibers to the LV muscle segments were still intact. Injection of norepinephrine into the artery close to a strain gauge mimicked the response seen during stimulation of a small thoracic nerve.

The hypothesis that the small thoracic cardiac nerves innervate discrete areas of the heart has been studied extensively by W. C. Randall and co-workers (5, 33, 47, 53, 63, 64, 65). In 1972 Randall et al. summarized this information during a symposium (62). Composite drawings of both epicardium and endocardium showed the relative innervation of the cardiac nerves. The left ventricle was shown to be extensively innervated by the ventrolateral cardiac nerve. The innominate and ventromedial cardiac nerves were shown to have minimal innervation to the epicardium but did innervate much more of the septum and papillary muscles. The sympathetic portion of the left vagosympathetic trunk when stimulated

resulted in only minimal force increase throughout the ventricle. The right side cardiac nerves innervated primarily the right side of the heart (both atrium and ventricle) but also innervated the left side. The recurrent cardiac nerve showed the most extensive innervation of the left ventricle including the base and apex of the epicardium, the septum and anterior papillary muscle. The stellate cardiac nerve, primarily a rate nerve, caused minimal force increase in the septum and anterior papillary muscle. The craniovagal and right vagosympathetic nerves exhibited similar innervation patterns. The diagrams indicate that these nerves innervate the septum and both papillary muscles with the craniovagal nerve also innervating the apical and basal anterior epicardium. The caudovagal nerve innervates only the lower septum and anterior apex of the left ventricle. The free wall endocardium was not included in the above descriptions of innervation patterns.

In a series of four papers (4, 51, 52, 61) W. C. Randall, D. C. Randall, J. A. Armour and their co-workers described the cardiac innervation of the baboon heart. They found (61) that, like the dog, there was anatomical variability from baboon to baboon. Also the anatomy of the cardiac nerves was slightly different from that seen in the dog. However, they found (51, 52) that the cardiac nerves when stimulated gave results similar to those seen

in dogs. Stimulation of the small cardiac nerves resulted in localized muscle segment force changes. The sympathetic fibers caused force increases and the parasympathetic fibers caused force decreases.

In 1966 Yanowitz, Preston and Abildskov (96) began a series of experiments designed to describe the innervation patterns of the thoracic cardiac nerves. Instead of using strain gauge arches as Randall and co-workers used, the authors measured the functional refractory period of the ventricles. The hearts were paced through the right atrium. Recording electrodes were placed on the epicardium. The interval between the pace stimulus and the test stimulus was varied until no premature beat could be elicited. This time interval was defined as the functional refractory period (FRP). Removal of the right stellate ganglion was found to prolong the FRP in all 16 test sites, but the muscle segments on the anterior surface exhibited the greatest prolongation. Removal of the left stellate ganglion caused the greatest change in the posterior surfaces.

In 1972 Burgess, Abildskov and co-workers (12) studied the sequence of normal ventricular recovery using the functional refractory period as a measure of recovery. Using multiple recording sites on the epicardium, endocardium and septum, the authors found the FRP was longer at the apex than at the base of the epicardium. The FRP's

measured in the endocardium were longer than the overlying epicardium with the FRP's becoming gradually shorter through the wall to the epicardium. The authors concluded that those areas of the heart activated early had long refractory periods while the areas activated later had shorter refractory periods. This resulted in the entire heart being repolarized almost simultaneously.

To study changes in the functional refractory periods during small thoracic cardiac nerve stimulation Kralios, Martin, Burgess and Millar (34) designed recording electrodes with multiple recording sites. This system allowed them to record the FRP's of many different areas of the heart simultaneously. Stimulation of the sympathetic nerves after atropine shortened refractory periods. Using the shortened FRP as an indication of innervation of a muscle segment by a nerve the authors reported the following results. Of the right side thoracic cardiac nerves, stimulation of the recurrent cardiac nerve resulted in shortened FRP's in the anterior epicardium and septum with the septum exhibiting the greatest change. Stimulation of the other right side nerves did not often change refractory periods or electrocardiographic waveforms. On the left side the ventrolateral cervical cardiac nerve caused changes in the FRP's throughout the posterior surface of the heart. The ventromedial nerve overlapped the recurrent cardiac nerve in that it also caused changes in

the FRP's in the anterior surface when stimulated. The innominate nerve stimulation resulted in little or no change in refractory periods. The authors concluded from this study that the innervation of the myocardium by the small thoracic cardiac nerves is localized, not diffuse.

C. Ventricular Activation

In 1915 T. Lewis and M. A. Rothschild (38) described the electrical activation of the ventricles. An interesting commentary on their description is that during the past 60 years, investigations with more sophisticated techniques have given the same results. Lewis and Rothschild used both bipolar and unipolar electrodes connected to string galvanometers to study the excitation patterns of both ventricles. The reference point employed to measure the time intervals was the take-off point of the R-wave in the Lead II ECG.

Though Lewis and Rothschild (38) described the Purkinje system anatomically in both ventricles, they had difficulty recording from the endocardium of the left ventricle. Their findings concerning the LV endocardium were that: (1) the earliest activation was in the middle left septum; and (2) most of the intervals were negative indicating that activation of the septum and apex occurred before the R-wave. In the right ventricle they found that the endocardial surface was electrically excited before its overlying epicardial surface. The time interval

between the respective activations was dependant upon the thickness of the myocardium between the electrodes. The authors felt that the action potentials spread rapidly through the Purkinje fibers and then through the muscle from endocardium to epicardium.

Their observations on the epicardium were much more extensive. The first area of the epicardium to be excited, according to Lewis and Rothschild, was the "central region" of the right ventricle. This was the area of the right ventricle midway between the base and the apex along the left anterior descending (LAD) artery. Activation there occurred before the upstroke of the R-wave. From this area the electrical activity appeared later and later as the electrodes were moved across the right ventricle to the base with the conus being one of the last RV muscle areas to be excited. The left ventricular epicardium displayed a slightly different pattern of electrical activation. The earliest area of the LV epicardium to show electrical activity was the apex. The intervals became longer as the recording sites moved closer to the base but were not always in sequence. Several figures in the Lewis and Rothschild paper suggest that it was common to find areas closer to the basal ring with shorter time intervals than in some areas further away from the ring. Many areas of the LV were electrically excited nearly simultaneously. The area of the left ventricle along the

LAD artery was always excited later than the corresponding areas of the RV. It was because of the simultaneous activation of many points of the left ventricle that the authors concluded that propagation through the ventricles was not from cell to cell along the epicardium, but from cell to cell from endocardium to epicardium. Lewis and Rothschild concluded that "the question of priority of base or apex is of little consequence." They felt that the activation times were so close together (the total time from first to last area was less than 30 msec) that there was little difference in times between the first and last segment to be activated.

In 1941 A. Sidney Harris (26) studied similar excitation patterns of the dog, cat and monkey along with the turtle heart. He also used the string galvanometer. All three of the mammalian hearts exhibited essentially the same patterns of excitation. The earliest area activated, as measured from the R-wave was the mid-portion of the right ventricle near the LAD artery. From there the intervals became longer as the electrodes approached the basal portions of either ventricle. The author does not show a posterior view of any of the hearts he studied so it is difficult to make direct comparisons with the Lewis and Rothschild data (38). However, Harris (26) did show the anterior apex being activated slightly later than the muscle segments on the left ventricular

side of the LAD artery. This is slightly different from Lewis and Rothschild's pattern (38). Also Harris showed that the difference between the earliest and latest site activated was only 18 to 22 msec as compared to 25 to 30 msec for Lewis and Rothschild's findings (38).

In 1952 Burchell, Essex and Pruitt (11) used both unipolar and bipolar electrodes connected to an oscilloscope to study the activation of the intraventricular septum. The heart was supported using a Langendorff apparatus. After the heart was stabilized on the apparatus, both the left and right ventricular free walls were removed so that the septum could be studied directly. Both direct electrograms and vectorcardiograms were recorded. These workers found that the septum was generally activated from apex to base in both ventricles with the right septum following the left septum slightly.

Three years later Allen Scher and his co-workers, Young, Malmgren and Erickson (78) used a multipolar electrode to investigate the total activation of the inter-ventricular septum. They used an electrode that had 15 separate wires, the ends of which were 1 mm apart, and the electrode was positioned perpendicular to the septum. In this manner the recording terminals at one end of the electrode were positioned in the left cavity and the terminals at the other end of the electrode were in the right cavity. The electrical activity from each recording

terminal was recorded on a separate channel of a 16-channel oscilloscope. Scher and co-workers (78) found that the earliest point to be excited in the septum was the mid-left septum near the level of the branching of the left bundle. From this point the activity spread through the endocardium of the septum. The septal muscle was activated as Lewis and Rothschild (38) postulated. The wave of depolarization spread to the muscle from its overlying endocardium. The right septum usually was excited later than the left side. The first area of right septum to show activity was near the base of the anterior papillary muscle. The excitation then spread throughout the endocardium and into the muscle. The septum was invaded electrically from both the right and left sides, with the left side invasion contributing to the excitation of the larger part of the septum. The endocardium was excited on both sides in an apex-to-base direction. Scher et al. (78) also found different conduction velocities of the excitation wave closer to the base. Near the apex the conduction velocity was 1 m/sec or greater; at the base it was 0.3 m/sec or less. Part of this difference may be due to the sparsity of Purkinje fibers in the basal portions of the septum.

There has been considerable disagreement over the activation of the left ventricular free wall. Following Lewis' paper (38) suggesting that the left ventricular free wall was activated from endocardium directly to overlying

epicardium, Robb and Robb (69) felt that Lewis was wrong. The latter workers recorded from the epicardial surface. They placed their electrode along what they felt were continuous muscle bundles, and reported that the apical end of the muscle bundle was activated first. From the apex the activation spread along the muscle bundle to the base. They postulated that the wave of excitation spread across the endocardium, then spread along the muscle bundles to the apex, passed to the epicardium at the apex and then to the base along the muscle bundles.

This hypothesis was challenged by Scher, Young, Malmgren and Paton (79) using the same technique described earlier. They inserted the multi-terminal electrodes in the muscle of the free wall of the left ventricle. Only the anterior and lateral surfaces were studied in both the right and left ventricles of dogs, cats and one monkey. By making multiple insertions in a single heart, it was possible to map the activation pattern of individual parts of the ventricle. In the left ventricle the earliest area to show electrical activity was at the junction of the wall and septum. From there the excitation spread toward the base and apex and from the endocardium toward the epicardium. The right ventricle showed essentially the same pattern. The earliest site of activation was at the junction of free wall and septum approximately midway along the LAD artery. From there the wave of excitation

spread toward the base and apex and from the endocardium toward the epicardium. The last area of the right ventricle to be activated was the conus. The authors felt that their data refuted the hypothesis of Robb and Robb (69) because Scher et al. (79) found no relationship between the spread of excitation and fiber orientation either in the endocardium or epicardium. The authors (79) concluded that the heart was excited through a rapid conduction system in the endocardium. The activity then spread into the wall through a "syncytial system" of cells or by a conduction system with slower rate than that of the Purkinje fibers. Scher et al. (79) favored the first hypothesis because no data was found which supported the conduction system hypothesis.

In 1956 Scher and Young (77) extended their studies. The electrodes were inserted into the heart in regular patterns and, at the conclusion of the experiment, the position of each of the electrodes was placed on an appropriate sketch of the heart. The results of these experiments confirmed and extended the data the authors had already published (78, 79). The earliest area of the ventricles to be activated was the mid-septum on the left side, this activation preceding the QRS complex. Five msec after the QRS the activation had spread to include the left ventricular apical endocardium. Ten msec following the QRS, the depolarization had spread to the intermediate myocardium

of the left and right ventricle. The first epicardial breakthrough occurred at this time at the junction of the right ventricular free wall and the septum. Five msec later most of the myocardium of both right and left ventricles was depolarized. Only a small portion of the basal portions of both ventricles was depolarized. The left ventricle epicardium was now activated. Twenty msec after the onset of the QRS the electrical activity continued to spread toward but did not reach the left ventricular lateral epicardium. Most of the right ventricular epicardium was also activated by this time. During the next 5 msec the activity spread to include most of the left ventricular epicardium. Between 25 and 30 msec after the QRS the left ventricular basal epicardium and the basal septum were finally excited.

In 1972, Myerburg, Nillsson and Gelband (43) reported on a large series of experiments designed to map the activation of the endocardium of both ventricles. The authors used microelectrodes to record transmembrane action potentials and bipolar electrodes to record surface electrograms. Although both ventricles were explored, only the results from the left ventricle will be discussed here.

The hearts were removed from the dogs and the section to be studied was placed in a tissue bath. For studies of the left ventricular endocardium three different preparations were utilized. Each preparation was designed

to include a main bundle branch and its ramifications. One preparation was the septum and the projection of the Purkinje fibers from the septum to the apical free wall. Another preparation included main left bundle branch, the anterior division of the left bundle branch, part of the septum, anterior papillary muscle and the free wall of endocardium. If the heart was small enough this preparation would also include the posterior papillary muscle. The third preparation was similar to the second except that it utilized the posterior division of the left bundle and its ramifications. The main left bundle was stimulated at a rate of 60 per minute, 1-2 msec duration at 1.1 to 1.2 times the threshold voltage.

Anatomically the left Purkinje network in the septum consisted of the main left bundle branch which divided into two subdivisions, the anterior division and the posterior division. These two divisions extend to and beyond their respective papillary muscles, and joined again in the free wall endocardium. Between the two divisions was an extensive network throughout the septum of subendocardial Purkinje fibers. These fibers continued down the septum onto the apical free wall endocardium and the basal portions of the papillary muscles. As a result of this anatomical make-up the free wall endocardium was activated from three different points.

Using several different septal preparations of

different sizes, Myerburg et al. (43) found that the earliest muscle area of the ventricle to be activated was approximately two-thirds distally along the septum from the base. This occurred 24 msec after stimulation. To that point on the septum the Purkinje network was isolated from the muscle and the activation did not pass into the muscle. From the point of entry into the muscle the wave of excitation spread in two directions. It spread up the septum to the base reaching there 60 msec after stimulation and down toward the apex arriving 24 to 26 msec after stimulation. Because of the lower conduction velocity through the muscle toward the base and the faster conduction velocity through the Purkinje fibers toward the apex, the net effect was for the depolarization to spread in an apex to base direction.

Following septal apex activation, the basal portions of the papillary muscles (26 msec) and the left ventricular apex (31 msec) were the next endocardial surfaces to be activated. The papillary muscles had a dual input from the Purkinje network. The apical portions of the papillary muscles received Purkinje fibers from the major divisions of the left bundle. The subendocardial network from the septum extended to the basal portions of the papillary muscles. The time intervals indicated that the Purkinje network depolarized from the apex toward the base of the papillary muscle while the muscle depolarization

occurred in the opposite direction from base to apex. The Purkinje fibers in the apical papillary muscles depolarized 13 msec after stimulation while the basal portions were activated 10 msec later. The muscle cells of the papillary muscle depolarized as follows: the base 26 msec and the apex 42 msec following stimulation of the main left bundle.

The interpapillary free wall was studied using all three preparations described earlier. It was found that the time intervals between the stimulation and activation of the Purkinje fibers in the free wall were similar with all preparations. The authors concluded that there were three inputs into the free wall Purkinje network: the two major divisions of the left bundle and from the subendocardial network in the septum. The Purkinje network throughout the free wall was activated nearly simultaneously. The time difference between the apical portion and basal portion of the free wall was only 3 to 5 msec. The muscle depolarization spread from apex to base with a time difference of 13 to 15 msec. The basal free wall was activated 44 msec after the stimulation of the main bundle branch.

The authors questioned whether the thin sections they had used for their experiments may have directed the pattern of excitation. To solve the problem, they also studied thick sections. The activation pattern was similar in both experiments, and indicated that the endocardium was

not activated from Purkinje fibers that plunged into the myocardium.

Brusca and Rosettani (9) using human fetal hearts and Durrer, van Dam, Freud, Janse, Meyler and Arzbaeher (16) using adult human hearts, confirmed what Lewis and Rothschild (38) reported in the dog heart. Activation spread throughout the endocardium and then from endocardium to epicardium. The earliest area to be activated was the lower third of the septum. The latest area was the posterolateral base.

D. Sequence of Muscle Segment Contraction

Until the 1920's it was generally assumed that all muscle segments contracted nearly simultaneously. In 1927 Carl Wiggers (91) introduced the term "Fractionate contraction." Based on the observations of Lewis and Rothschild (38) and his own (91), Wiggers concluded that ventricular muscle did not contract simultaneously but in what he called "many rapidly succeeding fractionate contractions." Wiggers based his conclusion on the results derived from the onset of electrical activity of a given area compared to the intraventricular pressure. The result of this electrical analysis corresponded to Lewis and Rothschild's data (38). Wiggers expanded on the data. He assumed that the time interval between the electrical activation of a muscle fraction and the onset of contraction in that cell was equal for all muscle fractions in the ventricle. This

meant that some fractions began to contract later than others.

He then constructed an intraventricular pressure curve from a series of isometric fractionate contractions. The constructed curve approximated the curves he recorded experimentally. Wiggers also noted that the T-wave of the ECG begins before the incisura in the pressure curve. This indicated to him that some contractions ceased before others.

Since Wiggers' report (91) many studies of the contraction of the ventricles have utilized some form of cineradiographic technique. These studies explored dimension changes during the cardiac cycle, but also provided an indication of the sequence of contraction. Robert Rushmer and his co-workers did much of the early work with the cineradiographic technique of studying ventricular dimension changes (72, 73).

Several techniques were used to study the dimension changes. Initially Diodrast was used (73) to visualize the ventricles under fluoroscopic examination. Rushmer thus found that left ventricular contraction resulted in a large reduction in width with only a minor change in length. He also found that wall thickness increased in systole with the radius of the endocardium undergoing a greater reduction than the radius of the epicardium.

In 1956, Rushmer changed his recording technique

to look at the isovolumetric phase of ventricular contraction (71). He placed variable induction gauges inside the left ventricle to measure diameter and length. He also used mercury filled length gauges on the epicardium to measure circumference and length. Thus, Rushmer found that during isovolumetric contraction with intraventricular pressure increasing, both the internal diameter and external circumference increased. The ventricle changed shape and became more spherical. The hypothesis proposed by Rushmer was that septal and papillary muscle contraction, which he supposed occurred first, caused the shortening. Then the areas that were activated later would contract later. Because of the distribution of the Purkinje fibers in the endocardium, Rushmer assumed that they would contract early in the cycle. This shortening of the length against a constant volume would force other muscle segments to be passively stretched until they began to contract.

It was not until 1970 that Armour and Randall (6) showed the left ventricular papillary muscles, while electrically activated early, contracted relatively late in the cardiac cycle. Walton-Brodie strain gauge arches were sutured directly to the left ventricular papillary muscles while the animal was on total cardiopulmonary bypass. In measuring the time interval between the Q-wave and the onset of contraction in the left ventricular

papillary muscles, they found the intraventricular pressure began to increase before the muscles contracted. The intraventricular pressure began to increase 71.9 msec after the Q-wave. The papillary muscles began to contract 88.5 and 87.8 msec, anterior and posterior muscles respectively, after the Q-wave. The left ventricular papillary muscles thus could not contribute to the initial shortening of the ventricle as Rushmer (71) hypothesized. In contrast to the papillary muscles, Armour and Randall showed that the anterior epicardium (61.2 msec) base epicardium (58.0 msec) and posterior epicardium (52.0 msec) all began to contract before the increase in intraventricular pressure. When an ectopic stimulus was placed in the papillary muscle the sequence of contraction between the papillary muscles and the epicardium was reversed. The papillary muscles contracted before the three epicardial segments.

In 1968 Hinds, Hawthorne, Mullins and Mitchell (28) measured internal dimensions by means of strain calipers and mercury-rubber gauges located between the mitral ring on the lateral wall and the apex to measure base-to-apex length. An electromagnetic induction system was used to measure the aorta-to-apex length; biplane cinefluorographic techniques were used to measure circumflex-to-apex length. The base-to-apex length decreased sharply during isovolumetric contraction then

lengthened slightly during ejection. In contrast to this, the aorta-to-apex length increased during isovolumetric contraction and did not shorten until during ejection. Circumflex-to-apex length shortened throughout ventricular systole. The above indicated that while the rest of the ventricle was shortening the septum (aorta-to-apex length) was not contracting. This resulted in the non-contracting muscle being stretched before it began to contract.

The above data were confirmed by Tsakiris, Donald, Strum and Wood (88) using biplane videometry. By measuring left ventricular dimensions from the angiograms, Tsakiris et al. found that during isovolumetric contraction there was a progressive inward movement of the posterior wall and a narrowing of the apex. At the same time the septal area showed slight expansion before contraction. It was also found that with an increase in emptying the major change in dimensions was in the circumference. The base-to-apex length was unchanged from control.

Both of these reports (28, 88) indicated that the free wall contracted slightly before the septum. The Tsakiris paper (88) also indicated that the apex contracted before the septum.

In 1964, Osadjan and Randall (46) utilized a different technique to study the synchrony of ventricular contraction. They sutured three strain gauge arches to

the anterior surface of the left ventricle. A fourth gauge with long sharp prongs for legs was inserted into the interventricular septum. In a second series of experiments, pin electrodes were positioned between the legs of the strain gauge arches. Using this system they were able to record both mechanical and electrical activity from a muscle segment. They found that during the control period, the anterior base and anterior apex each contracted first approximately 50% of the time. However, with left stellate ganglionic stimulation, the anterior base was always (49 out of 50 observations) the first to contract. Also, the time interval between the first segment and the last segment to contract was significantly shortened. In the second series of experiments utilizing the pin electrodes it was found that the septum had the shortest electromechanical (EM) coupling time (25 msec), the anterior apex (30 msec) and the anterior base (34 msec) following. With left stellate stimulation the electromechanical coupling intervals changed for all three muscle segments. The anterior base had the shortest interval (25 msec) followed by the septum (34 msec) and anterior apex (36 msec). Along with the shift in EM coupling time, Osadjan and Randall reported a change in the sequence of electrical activity. During the control period, electrical activity was first recorded in the septum with the apex and base following 5 msec and 10 msec later respectively.

With the stimulation the base was first with a 10 msec interval to the apical electrical activity and a 15 msec interval to the septal electrical activity. The authors stated that the synchrony of contraction of the left ventricle was increased by left stellate stimulation. This increased synchrony contributed to the more rapid rise of the pressure pulse that was seen during stellate stimulation.

Ventricular synchrony was also studied by Priola and Randall (49, 55) using simultaneously recorded ventricular pressures. It was found that during the control period, left ventricular systole preceded right ventricular systole by 22 msec. With right stellate stimulation the asynchrony between LV and RV disappeared. The pressures began to increase simultaneously. While pacing from the atrium, they found that the pace artifact-to-pressure onset time interval decreased for all four chambers during right stellate stimulation. The pace-to-pressure time interval for the RV decreased much more than the LV time interval which resulted in the more synchronous contractions. Left stellate ganglion stimulation gave similar results.

Priola, Osadjan and Randall (48) combined the use of intraventricular pressures and strain gauge arches to study the left ventricular inflow and outflow tracts. They found that the pressure began to increase in the

inflow tract 4 to 18 msec before the outflow tract. When the strain gauge arches were also used, an asynchrony occurred between the onset of contraction in the four muscle segments studied. The inflow tract muscle contracted 20 msec before the outflow tract muscle. As the strain gauge arches were moved closer together the asynchrony was less between the muscle segments.

In 1973, Armour, Lippincott and Randall (3) reported data concerning the onset of contraction of several different muscle segments in the left ventricle. Using strain gauge arches, it was found that during control the Q-wave-to-mechanical onset time interval in the left ventricle was shortest for the posterior epicardium (35.4 msec) followed by the anterior epicardium (40.4 msec) septal apex (48.4 msec) and septal base (54.0 msec). Left or right stellate stimulation shortened all four intervals but by varying degrees. The septal apex exhibited the greatest variation with the right stellate stimulation shortening the interval to 37.9 msec and the left stellate stimulation shortening the interval to 29.2 msec. In contrast, the other three muscle segments exhibited approximately equal shortening with either left or right stellate stimulation. The time intervals during left or right stellate stimulation for the other three areas were as follows: septal base, 40 msec, anterior epicardium, 32 msec, and posterior epicardium, 28 msec.

Isoproterenol and norepinephrine also caused the same degree of shortening of the Q-wave-to-force onset for all four muscle segments.

CHAPTER III

METHODS

A. Surgical Procedure

A total of 95 mongrel dogs, of both sexes weighing between 15 and 25 kg were used. They were anesthetized with phencyclidine hydrochloride (2.0 mg/kg) and alpha-chloralose (80-100 mg/kg). The animals were ventilated using a positive pressure respirator (Bird Mark 7) while a bilateral thoractomy was performed at the level of the fifth intercostal space.

In all experiments requiring placement of the Walton-Brodie strain gauge arches to the endocardial surfaces, the animals were placed on total cardiopulmonary bypass. The dogs were heparinized using 250 units/kg. The blood was drained from the right ventricle through a three-eighths inch Tygon tubing inserted through a right atriotomy. Oxygenation was achieved by bubbling 100% oxygen through the blood in a Travenol 1½ liter miniprime bag. The blood was then returned to the animal through a cannula inserted into a femoral artery. Mean blood pressure was maintained between 90 and 120 mm Hg by a Sarns model 3500 portable pump. A suction tube, connected to a duplicate pump, was used to remove any blood that

collected within the chest cavity. The oxygenator bag was primed using a 6% dextran (M.W. 40,000) and Ringers-Locke solution. This solution was slightly hyperosmotic to blood and only a small amount of fluid had to be added to the oxygenator bag to maintain vascular volume. After the animal was placed on the cardiopulmonary bypass the positive pressure respirator was turned off and the lungs were allowed to collapse. The animal was maintained on bypass for the duration of the experiment ($1\frac{1}{2}$ -3 hours).

A left atriotomy was performed and several chordae tendineae of the mitral valve were transected. From one to four Walton-Brodie strain gauge arches were then sutured to the endocardium. Four separate left ventricular endocardial muscle segments, the free wall base, the free wall apex, the septal apex, and the septal base (Fig. 1) were studied. The size and shape of the papillary muscles determined the number of strain gauge arches which could be sutured to the endocardial surface. Large papillary muscles made it difficult to suture a gauge to the free wall apex. In a small heart gauges successfully placed on the free wall apex and the septal apex tended to interfere with each other. After the gauges were placed on the endocardium the left atriotomy was left open. A suction tube was placed in the chest cavity to remove any blood that collected there. Strain gauge arches were then sutured to the following left ventricular epicardial

muscle segments; anterior, posterior, lateral base and lateral apex. The lateral base and the lateral apex gauges were positioned as closely as possible directly over their respective endocardial counterparts. This allowed for direct comparison of innervation patterns of the basal and apical muscle segments.

In those experiments dealing with the relationship between electrical and mechanical events two types of electrical activity were recorded. In those experiments using the R-wave of the QRS complex as the reference for electrical activity the lead II ECG was recorded. To record the electrical activity from the muscle segments directly, a modified strain gauge arch was employed. An insulated silver wire was inserted through a hole in one leg of the strain gauge arch. This wire, which protruded one to two millimeters below the foot of the arch, was used to record the local unipolar electrogram.

The thoracic autonomic nerves were identified and dissected according to the description by Mizeres (40), Figures 2 and 3. The cervical vagi were sectioned but the sympathetic nervous system was left intact. The vagi were sectioned to eliminate the arrhythmias that developed when the animal was on cardiopulmonary bypass. The nerves were stimulated using stainless-steel Porter electrodes connected to a Grass model SD9 stimulator. The stimulation parameters, 4-6 volts, 10 hertz and 5 msec, were monitored

Left Ventricular Endocardium

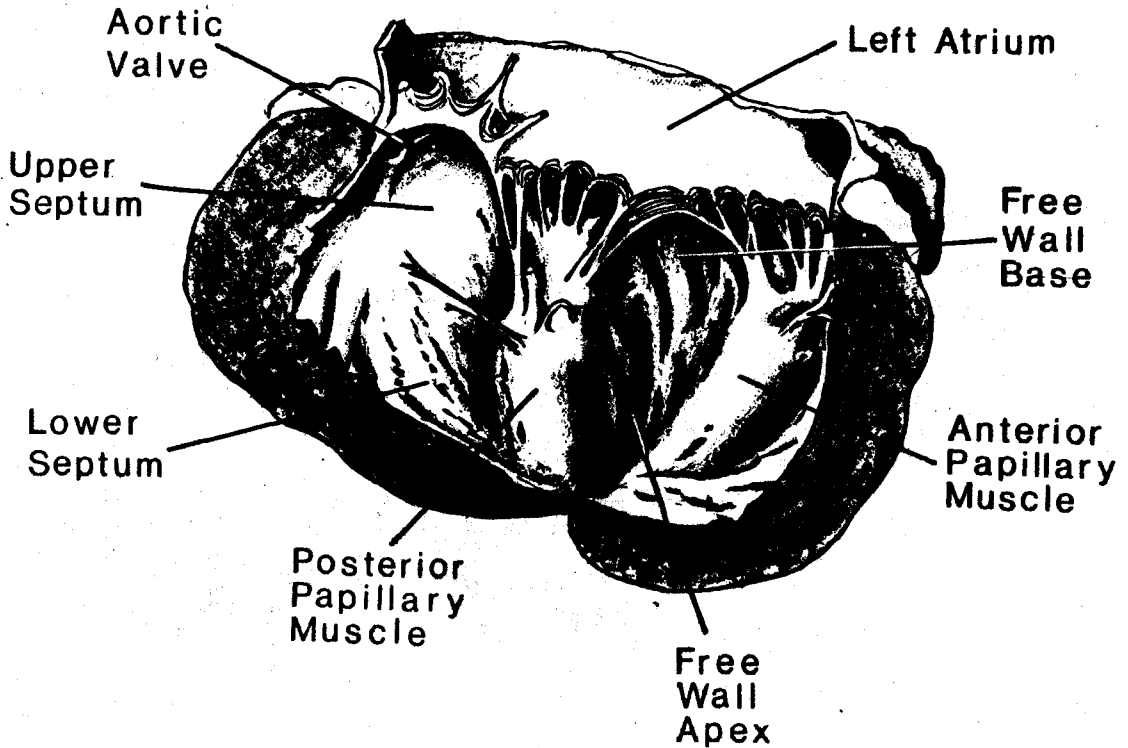


FIGURE 1

DRAWING OF THE LEFT VENTRICULAR ENDOCARDIUM

This view of the left ventricular endocardium shows the muscle areas studied. The heart was opened by cutting through the myocardium along the anterior descending artery. The areas labelled upper septum and lower septum are also referred to as the septal base and septal apex respectively.

using a Hewlett-Packard model 120B oscilloscope. Stimulation was maintained until maximal response was reached or for at least 20 seconds if no response to the stimulation was seen. Time duration between stimulation of the nerves was sufficiently long to allow for return to the control state of all muscle segments.

After all the nerves (Fig. 2 and 3) had been stimulated, atropine (2 mg/kg) was injected into the oxygenator bag to block the parasympathetic nervous system. Those nerves that induced cardiac slowing before atropine were then stimulated again. With the parasympathetic nervous system blocked, the stimulation of the nerves would result in stimulation of the sympathetic fibers in the nerve. As a result of this, the sympathetically induced changes in force and time intervals could be separated from the total response elicited by stimulation before atropine.

At the conclusion of the experiment the heart was opened and the placement of the endocardial strain gauges was confirmed. The recordings from any gauge that was improperly placed or tied down were discarded and not considered during the analysis of the data.

B. Walton-Brodie Strain Gauge Arch

The Walton-Brodie strain gauge arch used was a small U-shaped piece of brass with a variable resistor epoxied to its back surface. It measured eight millimeters

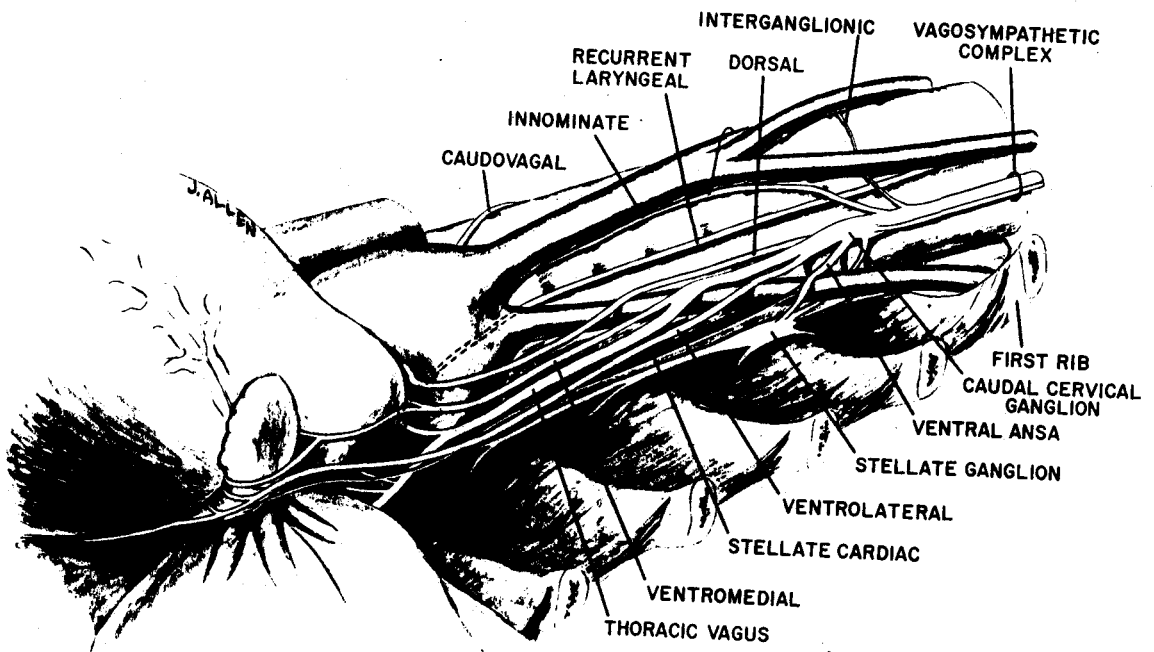


FIGURE 2

DRAWING OF THE THORACIC CARDIAC NERVES, LEFT SIDE

This drawing shows the anatomy of the left side thoracic autonomic nerves. The nerves are labelled according to Mizeres (40).

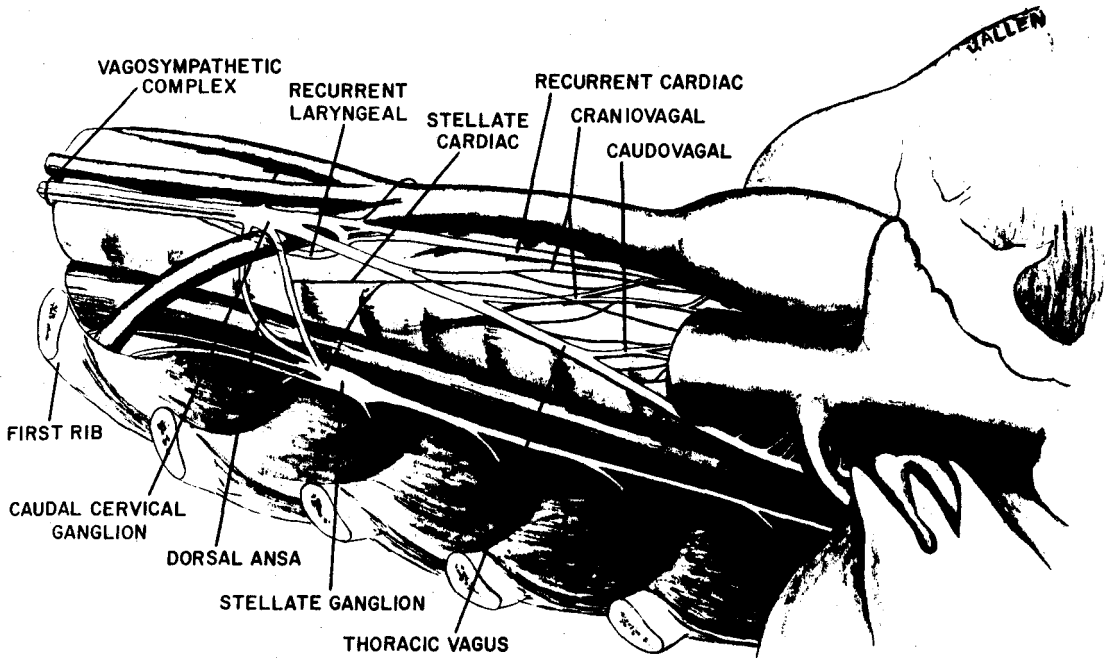


FIGURE 3

DRAWING OF THE THORACIC CARDIAC NERVES, RIGHT SIDE

This drawing shows the anatomy of the right side thoracic autonomic nerves. The nerves are labelled according to Mizeres (40).

long and three millimeters wide. The arch was sutured directly to the myocardium through two holes in each foot. The two sutures were placed approximately six millimeters apart so that when the gauge was tied down the muscle between the sutures was stretched. M. deV. Cotton and E. Bay (13) showed that to get maximal response from the gauge the muscle had to be stretched about 40 to 60% above the control length. Reeves and Hefner (67) in 1962 discovered that if the muscle stretch was greater than 25% over control length that there was damage done to the muscle segments. In a series of passive stretches they found that if the muscle was stretched out to more than 25% of its control length damage occurred to the muscle such that, when a second series of stretches was performed a diminution of passive tension was seen at any given length. In the present series of experiments attempts were made to keep muscle stretch to less than 30% of control.

The sutures on the epicardium were positioned such that the gauge was tied down parallel to the epicardial muscle fibers. The depth of the sutures was 1-2 millimeters. At this depth the muscle fibers are approximately parallel to the surface fibers. The endocardial gauges were also positioned parallel to the muscle fibers but the depth of the sutures could not be ascertained until the experiment was over. Usually the sutures were slightly

deeper than the sutures on the epicardium.

Shimosato, Herpfer and Etsten (80) examined the static and dynamic performance of the strain gauge arch. They studied the characteristics of both the enclosed gauge and the open gauge, which was similar to the ones used in these experiments. The dynamic characteristics were analyzed using a specialized piston pump. The static characteristics were studied by anchoring one end of the gauge and hanging weights on the other end. The two types of gauges studied were found to have similar characteristics in each of the tests. As a result, the following results and conclusions were considered valid for both types of gauges.

They found that in the static test the response of the strain gauge was linear over a range of zero to 300 gram load. They also showed that the stylus deflection of the weight recording was dependent upon the angle with which the force is applied to the gauge. The greater the angle between the gauge and the direction of force application the less the stylus deflection with a constant weight.

Studies using the piston pump showed that the gauges used had a flat response to 45 cycles per second. This is similar to the frequency response found for the gauges used in these experiments. The only parameter that had a major influence on the gauges was temperature. As

temperature was increased from 25 to 45°C, the baseline fell and the amplitude of the sinusoidal wave increased. This was reversible as temperature was decreased back to 25°C. The calibration curves did not change with temperature.

From these data the authors (80) concluded:

(1) the frequency response of the gauge was sufficient to record myocardial force as long as heart rate does not exceed 240 beats per minutes; (2) the validity of the data is temperature dependent; and (3) the orientation of the gauge on the heart can affect the results. By placing the gauge on the heart as described above, the conclusions of Shimosato et al., (80) were taken into account,

C. Analysis of the Data

1. Analysis of Force Changes

The strain gauge arch was connected to the Grass model 7 polygraph through a connector containing the other three resistors of the Wheatstone bridge. The preamplifier used was the Grass model 7P1.

Reeves, Hefner and co-workers (67, 68) pointed out that it is "impractical" to calibrate the strain gauge in situ. Because it is impossible to suture each gauge to a myocardial segment in exactly the same manner, with the sutures encompassing the same number of fibers and at the same tension, they concluded that the only valid comparison was between the percentage change for each gauge with

stimulation. Therefore, in these experiments, force data were presented by calculating the percentage change between the control state and the response to nerve stimulation. The control force was measured just before stimulation; the stimulation force was measured at the peak of the response or, if there was no change from control, the measurement was taken approximately 15 sec after initiation of stimulation. If the stimulation resulted in cardiac slowing, valid force measurements could not be made during the heart rate decrease. The time intervals between contractions varied from beat to beat resulting in unequal relaxation times. This variation in relaxation times accounts for the beat to beat change in force (See LTV in Fig. 9). As a result of the above problem the following procedure was used for measuring force during cardiac slowing. The percentage change in force was taken between the control force and the force of the first two beats following cessation of the stimulation when the heart rate had returned to control.

The percentage change in force was collected for each nerve stimulated and the mean and standard error were calculated. The analysis of variance, comparing all eight of the muscle segments investigated, was calculated for each nerve stimulated.

2. Analysis of Time Intervals

(a) R-wave Reference

In this series of experiments the Lead II ECG was recorded simultaneously with the strain gauge arch recordings. The coupling interval between electrical activation and mechanical activity was taken as the interval from the beginning of the upstroke of the R-wave to the beginning of the upstroke of the force recording. This interval was measured for three separate beats during control and three separate beats during stimulation. These three intervals were then averaged and recorded. At a paper speed of 100 mm/sec the intervals could be measured with accuracy to 5 msec.

It was noticed in the early experiments that sometimes the time interval would change drastically during stimulation, in some instances the change approached 100 msec. When this happened the shape of the R-wave also was seen to change. As a result of this observation care was taken to measure the intervals using R-waves of similar shape and duration during control and stimulation. If no R-wave during stimulation was found which resembled the control R-wave the stimulation was repeated. If an R-wave during stimulation similar to those during control could not be found, the intervals measured during that stimulation were not used.

After the time intervals were measured they were

collected and statistically analyzed in the following manner. The control and stimulation time intervals for each muscle segment for each nerve stimulation were analyzed using the paired t-test. Since the control intervals were measured before each nerve stimulation, they could be analyzed in this manner.

The control electromechanical (EM) coupling intervals of the eight muscle segments analyzed for each nerve stimulated were statistically compared using the analysis of variance. The EM coupling intervals during stimulation also were analyzed using the analysis of variance.

(b) Left Ventricular Anterior Electrogram
Reference

Two different series of experiments using local unipolar electrograms were conducted. In both series the reference electrical activity was that of the left ventricular anterior muscle segment. The electrical activity of this area was used as the reference for two reasons:

1. Lewis and Rothschild (38) showed that the anterior epicardial surface was one of the first epicardial areas to be electrically activated.
2. The gauge was easily sutured to the anterior segment and good clean records were assured.

In both series of experiments up to four strain

gauges with the electrodes inserted through the foot could be sutured to the heart in any given dog. In all experiments both the electrical and mechanical activity was amplified using the Grass model 7 polygraph with the model 7P1 preamplifiers. In some experiments the output of the amplifiers was recorded using the Midwest Optical Oscillograph model 591 with optical galvanometers flat to 3 kilohertz on photographic paper. Comparisons of time intervals recorded using the two recording systems were in good agreement. The wave forms were also identical. Because of these two facts the time intervals measured from the polygraph paper and the intervals measured from the optical recorder were averaged together.

Figure 4 illustrates the various time intervals measured and analyzed. The electrical-electrical coupling interval is the time from the first positive deflection in the left ventricular anterior (LVA) electrogram to the first positive deflection in the electrogram recorded from another muscle segment. The time interval from the first positive deflection in the LVA electrogram to the onset of mechanical activity in any muscle segment will be called the sequence interval. The electromechanical coupling interval is the time between the first positive deflection in an electrogram from a muscle segment and the onset of mechanical activity in that muscle segment.

Unipolar electrograms present problems in that it

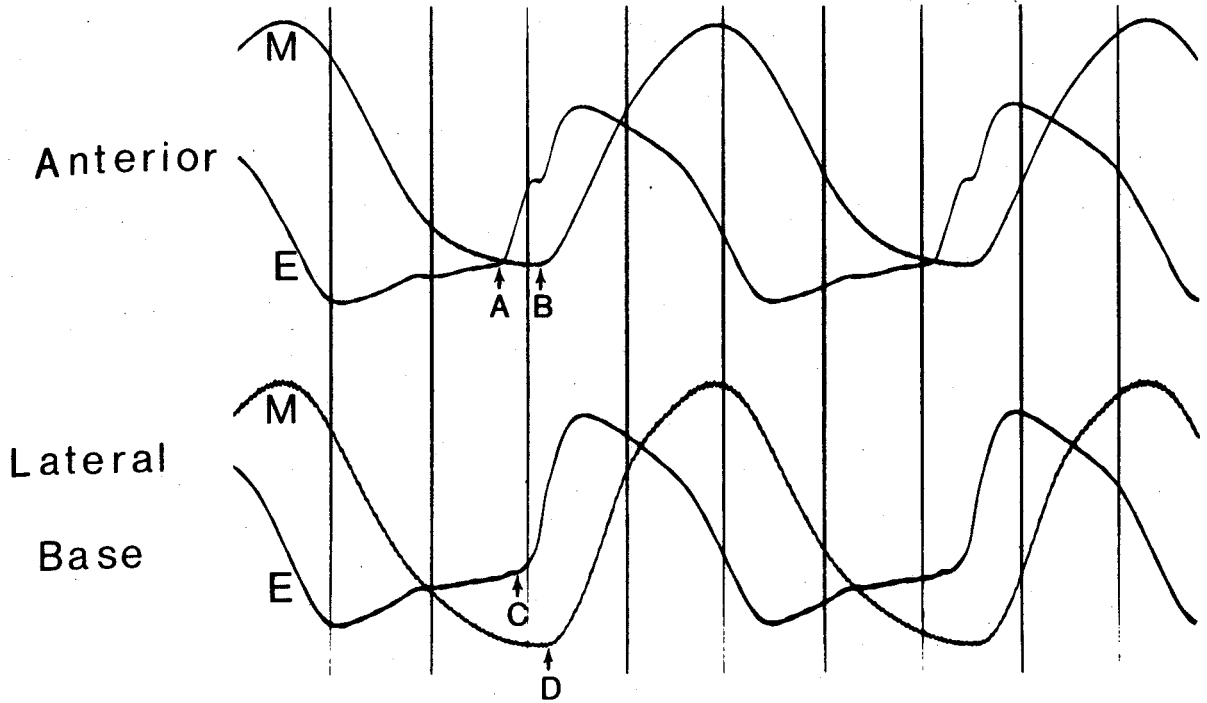


FIGURE 4

MEASURED TIME INTERVALS

This figure illustrates the various time intervals measured using the local electrograms as the reference. The electrical-electrical time interval was measured from the upstroke in the electrogram of the anterior segment (A) to the upstroke in the electrogram of one of the other segments studied (C). The electro-mechanical coupling interval was measured from the upstroke in the electrogram from a muscle segment to the onset of mechanical activity in that same segment. In the anterior segment the time between A and B and in the lateral base the time between C and D are the respective electro-mechanical intervals.

is difficult to differentiate between the extrinsic and intrinsic excitation. Lewis (37) defined the extrinsic deflection as the activation of the electrode by the approaching wavefront which has not yet activated the tissue under the electrode. The intrinsic deflection occurs when the tissue directly under the electrode is electrically activated. Several investigators (74, 83) have attempted to relate the bipolar electrogram and transmembrane potentials to various parts of the unipolar electrogram. No specific part of the unipolar electrogram could be found to correlate with either of the intrinsic or extrinsic electrical activation. Because the intrinsic activation cannot be easily found in the unipolar electrogram, an arbitrary point was picked in the electrogram for the reference point. The first positive deflection was chosen as the point in the electrogram to measure from. Also the wave form had to be the same before and during stimulation for the interval measurements to be included. The data were analyzed as described for the R-wave analysis. The paired t-test and analysis of variance were performed on the E-E interval, the E-M interval and the sequence interval.

This setup and analysis was used for two series of experiments. In one series the strain gauges were only applied to the epicardium. Following stimulation of the left and right stellate ganglia, norepinephrine (1 γ /kg)

and calcium ($\frac{1}{4}$ gm) were injected. The right atrium was then paced at 175, 200 and 225 beats per minute. Following the injection of propranolol (0.5 mg/kg) the norepinephrine and then the calcium were injected again.

In the second series of experiments the strain gauge arches were sutured to both the endocardium and the epicardium. The small thoracic autonomic nerves were stimulated before and after atropine (2 mg/kg).

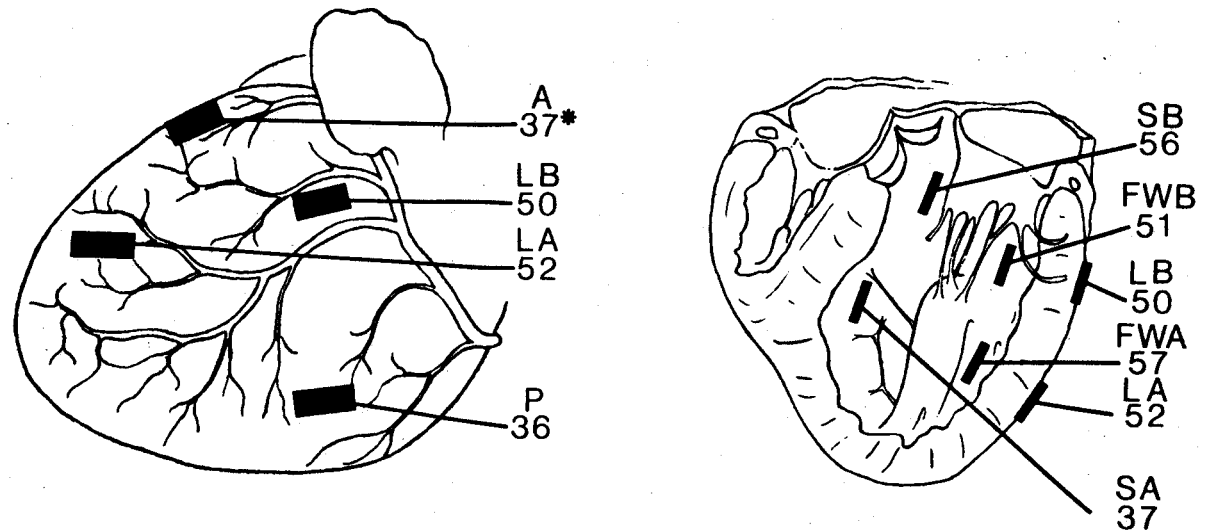
CHAPTER IV

RESULTS

A. Control Time Intervals

Several different control time intervals were measured including: (1) the interval between the R-wave upstroke of the ECG to the onset of mechanical activity in each of the muscle segments studied; (2) the interval between the first positive deflection in the local electrogram to the onset of mechanical activity in each muscle segment; (3) and the interval between the first positive deflection in the LVA electrogram to the first positive deflection in the electrogram from one of the other muscle segments. Figure 5 illustrates the average control time interval using the R-wave as the reference electrical activity. This time interval is the time between the upstroke of the R-wave of the ECG and the onset of mechanical activity of the respective muscle segments. A total of 434 different control intervals were analyzed using the analysis of variance. Table I lists the complete analysis showing the significances between the intervals. The muscle segments studied are the anterior (A), lateral base (LB), lateral apex (LA) and the posterior (P) areas of the epicardium and the septal base (SB), septal apex (SA), free wall base (FWB) and the free wall apex (FWA)

Sequence of Muscle Segment Contraction



*Time in msec from R-wave upstroke

FIGURE 5

CONTROL R-WAVE TO MECHANICAL ONSET TIME INTERVALS

This figure shows the time interval in msec between the R-wave upstroke to the onset of mechanical activity in the following left ventricular epicardial and endocardial areas; anterior (A), lateral base (LB), lateral apex (LA), posterior (P), free wall base (FWB), free wall apex (FWA), septal base (SB) and septal apex (SA). The statistical analysis for this data is shown in Table I.

TABLE I
R-WAVE TO MECHANICAL ONSET TIME INTERVALS

N = 434
SD = 16.3

	A	LB	LA	P	FWA	FWB	SB
	37	50	52	36	57	51	56
LB 50	**						
LA 52	**	0					
P 36	0	**	**				
FWA 57	**	*	0	**			
FWB 51	**	0	0	**	0		
SB 56	**	*	0	**	0	0	
SA 37	0	**	**	0	**	**	**

*P<0.05

**P<0.01

0 Not significantly different

This table shows the results of the analysis of variance of the control time intervals in milliseconds from the R-wave upstroke to the onset of mechanical activity in a muscle segment. The left ventricular muscle segments studied are the anterior (A), lateral base (LB), lateral apex (LA) and posterior (P) areas of the epicardium and the free wall apex (FWA), free wall base (FWB), septal base (SB) and septal apex (SA) areas of the endocardium. The asterisks indicate whether the differences between the means are significantly different. N is the total number of observations analyzed. SD is the standard deviation of the analysis.

of the endocardium.

In the non-stimulated heart, the anterior (37 msec) and posterior epicardium (36 msec) and septal apex (37 msec) all began to contract simultaneously. The lateral base (50 msec) was the next segment to contract. The difference between the onset of contraction by the lateral base and the first three areas to contract was significant ($P < 0.01$). The intervals for the lateral base, lateral apex (51 msec) and the free wall base (52 msec) were not significantly different ($P > 0.05$) from each other. The free wall apical muscle segment interval (57 msec) was not different from the free wall base and the lateral apex but was different ($P < 0.05$) from the lateral base. The septal base interval (56 msec) contracts at the same time as the free wall apex.

The sequence of electrical activation using unipolar electrodes was determined by measuring the electrical to electrical time interval. Figure 6 and Table II show the time interval from the LVA electrical to the electrical activity in the other muscle segments. These intervals were measured from the first positive deflection in the LVA electrogram to the first positive deflection in the electrogram from one of the other segments studied. The septal apex was the first area to be electrically activated ($P < 0.01$) 8.5 msec before the reference area, the anterior epicardium of the left ventricle. The septal base (-2.7 msec) and the

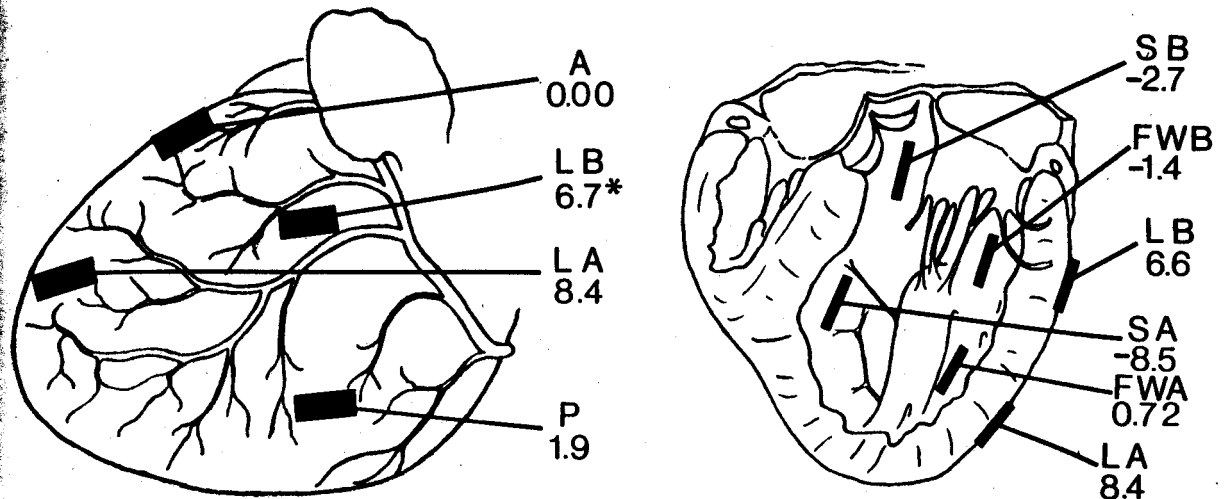
free wall base (-1.4 msec) were excited at the same time and slightly before the anterior segment. Following the anterior area the next area excited was the final endocardial area, the free wall apex (0.7 msec). This area was excited at the same time as the free wall base ($P > 0.05$ significance between the means) but was activated after the septal base ($P < 0.01$). The posterior muscle segment was excited next (1.9 msec). This was not significantly different from the free wall apex. The last two areas to be electrically activated were the lateral base (6.6 msec) and the lateral apex (8.4 msec). Both of these time intervals, which were not different from each other ($P > 0.05$), were significantly longer ($P < 0.01$) than all the other intervals.

Lewis and Rothschild (38) and Scher and Young (77), found similar activation patterns of the canine ventricle using both unipolar and bipolar electrodes.

Both lateral epicardial areas were excited after their underlying endocardial segments ($P < 0.01$). However, there was no significant difference ($P > 0.05$) between the R-wave to mechanical onset interval for the basal areas or the apical areas.

Because of this dichotomy between the onset of mechanical activity and the onset of electrical activity, as seen in Figures 5 and 6, the electromechanical coupling interval was studied. Figure 7 and Table III show the

Electrical-Electrical Time Interval



*Time in msec

FIGURE 6

CONTROL ELECTRICAL-ELECTRICAL COUPLING INTERVALS

This figure shows the time interval in msec between the upstroke in the electrogram in the anterior (A) segment and the upstroke in the electrogram in the seven other segments studied. See Figure 5 for an explanation of the abbreviations. The negative signs indicate that those segments were electrically activated before the anterior segment.

TABLE II
ELECTRICAL-ELECTRICAL COUPLING INTERVALS

N = 326
SD = 6.4

	LB	LA	P	FWB	FWA	SA
	6.7	8.4	1.9	-1.4	0.7	-8.5
LA 8.4	0					
P 1.9	**	**				
FWB -1.4	**	**	*			
FWA 0.7	**	**	0	0		
SA -8.5	**	**	**	**	**	
SB -2.7	**	**	**	0	**	**

*P<0.05

**P<0.01

0 Not significantly different

This table shows the results of the analysis of variance of the electrical-electrical coupling time interval. This time interval is measured, in milliseconds, from the first positive deflection in the LVA electrogram to the first positive deflection in the electrogram from a second muscle segment. A negative number indicates that segment was electrically excited before the LVA. The asterisks indicate whether the difference between the means is significant. See Table I for an explanation of the abbreviations.

time interval between the first positive deflection in the electrogram from a muscle segment and the onset of mechanical activity in that segment. This interval is called the electromechanical coupling interval (EM). Three of the four epicardial muscle segments have the same EM coupling interval. The anterior (50 msec), lateral base (50 msec) and lateral apex (48 msec) all have the same EM interval. Only the posterior segment (57 msec) of the epicardium has a longer ($P < 0.01$ anterior and lateral apex, $P < 0.05$ lateral base) EM coupling interval. Of the four endocardial areas only the septal apex EM coupling interval (51 msec) was not different from the four epicardial intervals. The septal base (73 msec) has the longest EM interval ($P < 0.01$) of all the segments studied. The EM intervals of the free wall base (66 msec) and the free wall apex (64 msec) were both significantly different ($P < 0.01$) from their respective overlying epicardial segments.

Using the R-wave as the reference electrical activation, the two free wall basal segments and the two free wall apical segments each begin to contract at the same time. However, using the LV anterior electrical activation as the reference point, summation of the E-E coupling interval and the EM coupling interval gives a slightly different relationship. The summation results in the following lapse intervals: lateral base contraction

Electromechanical Coupling Interval

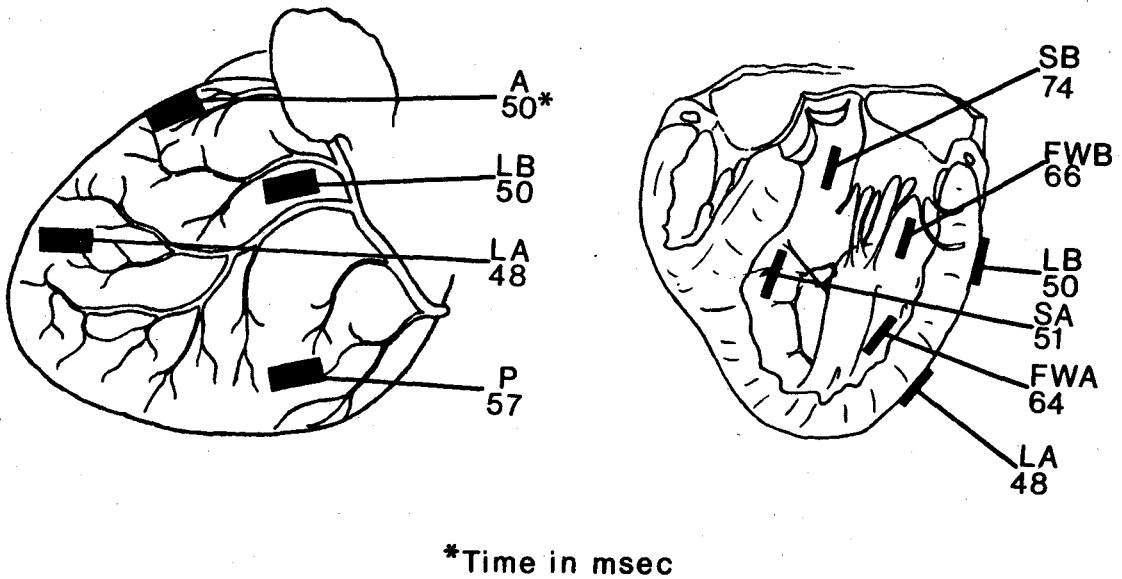


FIGURE 7

CONTROL ELECTROMECHANICAL COUPLING INTERVALS

This figure shows the control electromechanical coupling intervals for the eight muscle segments studied. The electromechanical coupling interval is the time between the first positive deflection in a local electrogram from a muscle segment and the onset of mechanical activity in that segment. See Figure 5 for an explanation of the abbreviation.

TABLE III
ELECTROMECHANICAL COUPLING INTERVALS

N = 420
SD = 13.7

	A 50	LB 50	LA 48	P 57	FWB 66	FWA 64	SA 51
LB 50	0						
LA 48	0	0					
P 57	**	*	**				
FWB 66	**	**	**	**			
FWA 64	**	**	**	*	0		
SA 51	0	0	0	0	**	**	
SB 74	**	**	**	**	**	**	**

*P<0.05

**P<0.01

0 No significance

This table shows the analysis of variance of the time interval from the first positive deflection in the electrogram from a muscle segment to the onset of mechanical activity in that segment. The times are in msec. See Table I for explanation of the abbreviations.

and the free wall base contraction begin 56 msec and 65 msec after the electrical activation of the LVA. The lateral apex and the free wall apex contractions begin 57 msec and 65 msec after the LVA. Both of the endocardial segments contract simultaneously; the epicardial segments contract simultaneously but 8 msec before the endocardial segments.

B. Heart Rate and Force Changes During Autonomic Stimulation

Stimulation of the autonomic cardiac nerves results in a heart rate change, a force change or both. Figure 8 shows the heart rate changes due to stimulation of the thoracic autonomic nerves. The figure shows the control rate, from zero to the end of the enclosed bar, and the rate during stimulation, from zero to the end of the open bar. The black bar columns are the heart rates before the injection of atropine. The black and white striped bar columns are the heart rates after atropine. The data were analyzed using the paired t-test. The asterisks at the left end of the bar graphs indicate the significant differences between the control rate and the stimulation rate. The data are presented in Tables A-1 and A-2 in the Appendix.

The cervical vagi were cut and the sympathetics left intact for all stimulations. Before atropine only the left stellate (LSS), right stellate (RSS), ventral

HEART RATE

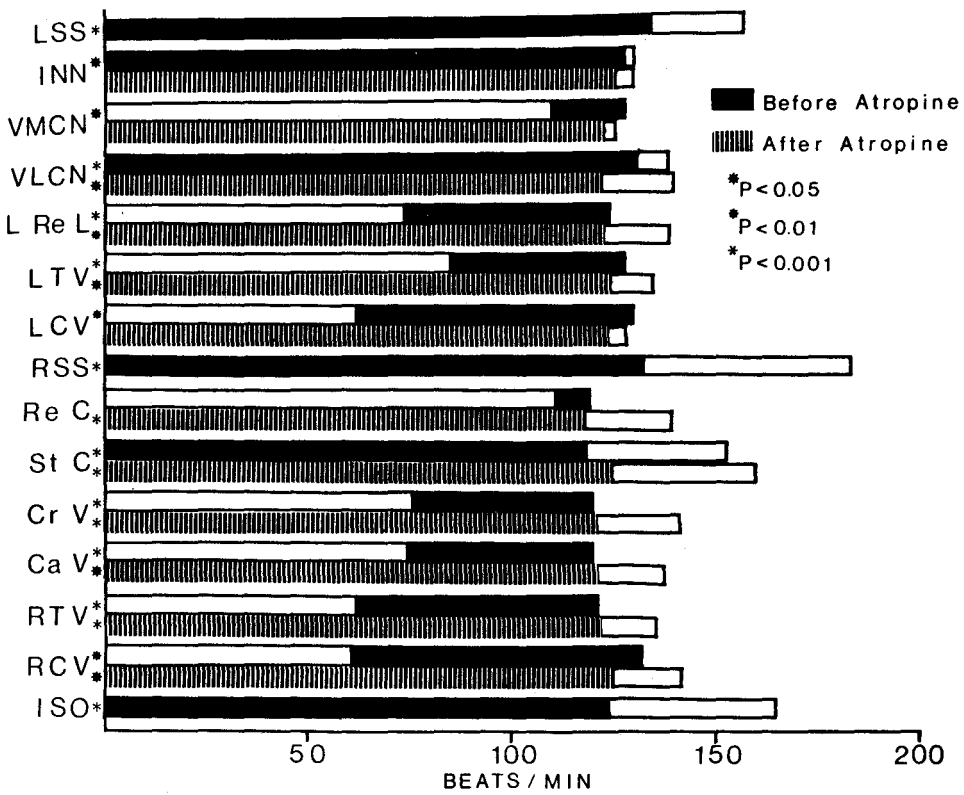


FIGURE 8

HEART RATE: CONTROL AND STIMULATION

FIGURE 8

LEGEND

Figure 8 is a bar graph showing the heart rate during control and during stimulation for each of the nerve stimulations. The control rate is represented by the length of the enclosed bar; the stimulation rate is represented by the bar from zero to the end of the open bar. For example, left stellate control rate is 135 beats/min and the rate during stimulation is 157 beats/min. The totally black bar shows the control and stimulation rates before atropine. The black and white striped bar shows the control and stimulation rates after atropine. The significant differences between the means, as calculated using the paired t-test, are shown to the left of the bar graph.

LSS	Left Stellate Ganglion
INN	Innominate Nerve
VLCN	Ventral Lateral Cervical Cardiac Nerve
VMCN	Ventral Medial Cervical Cardiac Nerve
L Re L	Left Recurrent Laryngeal Nerve
LTV	Left Thoracic Vagus Nerve
LCV	Left Cervical Vagus Nerve
RSS	Right Stellate Ganglion
Re C	Right Recurrent Cardiac Nerve
St C	Right Stellate Cardiac Nerve
Cr V	Cranial Vagus Nerve
Ca V	Caudal Vagus Nerve
RTV	Right Thoracic Vagus Nerve
RCV	Right Cervical Vagus Nerve
ISO	Isoproterenol (1 γ /kg)

lateral cervical cardiac nerve (VLCN), innominate nerve (INN) and the right stellate cardiac nerve (St C) stimulations resulted in significant increases in heart rate. The stimulation of the rest of the thoracic cardiac nerves caused a significant decrease in heart rate. Recurrent cardiac (Re C) stimulation caused only minimal slowing ($P < 0.1$). Following the injection of atropine none of the stimulations elicited a slowing of cardiac rate. With the exception of the ventral medial cervical cardiac nerve (VMCN), INN and the left cervical vagus (LCV), the rest of the stimulations cause significant increases in cardiac rate. Isoproterenol injection ($1\gamma/\text{kg}$) also elicited a significant increase in heart rate.

Figures 9, 10 and 11 are recordings from a typical experiment. The responses of the different areas to left side thoracic cardiac nerve stimulations are shown in Figure 9. The VMCN and INN stimulation did not cause any change in force in the left ventricle in this particular experiment. The INN stimulation did cause an increase in force in the sinus region of the right ventricle. Stimulation of either the LSS or the VLCN caused a generalized force increase throughout the left ventricle. Comparison of the endocardial and epicardial force recordings from both the lateral base and lateral apex during both LSS and VLCN stimulation showed a greater force increase in the endocardial segments than in their respective overlying

epicardial segments. Stimulation of the left thoracic vagus first caused cardiac slowing. When the stimulation was turned off and the rate returned to normal, the lateral apex endocardium and epicardium, the anterior and the posterior force recordings were depressed compared to control. The lateral base endocardium and epicardium and the right ventricular sinus all showed a greater force following stimulation.

Stimulation of the right side thoracic nerves elicited the same types of changes and are shown in Figure 10. Right stellate (RSS) and stellate cardiac (St C) stimulation increased both the rate and force. During RSS stimulation the larger force increases occurred in the anterior and the lateral base epicardium and endocardium of the left ventricle and the right ventricular sinus. As with the left stellate the endocardial force increased more than the epicardial force in the lateral base. However, in the lateral apex the force increase was the same for endocardium and the epicardium. In this experiment, stimulation of the rest of the right side nerves caused cardiac slowing. When the stimulation of the recurrent cardiac (Re C), cranial vagus (Cr V) and the caudal vagus (Ca V) was turned off, the rate returned to a level higher than control. The rate eventually returned to control. The force recorded from some of the muscle segments also increased to a level higher than

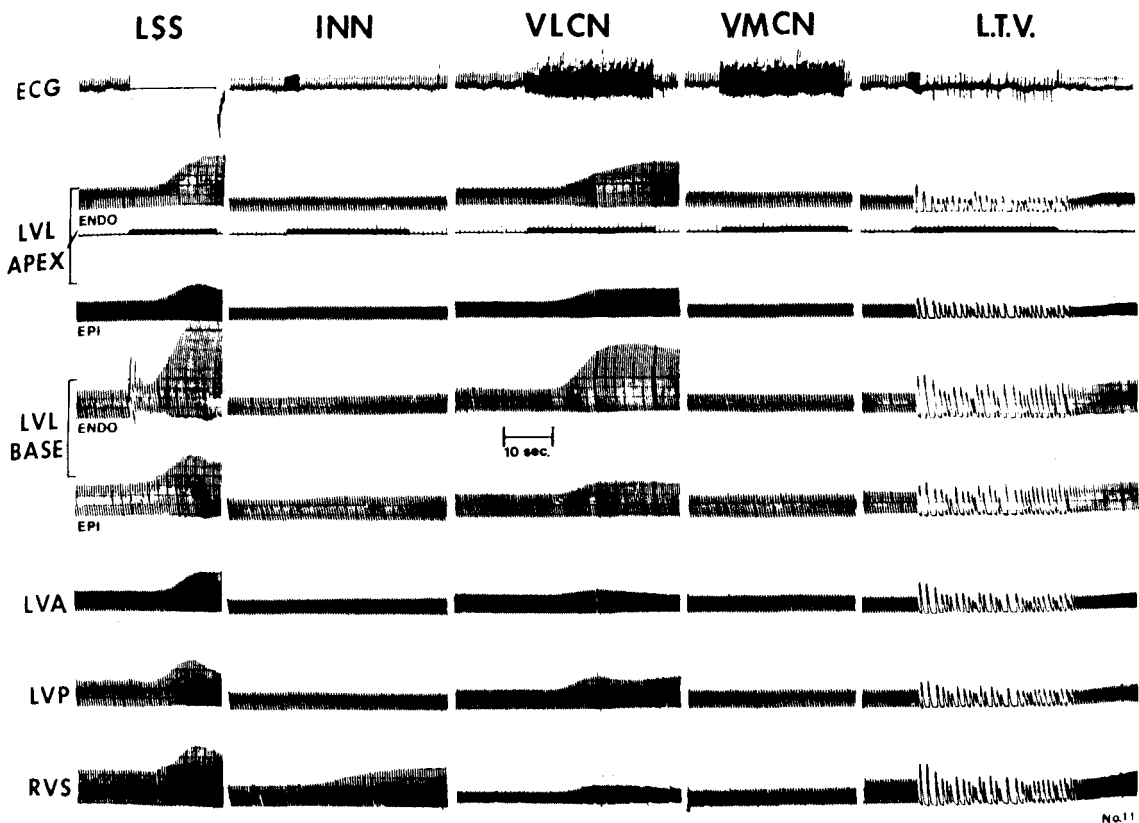


FIGURE 9

TYPICAL FORCE RECORDING, LEFT SIDE NERVE STIMULATIONS

This figure shows typical recordings of force changes during stimulation of the left side cardiac nerves. The nerves stimulated were the left stellate ganglion (LSS), innominate nerve (INN), ventral lateral cervical cardiac nerve (VLCN), ventral medial cervical cardiac nerve (VMCN), and left thoracic vagus (LTV). The recordings are, from top to bottom, Lead II electrocardiogram (ECG), left ventricular lateral apex endocardium and epicardium (LVL apex), left ventricular lateral base endocardium and epicardium (LVL base), left ventricular anterior (LVA), left ventricular posterior (LVP) and right ventricular sinus (RVS).

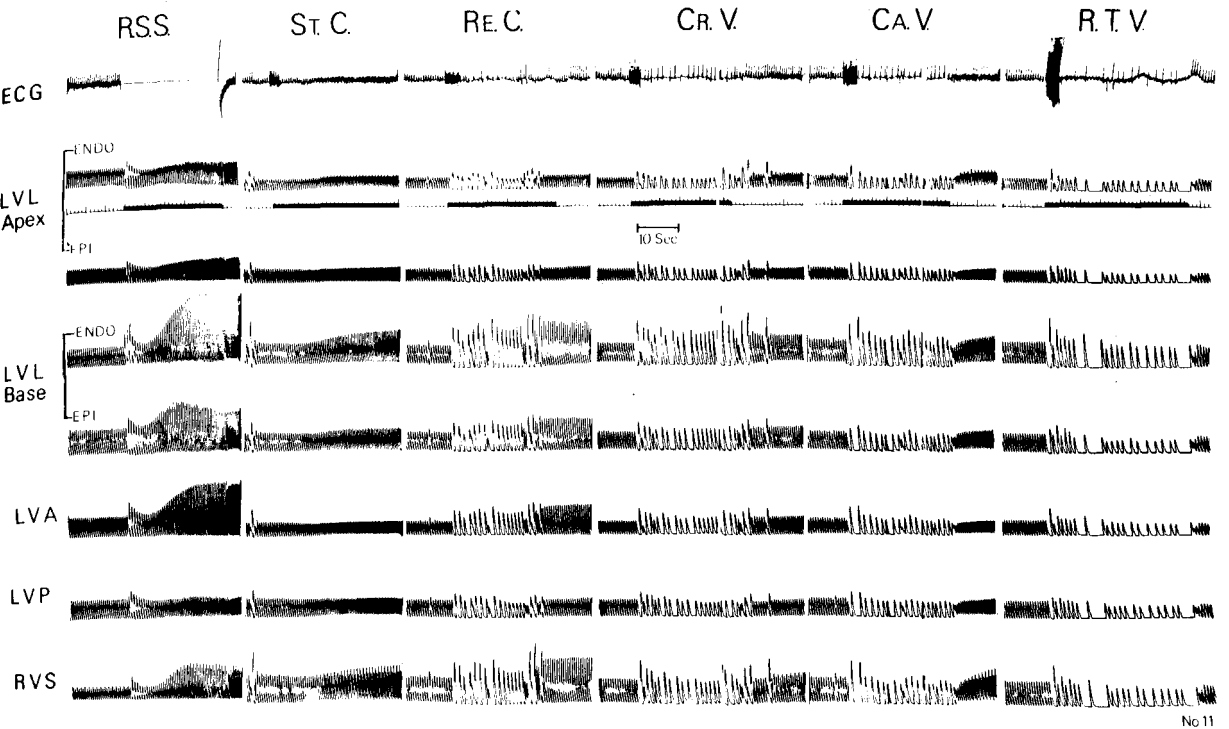


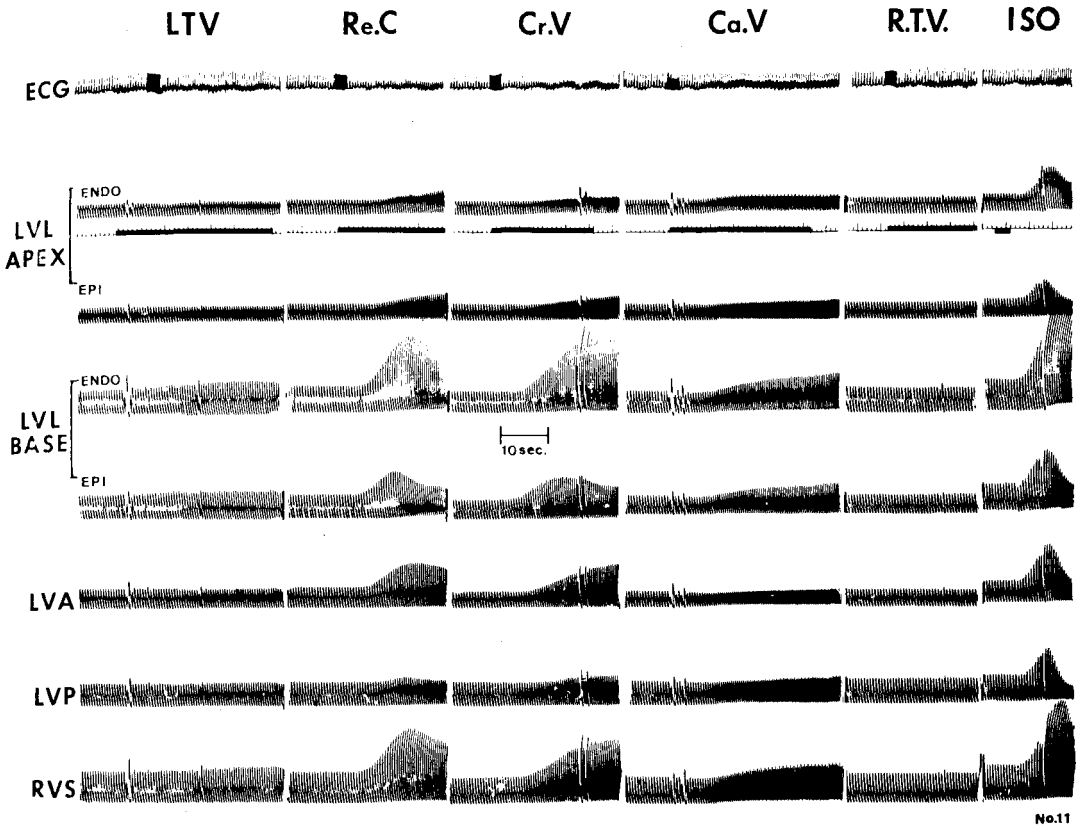
FIGURE 10

TYPICAL FORCE RECORDINGS, RIGHT SIDE NERVE STIMULATIONS

This figure shows the force recordings before and during stimulation of the right side cardiac nerves. The nerves stimulated were the right stellate ganglion (RSS), right stellate cardiac nerve (St C), recurrent cardiac (Re C), cranial vagus (Cr V), caudal vagus (Ca V) and right thoracic vagus (RTV). See Figure 9 for explanation of the designations of the force recordings.

control. This was seen especially in the LV lateral base endocardium and epicardium, LV anterior and RV sinus following Re C stimulation. The first two beats in all muscle segments following cessation of stimulation of the Ca V are an example of the depression of force as a result of stimulation of the parasympathetic fibers in that nerve. This same type of depression is seen following RTV stimulation. This same depression could be shown during ventricular pacing but the ventricles were not paced in these experiments.

Atropine is a muscarinic blocker and therefore blocks the parasympathetic component in the responses to nerve stimulation. Figure 11 shows the result of stimulation following atropine injection (2 mg/kg) of those nerves which contained a high number of parasympathetic fibers as seen by cardiac slowing during stimulation before atropine (Figures 9 and 10). Stimulation of either the left or right thoracic vagi was ineffective in changing force. In this particular experiment there was a large increase in rate with Re C, Cr V and Ca V nerves. Along with the rate changes contractile force in all muscle segments increased during Re C and Cr V stimulation. Ca V stimulation caused force increases only in the lateral base endocardium and epicardium and the right ventricular sinus. In contrast, injection of isoproterenol (1 γ /kg) directly into the aorta resulted in force increases in all



No.11

FIGURE 11
 TYPICAL FORCE RECORDINGS, PARASYMPATHETIC
 NERVES AFTER ATROPINE

This figure shows the force recordings following atropine injection (2 mg/kg) before and during stimulation of those nerves which caused cardiac slowing before atropine. See Figures 9 and 10 for an explanation of the abbreviations.

segments studied. As with the LSS stimulation the force increases in the two endocardial areas were greater than in their respective overlying epicardial segments.

The analyses of variance of the force changes induced by cardiac nerve stimulation are shown in Table IV. The table lists the mean percentage change for each area that occurred with the respective nerve stimulation. The number directly below the percentage change is the number of observations included in the mean. The analysis of variance was applied to all eight muscle segments for each nerve stimulation. The standard deviation of each analysis is given at the bottom of the respective column. Control force was taken as 100%. The analysis of variance calculates the probability that the difference between the mean percentage change for one segment and the mean percentage change for another segment is due to the experimental procedure. The results of the analyses of variance are shown in Figures 12 through 16. Only those pairs of mean percentage changes that were significantly different are shown in the Figures 12 through 16. Any pairs of muscle segments that are not shown did not have significantly different mean force changes with stimulation.

Four different views of the heart are used in Figures 12 through 16. Figure 12E is the left lateral view of the epicardium. Figure 12A is a frontal section of the heart showing the endocardial surface of the

TABLE IV
CONTRACTILE FORCE CHANGES

	<u>LSS</u>	<u>INN</u>	<u>VMCN</u>	<u>L Re L</u>	<u>VLCN</u>	<u>LTV</u>	<u>LCV</u>
Anterior	204.4	118.0	111.4	136.5	143.2	74.5	71.8
	25	24	24	19	24	24	5
Posterior	277.1	116.1	101.1	123.7	242.9	73.3	86.8
	16	16	17	12	16	15	4
Lateral Base	250.3	135.3	115.3	135.9	174.7	71.7	69.5
	24	23	23	17	23	23	4
Free Wall Base	340.0	124.0	113.7	143.3	276.4	71.8	66.8
	21	20	21	15	21	20	5
Septal Base	259.5	111.4	125.8	139.2	159.6	84.1	74.2
	26	18	26	9	25	16	13
Lateral Apex	227.4	115.0	103.5	125.4	212.2	75.2	66.8
	17	15	18	10	17	16	4
Free Wall Apex	329.9	112.3	116.3	131.9	233.0	85.7	67.0
	21	18	22	14	21	20	84
Septal Apex	267.9	128.9	123.2	166.4	171.4	78.6	72.9
	20	15	16	5	19	11	11
S. D.	106.7	34.4	41.9	76.4	73.7	25.5	22.7
	<u>RSS</u>	<u>St. C</u>	<u>Re C</u>	<u>Cr V</u>	<u>Ca V</u>	<u>RTV</u>	<u>RCV</u>
Anterior	221.0	128.6	181.4	98.0	75.3	73.9	75.7
	25	14	26	22	22	16	7
Posterior	198.6	116.8	146.7	78.9	73.4	75.1	80.8
	14	10	14	14	13	8	6
Lateral Base	255.8	127.4	192.3	89.8	70.2	70.1	91.1
	24	14	25	20	20	15	6
Free Wall Base	301.2	119.0	198.1	95.3	70.2	50.8	63.3
	21	12	20	18	18	12	7
Septal Base	209.3	113.8	154.3	92.8	77.9	78.9	75.8
	25	9	27	18	18	14	13
Lateral Apex	220.3	125.1	150.6	87.2	79.6	76.8	76.7
	17	10	16	14	14	9	6
Free Wall Apex	251.1	132.9	186.6	94.4	91.5	88.4	81.0
	21	11	22	19	19	13	6
Septal Apex	184.2	106.4	150.1	98.0	84.6	63.1	75.6
	20	7	19	11	11	8	11
S. D.	88.0	38.0	65.0	36.9	28.2	29.6	34.7

TABLE IV

LEGEND

Table IV shows the contractile force for each muscle segment as a percentage of control. Control is taken as 100%. Those percentages greater than 100% mean an increase of contractile force occurred with stimulation. A percentage less than 100% indicates that contractile force decreased with stimulation. Directly under each mean value is the number of observations that are included in the mean. The data were analyzed using the analysis of variance for each nerve stimulation. The standard deviation of each analysis is shown at the bottom of each column. See Figure 9 for an explanation of the abbreviations.

LEFT STELLATE GANGLION

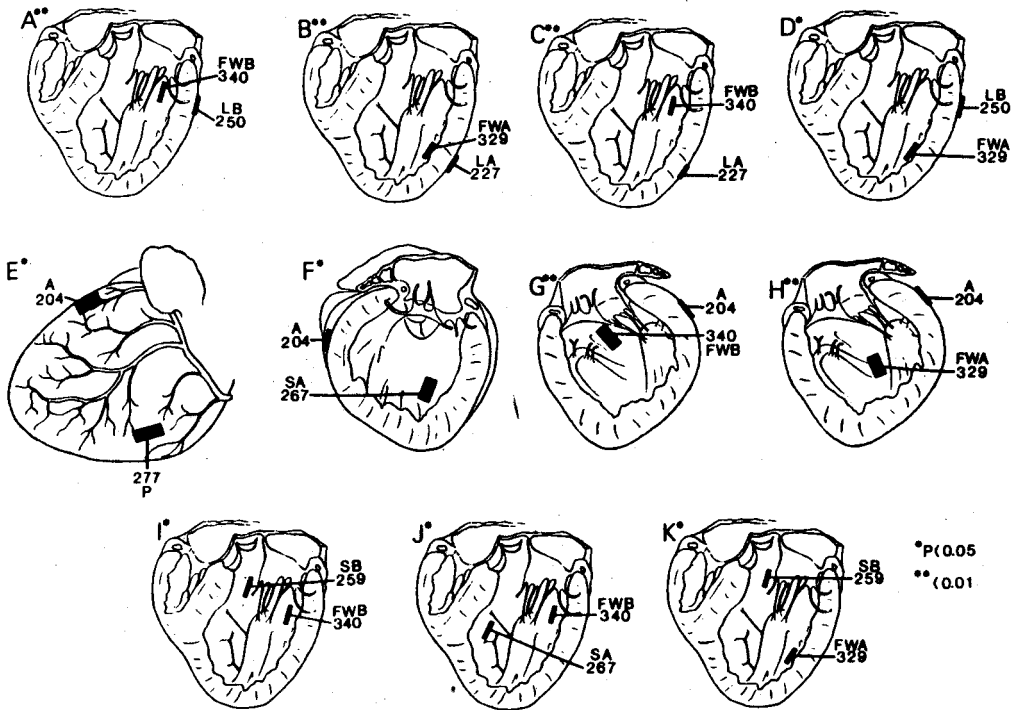


FIGURE 12

FORCE COMPARISONS DURING LEFT STELLATE
GANGLION STIMULATION

Figure 12 shows the results of the analyses of variance of the force changes due to left stellate ganglion stimulation. Each drawing shows a pair of means that are significantly different. The eight muscle segments are the anterior (A), lateral base (LB), lateral apex (LA) and posterior areas of the epicardium and the septal apex (SA), septal base (SB), free wall base (FWB) and the free wall apex (FWA) areas of the endocardium. The asterisks indicate if the difference between the means is significant at the 0.05 level (*) or the 0.01 level (**). See Table IV for the complete list of mean percentage changes.

right ventricle, interventricular septum and the endocardium of the left ventricle with the posterior papillary muscle. Figure 12F is a drawing of the interventricular septum. Figure 12G is a drawing of the interpapillary muscle free wall of the left ventricular endocardium.

Figure 12 shows the results of the left stellate ganglion stimulation (LSS). Each drawing shows two muscle segments which had significantly different mean increases in contractile force. For example, in Figure 12A the free wall base (FWB) had a total contractile force of 340% and the lateral base (LB) had a total contractile force of 250%. These were 240% and 150% above control (100%). As can be seen from the figure the increase in the FWB was statistically greater ($P < 0.01$) than the increase in the LB with LSS stimulation. Drawings 12A and 12B show that the relationships described in Figure 8 between the endocardium and epicardium of the lateral wall base and apex contractile force changes were statistically significant ($P < 0.01$) for both comparisons. Each of the lateral wall endocardial segments showed a greater force increase than their respective overlying epicardial segments. The anterior force increase was significantly less ($P < 0.05$) than the force increases in either the posterior or septal apex muscle segments (Drawings E and F). Drawings C, D and G through K show that the free wall base (FWB) and the free wall apex (FWA) each increase in contractile force more

than most of the muscle segments studied except the posterior segment. Also, the free wall apex and septal apex contractile force increases were not significantly different.

The analyses of variance of the force changes during RSS stimulation resulted in fewer pairs of means that were significantly different. Figure 13 illustrates those pairs. The free wall base had the largest increase in force with stimulation and that increase was significantly different ($P < 0.01$) from the rest of the force increases except for the overlying lateral base and the free wall apex (Drawings C-G). It can be seen in Drawings A and B that the septal apex, which had the smallest force increase, increased less than the free wall apex ($P < 0.05$) and the lateral base ($P < 0.01$).

The next three figures show the results of the analysis of variance of the contractile force changes during stimulation of the rest of the thoracic cardiac nerves. While stimulation of each of the nerves caused changes in contractile force, only stimulation of the five nerves shown in the figures resulted in muscle segments that had force changes that were significantly different from the force changes in other areas.

The VLCN stimulation (Figure 14) resulted in the greatest number of significantly different pairs of means. Each one of the drawings contains one of the following muscle segments, posterior or lateral free wall endocardial

RIGHT STELLATE GANGLION

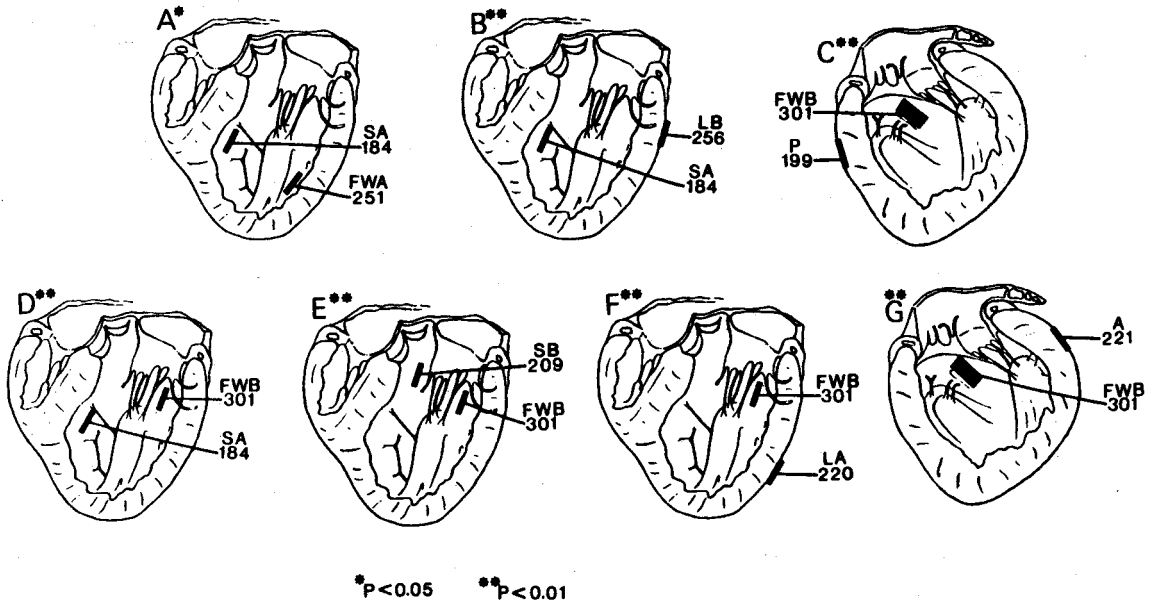


FIGURE 13

FORCE COMPARISONS DURING RIGHT STELLATE GANGLION STIMULATION

This figure shows the results of the analysis of variance of the force changes due to right stellate stimulation. Each drawing shows a pair of means that were significantly different. See Figure 12 for further explanations.

VENTROLATERAL CARDIAC NERVE

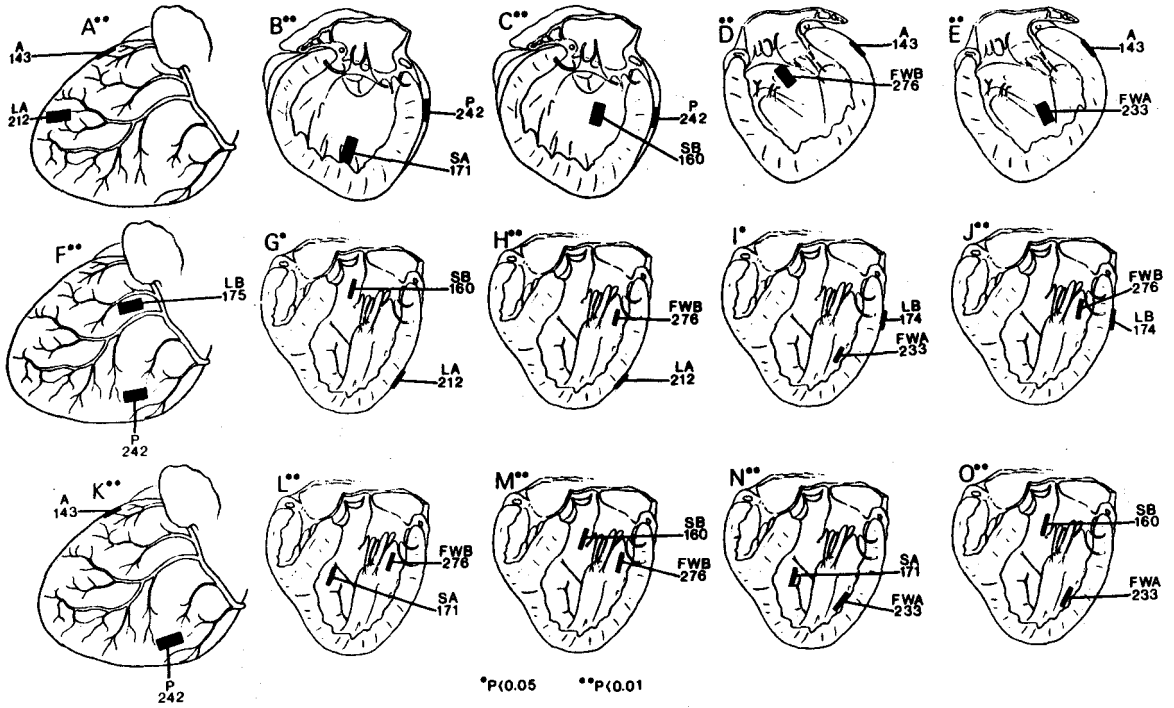


FIGURE 14

FORCE COMPARISONS DURING VENTROLATERAL CARDIAC NERVE STIMULATION

This figure shows the results of the analysis of variance of the force changes due to ventrolateral cervical cardiac nerve stimulation. Each drawing shows a pair of means that were significantly different. See Figure 12 for further explanations.

and epicardial muscle segments. These five areas all showed a greater force increase than the areas they are compared to. Drawing J shows that as with the LSS the force increase in the FWB was greater than in the overlying epicardial segment ($P < 0.01$). However, the two apical free wall segment's force increases were not different ($P > 0.05$).

Figure 15 shows the pairs of means that are different ($P < 0.05$ for all pairs) during recurrent cardiac nerve stimulation. This figure illustrates that the lateral base (A, E and F) and the free wall base (B, C and D) both had larger force increases as a result of the stimulation. The FWB also had a greater force increase than the lateral apex but the lateral base increase is not significantly different ($P > 0.05$) from the lateral apex. The difference between the lateral base force and the lateral apex (42%) was almost as great as the difference between the free wall base and the lateral apex (44%). The anterior force (181%) and the free wall apex force (187%) reached an intermediate level compared to the rest of the force means.

Stimulation of the rest of the thoracic nerves results in only seven pairs of means that are significantly different. These seven pairs are shown in Figure 16. The innominate nerve stimulation (A and B) causes a slight general force increase (Table IV). The three areas that are significantly different are those with the greatest

RECURRENT CARDIAC NERVE

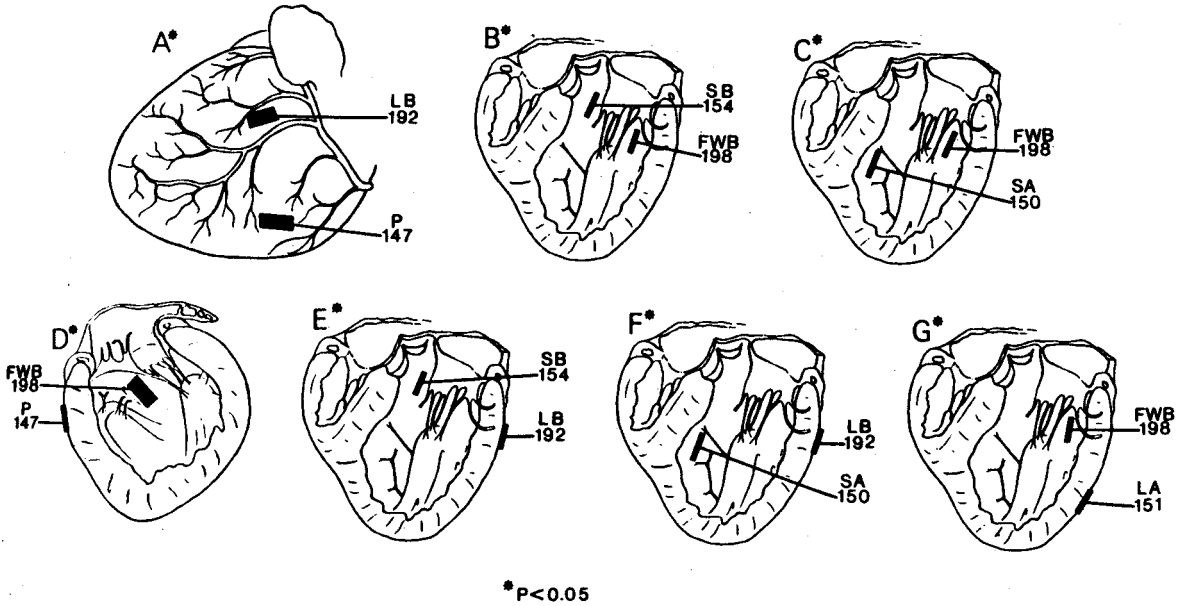
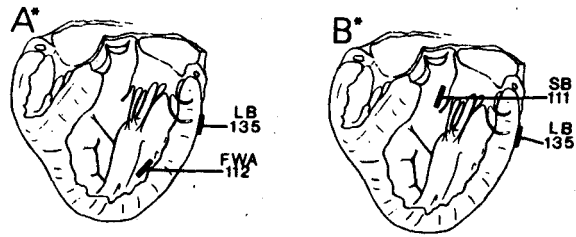


FIGURE 15

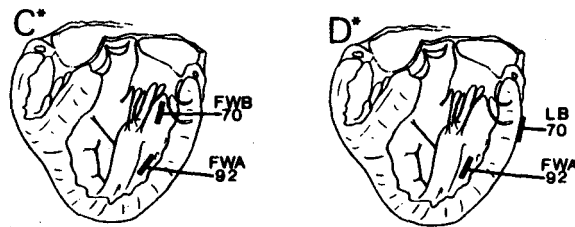
FORCE COMPARISONS DURING RECURRENT CARDIAC NERVE STIMULATION

This figure shows the results of the analysis of variance of the force changes due to recurrent cardiac nerve stimulation. Each drawing shows a pair of means that were significantly different. See Figure 12 for further explanations.

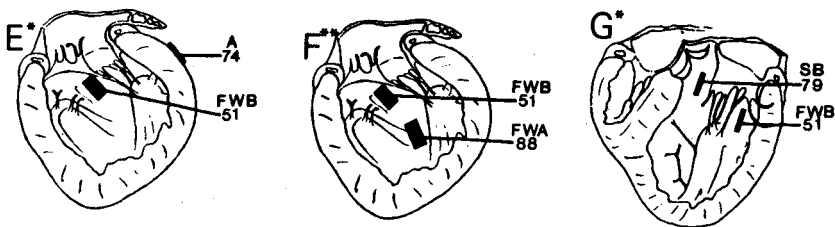
INNOMINATE NERVE



CAUDAL VAGAL NERVE



RIGHT THORACIC VAGUS



* $P < 0.05$

** $P < 0.01$

FIGURE 16

FORCE COMPARISONS DURING INNOMINATE, CAUDAL VAGAL
AND RIGHT THORACIC NERVE STIMULATIONS

FIGURE 16

LEGEND

Figure 16 shows the results of the analysis of variance of the force changes due to stimulation of the following nerves, the innominate, the caudal vagal, and the right thoracic vagus. Each drawing shows a pair of means that were significantly different. All other pairs of means from all of the nerve stimulations were not significantly different ($P < 0.05$). See Figure 12 for further explanations.

increase, the lateral base at 135%, and the two areas with the smallest force increases, the free wall apex at 112% and the septal base at 111%. Stimulation of six different cardiac nerves resulted in generalized force decreases when compared to control. These nerves were the left and right thoracic and cervical vagi and the cranial vagus and caudal vagus of the right side. Of these, only stimulation of the caudal vagal nerve (Drawings C and D) and the right thoracic vagus (E, F and G) resulted in significantly different force changes. As a result of Ca V stimulation the FWA force decreased less than the two basal free wall areas ($P < 0.05$). With right thoracic vagal stimulation the FWB force decreased (E, F and G) more than the A ($P < 0.05$), FWA ($P < 0.01$) and SB ($P < 0.05$).

The force changes due to stimulation of the cardiac nerves following the injection of atropine (2 mg/kg) are shown in Table V. The analysis of variance was calculated for all of the force changes for each nerve stimulation and the results of that analysis are shown in Figures 17, 18 and 19. Following the atropine injection neither the left nor right stellate ganglions were stimulated.

Figure 17 shows responses to excitation of the three left side nerves which elicited force changes that were significantly different from each other. Stimulation of the left thoracic vagus, which before atropine caused a depression of force, now caused an increase in force in

TABLE V

CONTRACTILE FORCE CHANGES, AFTER ATROPINE

	<u>INN</u>	<u>VMCN</u>	<u>L Re L</u>	<u>VLCN</u>	<u>LTV</u>	<u>LCV</u>	
Anterior	148.7 12	125.8 16	172.4 14	159.7 10	108.6 16	109.6 5	
Posterior	123.7 10	120.2 11	159.8 10	202.8 9	134.2 11	121.8 4	
Lateral Base	144.4 11	132.8 16	181.4 14	175.6 10	123.3 14	112.8 5	
Free Wall Base	156.2 10	141.8 13	206.8 12	276.0 8	124.8 12	112.4 5	
Septal Base	-----	110.6 10	140.0 10	-----	111.4 12	104.2 4	
Lateral Apex	139.5 8	125.6 12	158.0 9	174.7 7	128.4 11	121.7 3	
Free Wall Apex	146.3 9	125.9 14	150.2 11	236.1 8	115.4 14	104.0 4	
Septal Apex	-----	106.8 5	138.3 6	-----	114.2 8	105.0 2	
S. D.	59.9	40.0	62.9	61.3	22.6	14.9	
	<u>Re C</u>	<u>Cr V</u>	<u>Ca V</u>	<u>St C</u>	<u>RTV</u>	<u>RCV</u>	<u>ISO</u>
Anterior	205.5 17	130.8 16	112.5 16	116.2 8	102.7 15	119.3 6	207.3 9
Posterior	173.1 11	132.8 13	107.9 11	119.3 7	102.4 11	111.8 5	272.2 8
Lateral Base	208.2 17	146.4 14	106.8 13	128.5 8	103.8 13	126.0 6	302.0 9
Free Wall Base	215.8 13	144.1 14	118.8 13	134.5 8	109.1 13	115.2 5	322.7 7
Septal Base	159.2 9	113.2 13	113.5 11	-----	100.9 12	98.5 4	250.5 12
Lateral Apex	155.8 12	136.7 11	103.4 10	126.8 6	101.4 10	99.8 4	279.4 5
Free Wall Apex	176.5 15	119.6 14	101.0 12	121.3 7	105.3 12	112.0 5	252.6 7
Septal Apex	149.8 6	106.5 8	98.0 7	-----	97.7 9	100.0 2	184.9 7
S. D.	58.95	40.8	22.7	30.0	12.0	22.5	78.3

TABLE V

LEGEND

Table V shows the contractile force for each muscle segment as a percentage of control. Control is taken as 100%. Atropine (2 mg/Kg) was injected into the animal prior to the stimulations shown in this table. Directly under each mean value is the number of observations that are included in the mean. The data were analyzed using the analysis of variance for each nerve stimulation. The standard deviation of each analysis is shown at the bottom of each column. See Figure 9 for an explanation of the abbreviations.

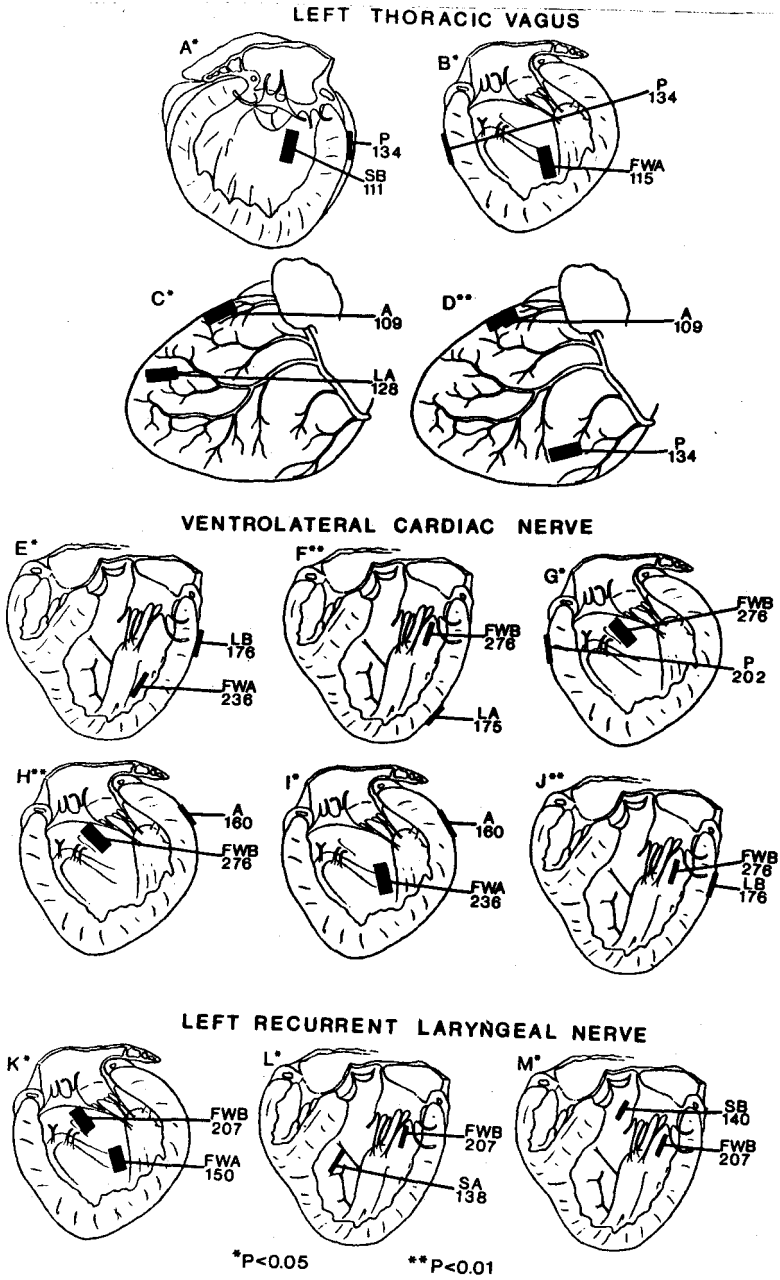


FIGURE 17

FORCE COMPARISONS DURING LEFT SIDE NERVE
STIMULATIONS FOLLOWING ATROPINE

FIGURE 17

LEGEND

Figure 17 shows the results of the analysis of variance of the force changes resulting from left side autonomic nerve stimulation following the injection of atropine (2 mg/Kg). Each drawing shows a pair of means that were significantly different. Only those nerves and pairs of means shown were significantly different. The left stellate ganglion was not stimulated following atropine. See Figure 12 for further explanations.

all areas. Drawings A, B and D show that the posterior segment force increase, which was the largest increase, was significantly greater than the anterior ($P < 0.01$), septal base ($P < 0.05$) and the free wall apex ($P < 0.05$). The increase in contractile force of the anterior segment was also less than the lateral apex increase ($P < 0.05$). Drawings E through J show the pairs of means that were significantly different during VLCN stimulation. The VLCN stimulation never caused cardiac slowing and as a result the number of observations (N) after atropine was small. The N for the septal apex and the septal base during VLCN stimulation was too small for the means to be included in the table. Of the six pairs of means that were significantly different after atropine, five pairs (E, F, H, I and J) were also different before atropine. Drawing G shows that the FWB force increase (276%) is greater ($P < 0.05$) than the posterior (202%). This pair was not different ($P > 0.05$) before atropine. The FWB force was the same before (276%) and after (276%) atropine. The posterior force increase was different before (243%) and after (203%) atropine and therefore, the difference between the means was not significant before but was significant following atropine. Stimulation of the left recurrent laryngeal nerve (L Re L), which before atropine resulted in small force increases, none of which were different from each other ($P < 0.05$), resulted in a force increase in the

FWB (207%) which was greater ($P < 0.05$) than the FWA (150.2%), septal apex (138%) and septal base (140%). In general, all of the segmental forces increased more after atropine than before. These changes after atropine in the pattern of response to the nerve stimulation are indicative of the competitive influences of the adrenergic and cholinergic systems.

Those right side nerves which when stimulated before atropine caused force depression now caused force to increase. Only the cranial vagus and the recurrent cardiac nerve stimulations caused a varied force response that results in significantly different pairs of means. These are shown in Figure 18. With cranial vagal stimulation the lateral base (C) and free wall base (A) forces were both greater ($P < 0.05$) than the septal apex. The lateral base force also increased more than the septal base ($P < 0.05$) (B). Stimulation of the recurrent cardiac nerve after atropine caused slightly larger force increases in all the basal areas, except the septal base, compared to the increases before atropine. In contrast, the apical segments had approximately the same force changes before and after atropine. Five of the seven pairs in Figure 18 were also different before atropine (D, E, F, I and J). Because of the slight increase in the force recorded from the basal segments, the anterior (G) and the lateral base (H) generated more force than the lateral apex ($P < 0.05$).



FIGURE 18

FORCE COMPARISONS DURING RIGHT SIDE NERVE
STIMULATION FOLLOWING ATROPINE

FIGURE 18

LEGEND

Figure 18 shows the results of the analysis of variance of the force changes resulting from the right side autonomic nerve stimulation following the injection of atropine (2 mg/Kg). Each drawing shows a pair of means that were significantly different. Only those nerves and pairs of means shown were significantly different. The right stellate ganglion was not stimulated following atropine. See Figure 12 for further explanations.

Table V shows that injection of isoproterenol (1 γ /kg) into the aorta resulted in force increases in all eight segments. It can also be seen that these increases were not equal in all areas. They range from 185% in the anterior segment to 323% in the free wall base. The results of the analysis of variance of the force changes with isoproterenol are shown in Figure 19. Both free wall basal endocardium and epicardium increased in force more than the anterior and septal apex (A, B, C and F). The septal apex also increased less than the lateral apex (D) and the posterior segments (E).

C. Time Interval Changes

1. R-wave Reference--Autonomic Nerve Stimulation

Figures 20 and 21 show the typical responses to autonomic nerve stimulation of the time interval between the beginning of the R-wave upstroke and the onset of mechanical activity as measured by the strain gauge arch attached to the muscle segments studied. The muscle segments involved in this experiment were the septal base (SB), septal apex (SA) free wall base (FWB) areas of the endocardium and from the anterior (LVA), lateral base (LVLB) and posterior (LVP) areas of the epicardium. The ECG recording is of Lead II.

Figure 20 shows the results of the stimulation of the left stellate (LSS), left recurrent laryngeal (L Re L)

ISOPROTERENOL

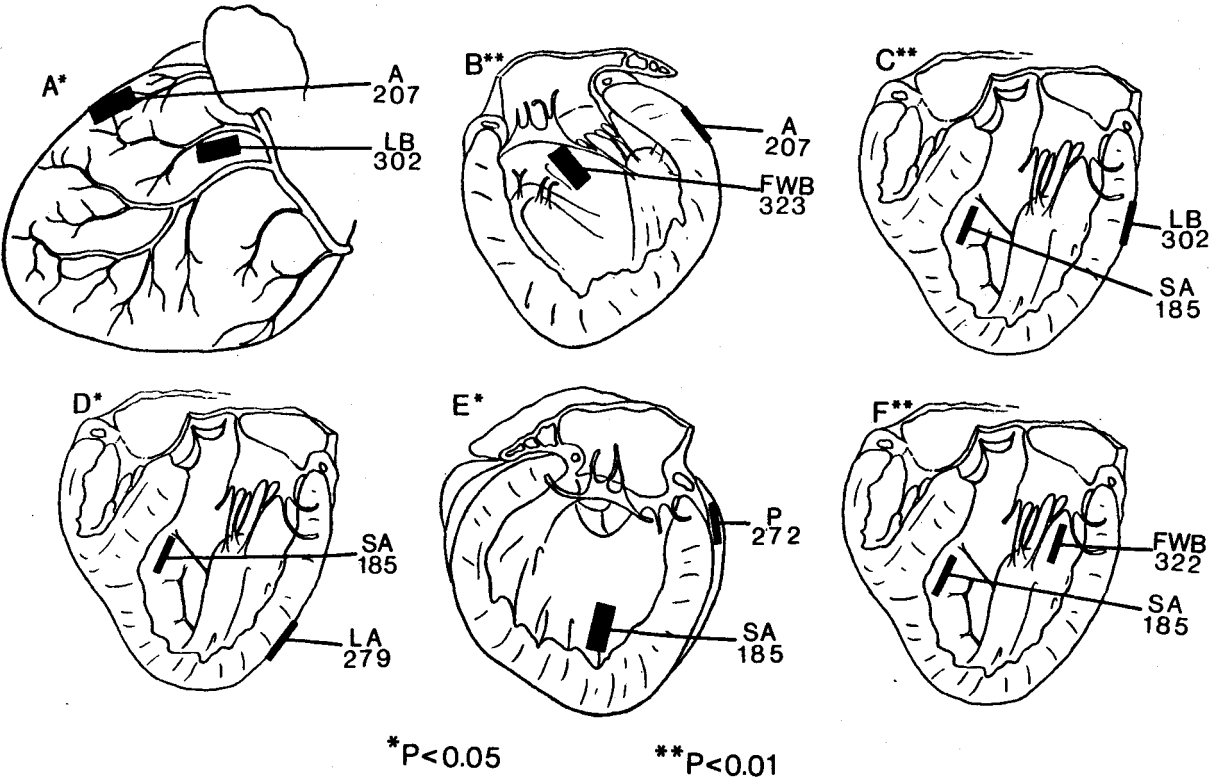


FIGURE 19

FORCE COMPARISONS FOLLOWING ISOPROTERENOL INJECTION

This figure shows the significantly different pairs of means of force increases following the injection of isoproterenol (1 γ /Kg). See Figure 12 for further explanations.

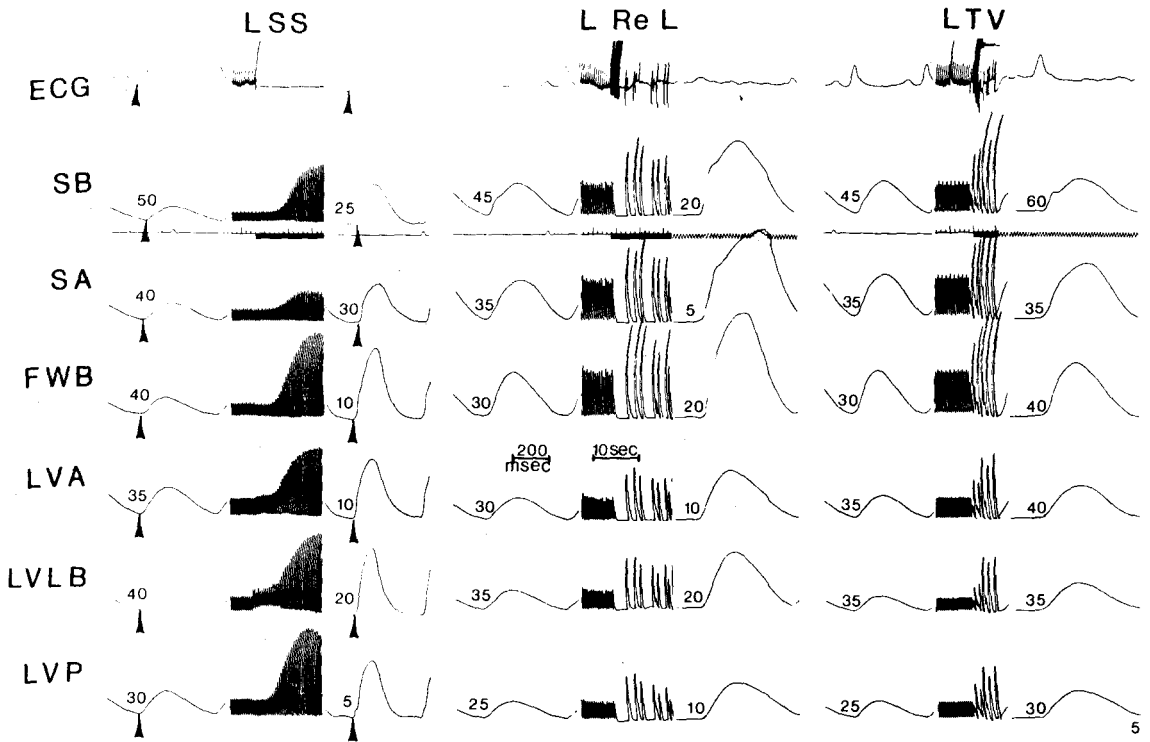


FIGURE 20
 TYPICAL R-WAVE UPSTROKE TO MECHANICAL ONSET
 RECORDINGS, LEFT SIDE NERVES

FIGURE 20

LEGEND

Figure 20 shows the time interval changes as a result of left stellate (LSS), left recurrent laryngeal (LReL) and left thoracic vagus nerve (LTV) stimulation. The time interval is the time from the upstroke of the R-wave to the onset of mechanical activity in the respective muscle segment. The recordings are from the following left ventricular muscle segments, septal base (SB), septal apex (SA) and free wall base (FWB) areas of the endocardium and the anterior (LVA), lateral base (LVLB) and posterior (LVP) areas of the epicardium. The ECG is the Lead II electrocardiogram. The arrows indicate the points of take-off of the respective recordings. The numbers above each recording is the time in msec from the R-wave upstroke to the onset of mechanical activity in that muscle segment.

and left thoracic vagus (LTV) nerves. The time intervals are shown in msec by the numbers located just above the strain gauge recordings. The control intervals for the LSS stimulus-response curves are different from the intervals presented in Figure 5. The sequence is also different, and illustrates the variability in these experiments. With stimulation of the left stellate the interval between the R-wave upstroke and mechanical activity shortened in all areas studied. The biggest change occurred in the FWB (30 msec change) with septal base, anterior and posterior areas all shortening 25 msec. The smallest change was in the septal apex (10 msec). The stimulation of the left recurrent laryngeal caused the heart rate to decrease. It also caused the R-wave to mechanical interval to shorten in all segments. However, the pattern of changes was different during L Re L stimulation as compared with that during LSS stimulation. With L Re L stimulation the septal apex had the greatest amount of shortening in time interval. The septal base time interval still shortened 25 msec but the anterior (20 msec) and the posterior (15 msec) intervals were shorter than with LSS stimulation. The FWB interval shortened only 10 msec. The left thoracic vagal stimulation elicited cardiac slowing similar to that induced by L Re L stimulation. However, the time intervals actually lengthened in some of the muscle segments. The largest changes were in the septal base (15

msec) and free wall base (10 msec). The septal apex and lateral base segment intervals did not change from control.

Figure 21 shows the response of the muscle segments to stimulation of three of the right side cardiac nerves. The nerves stimulated were the right stellate (RSS), caudal vagus (CaV) and the right thoracic vagus (RTV). RSS stimulation increased rate to the extent that pulsus alternans occurred. The R-wave-contraction time interval for the large beat and the small beat were identical. As with LSS stimulation, the RSS stimulation caused a shortening of the R-wave upstroke to mechanical onset time interval. The amount of shortening with RSS stimulation was about the same for all six of the muscle segments shown. However, there was a slight change in the sequence of mechanical activity. During control the anterior and posterior segment contractions preceded the lateral base by 5 msec; with stimulation they all contracted simultaneously. Before stimulation the free wall base and septal apex contractions followed the lateral base by 5 msec and preceded the septal base by the same amount. During stimulation the free wall base time interval shortened 25 msec so that the onset of contraction followed the epicardial areas by 5 msec. The septal areas, with stimulation, had an onset of contraction that was simultaneous and followed the FWB by 10 msec. Caudal vagal stimulation (CaV) caused the heart rate to decrease.

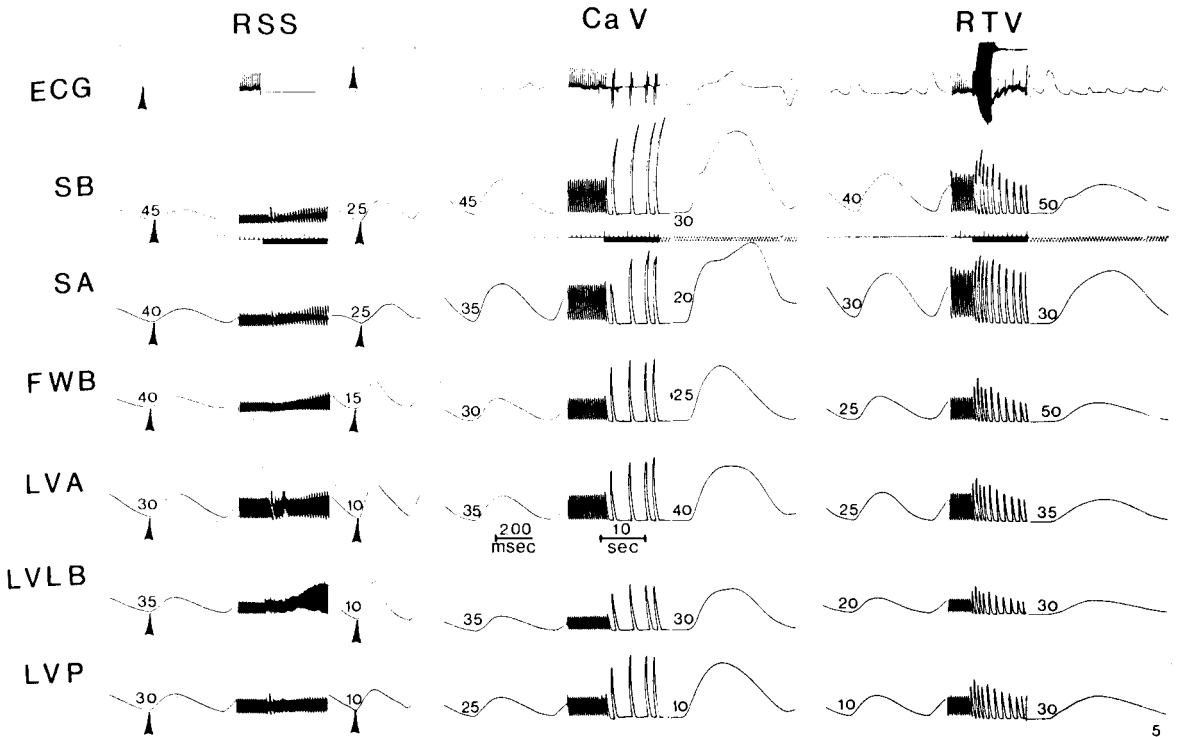


FIGURE 21

TYPICAL R-WAVE UPSTROKE TO MECHANICAL ONSET

RECORDINGS, RIGHT SIDE NERVES

Figure 21 shows the time interval changes as a result of right stellate (RSS) caudal vagus (CaV) and right thoracic vagus (RTV) stimulation. The time interval is the time from the upstroke of the R-wave to the onset of mechanical activity in each of the muscle segments. See Figure 20 for explanation of the abbreviations.

(See also Figure 8.) However, as with L Re L stimulation (Figure 20) there was a decrease in the R-wave to mechanical onset interval for all muscle segments except the anterior, which increased by 5 msec. This change in the onset time may be due to the change in the activation pattern of the ventricle, as indicated by gross change in the ECG recording. Right thoracic vagus stimulation caused either no change or an increase in the time interval. However, the control intervals were shorter than the control intervals seen before RSS or CaV stimulation. Comparison of the RTV stimulation intervals to the control intervals for the CaV shows that there is still a lengthening of the time intervals in some of the muscle segments. In making the above comparison several of the intervals (SA and LVLB) appear to shorten (5 msec for each segment).

The statistical analyses of the R-wave to mechanical activity time intervals are shown in Figure 22 and 23. The data used in preparing Figures 22 and 23 can be found in the Appendix in Tables A-3 through A-10. Each figure consists of a bar graph which shows the average control interval and the average stimulation interval for each of the eight muscle segments and the cardiac nerves stimulated. The standard error for each average is indicated by the thin black vertical bar. The control values and stimulation values were compared using the paired t-test and the degree of significance is indicated at the bottom of each

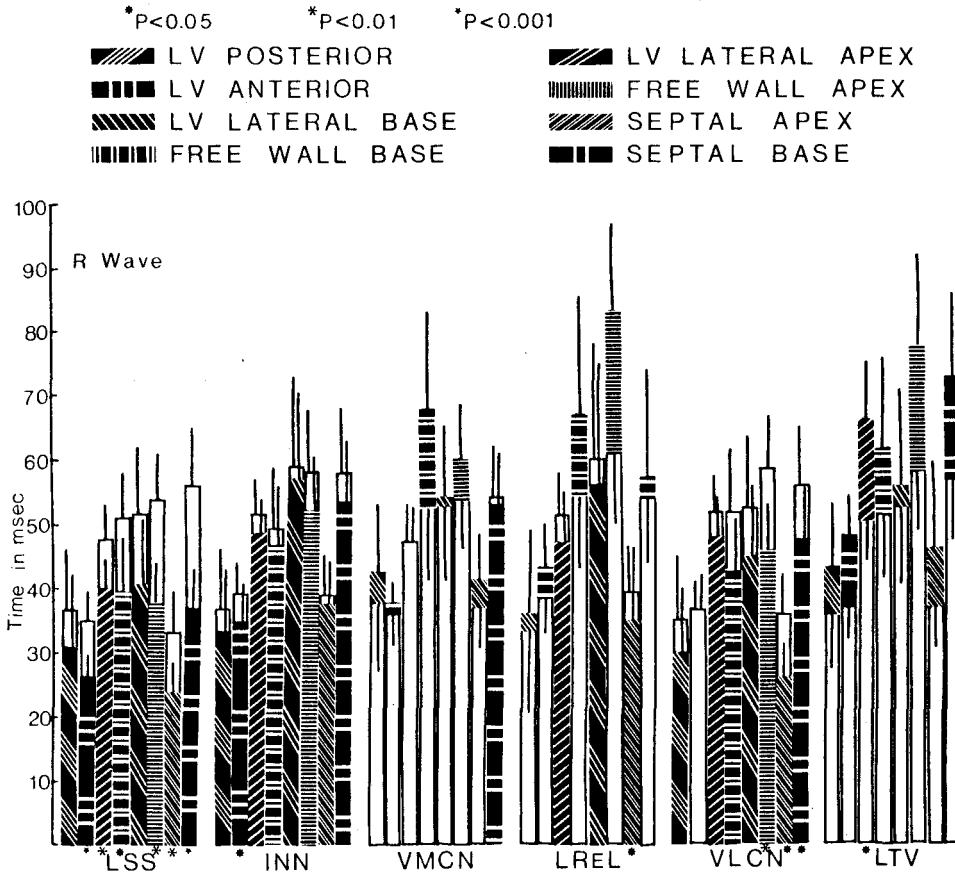


FIGURE 22

R-WAVE TO MECHANICAL ONSET TIME INTERVAL
 CHANGES, LEFT SIDE NERVES

FIGURE 22

LEGEND

Figure 22 shows the statistical analyses of the R-wave upstroke to onset of mechanical activity time intervals during control and left side thoracic cardiac nerve stimulation for all ventricular areas studied. The control time interval is shown by the top of the white bar. The time interval found during stimulation is shown by the black and white striped bars. The standard error of each time interval is indicated by the black vertical bar. The data were analyzed using the paired t-test. The degree of significance between the control and stimulation time interval for each muscle segment is indicated at the bottom of each column. No asterisk means that there is no significant difference between the control interval and the stimulation interval. The nerves stimulated were:

LSS	Left stellate ganglion
INN	Innominate nerve
VMCN	Ventromedial cardiac nerve
LReL	Left recurrent laryngeal nerve
VLCN	Ventrolateral cardiac nerve
LTV	Left Thoracic nerve

The data presented in this figure can also be found in Tables A-3 through A-10 in the Appendix.

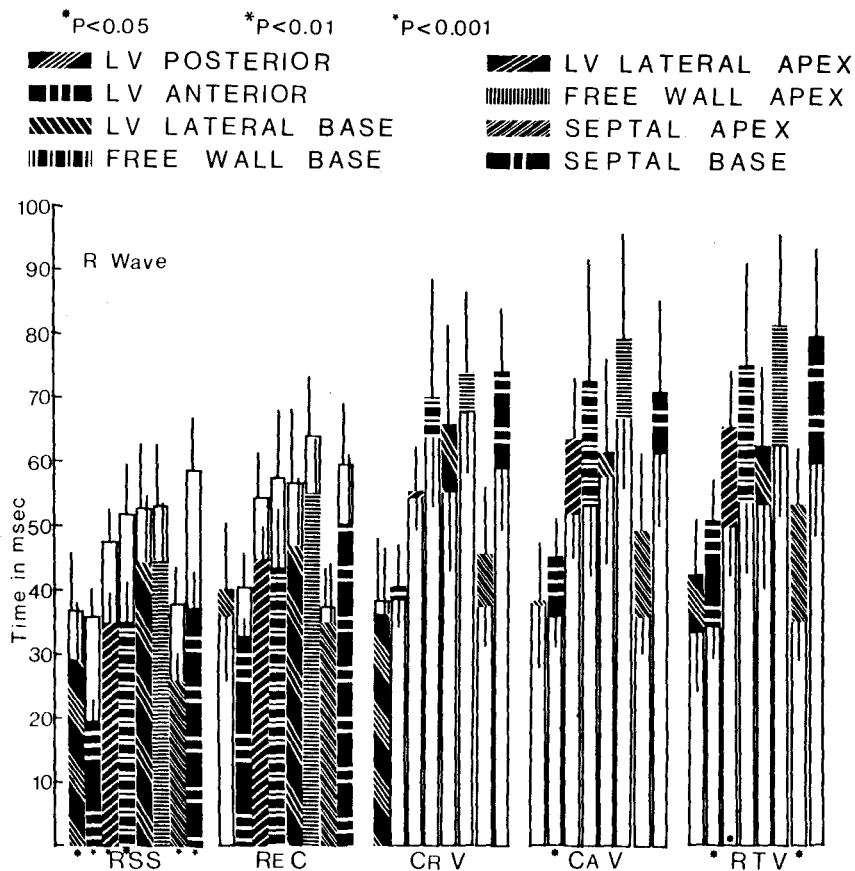


FIGURE 23

R-WAVE TO MECHANICAL ONSET TIME INTERVAL
CHANGES, RIGHT SIDE NERVES

FIGURE 23

LEGEND

Figure 23 shows the statistical analyses of the R-wave upstroke to onset of mechanical activity time intervals during control and right side thoracic cardiac nerve stimulation for all ventricular areas studied. See Figure 22 for further explanations. The nerves stimulated were:

RSS	Right stellate ganglion
ReC	Recurrent cardiac nerve
CrV	Cranial vagus
CaV	Caudal vagus
RTV	Right thoracic vagus

The data presented in this figure can also be found in Tables A-3 through A-10 in the Appendix.

bar. The control time interval is indicated by the top of the white bar. The stimulation time interval is indicated by the top of the black and white bar. In Figure 22, LSS stimulation caused the septal base (right hand bar) to shorten from an average control value of $59.0 \text{ msec} \pm 7.22$ (top of white bar) to an average stimulation value of $37.0 \text{ msec} \pm 4.67$ (top of black bar). In two instances in Figure 22, LV lateral base during VMCN stimulation and LV anterior during VLCN stimulation there was no change in the interval. This is shown by a white bar with both standard error bars from the top of the bar. The left-hand S.E. bar is for the control interval and the right-hand S.E. bar is for the stimulation interval.

Figure 22 shows the results of stimulation of the left side thoracic cardiac nerves. LSS stimulation shortened the R-wave upstroke to onset of mechanical activity time interval in all muscle segments but in two of those, the posterior and lateral apex, the interval change was not significant. The other six areas, SA, SB, FWB, FWA, A and LE all showed significant shortening of the time interval (see figure for degree of significance). The sequence of contraction was not changed with LSS stimulation. Stimulation of the rest of the left side cardiac nerves caused changes in the R-wave to mechanical onset time interval but few of these changes were significant by the paired t-test. With innominate stimulation,

although all of the intervals shorten, only the anterior segment time interval shortens significantly ($P < 0.05$). Most areas showed a lengthening of the R-wave to mechanical onset time interval during VMCN stimulation but the responses from animal to animal were so varied that no change proved to be significant. With left recurrent laryngeal nerve stimulation the changes were varied. While some areas showed a slight increase in the time interval and some areas showed a slight decrease, only the shortening in the septal apex was significant ($P < 0.05$). VLCN stimulation caused all areas except the anterior to show a shortened interval with three of the four endocardial segments exhibiting significant decreases in the time interval. These segments were the free wall apex ($P < 0.01$), septal base and septal apex (both $P < 0.05$). Left thoracic vagal stimulation caused a lengthening of the time interval but of those changes only the lateral base change was significant ($P < 0.05$).

Figure 23 shows the results of the paired t-test analysis of the changes in the time interval from the upstroke of the R-wave to the onset of mechanical activity due to the stimulation of the right side thoracic cardiac nerves. As with left stellate stimulation, right stellate stimulation caused all areas to show a decreased time interval with all but two being significant. The two lateral apical segment intervals shortened but not

significantly ($P > 0.05$). The changes in the anterior, lateral base, septal base and septal apex are highly significant ($P < 0.001$) and the posterior and free wall base changes are significant at the 0.05 level. The recurrent cardiac and cranial vagus stimulations caused slight shortening and lengthening respectively, but none of these changes were significant. Of the increase in all segments with caudal vagus stimulation only the anterior segment change was significant ($P < 0.05$). The right thoracic vagal stimulation also caused increased time intervals in all areas but only the changes in the anterior, lateral base and septal apex were significant (all $P < 0.05$).

2. Electromechanical Coupling Interval-Calcium, Norepinephrine and Atrial pace

As a result of the changes in time interval from the R-wave reference point to mechanical onset of contraction, experiments were carried out to determine if it was the electrical activity or the mechanical activity that was changing with the stimulation. A series of experiments were carried out to see if the changes seen in the previous experiments were related to the norepinephrine (NE) released or to heart rate changes.

Figure 24 shows the results of left and right stellate stimulation on the electromechanical (EM) coupling time interval for the posterior (LVP) and anterior

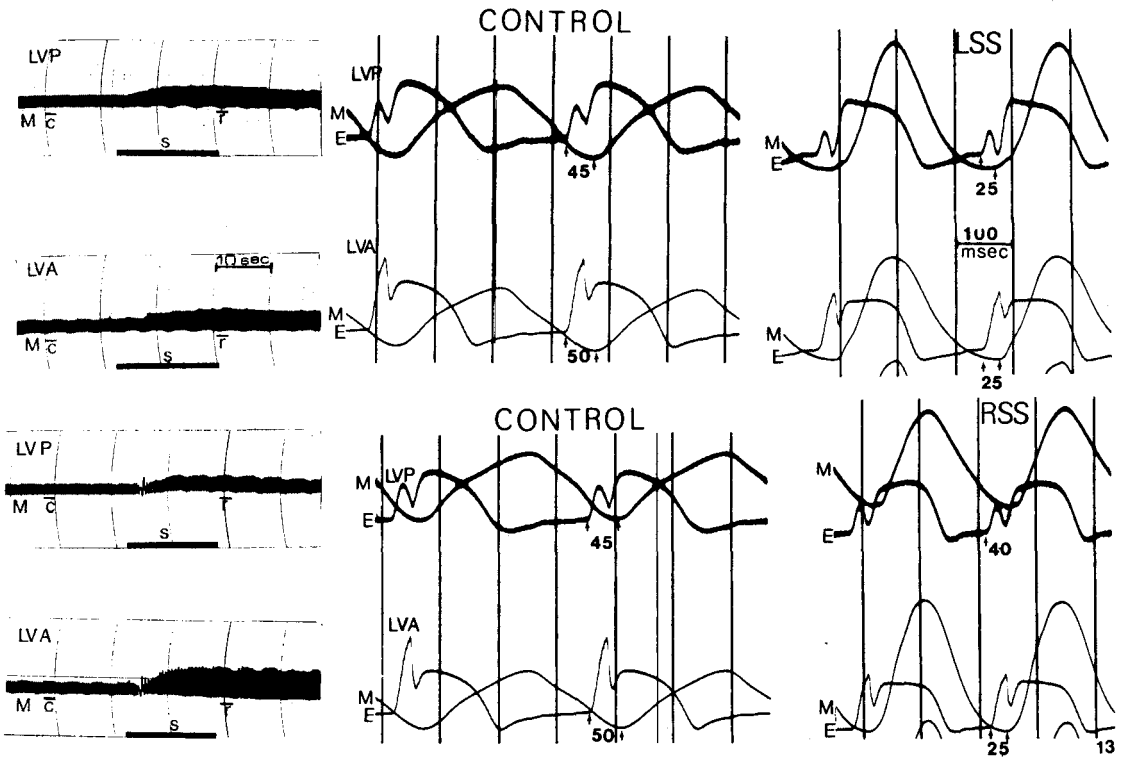


FIGURE 24

EFFECT OF STELLATE STIMULATION ON THE ELECTROMECHANICAL
COUPLING INTERVAL

FIGURE 24

LEGEND

Figure 24 shows the effect of stimulation of the left (LSS) and right (RSS) stellate ganglions on the electromechanical (EM) coupling interval. The EM coupling interval is the time between the upstroke of the local electrogram (E) to the beginning of the upstroke of the mechanical (M) activity.

Other abbreviations are:

LVP Left ventricular posterior
LVA Left ventricular anterior
c Control
s Stimulation
r Response

On the left of the figure are the tracings taken from the polygraph showing the total force response to the stimulation. The panels marked "control" were recorded on the Midwest Optical Oscillograph during the period marked by the "c." The panels marked LSS and RSS are the response to the stimulation and were recorded during the period marked "r" on the polygraph recordings. The bar labelled "s" shows the duration of the stimulus. The small arrows on the center and right panels indicate the take-off points for the electrical and mechanical activity. The numbers between the arrows are the electro-mechanical coupling intervals in msec.

(LVA) muscle segments. In this series of experiments the modified strain gauge arches were placed only on the epicardium. These strain gauges were the type with the single electrode positioned through one foot of the arch. Recordings from both the polygraph and the Midwest Oscillograph recorder are shown. The left column shows the force records from the polygraph. The middle or control column is from the oscillograph and was recorded during the period labelled "c" on the force recording. The response to stimulation is shown in the right column and was recorded during the interval marked "r" on the polygraph recording. Stimulation of the left stellate (top) caused the electromechanical (EM) coupling intervals for both segments to shorten. The electrical reference used was the recording of the local electrogram. This was the electrical activity of the tissue under the strain gauge and the surrounding tissue. During stimulation of the right stellate (bottom), both EM coupling intervals shortened but the posterior segment interval shortened only 5 msec while the anterior segment interval shortened 25 msec.

To check the possibility that the time interval, both R-wave referenced and local electrogram referenced, was or was not related to heart rate, the right atrium was paced. Figure 25 shows the results of this part of the experiment. The control rate in this experiment was

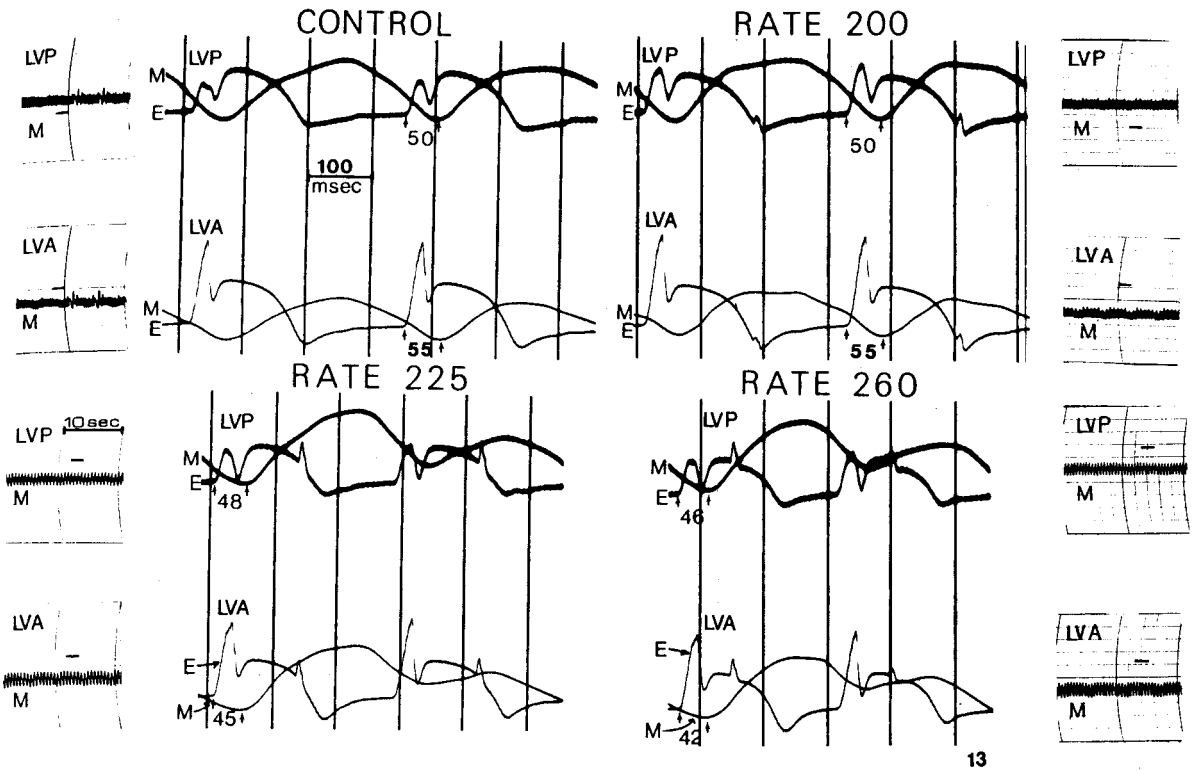


FIGURE 25

EFFECT OF ATRIAL PACING ON THE ELECTROMECHANICAL
COUPLING INTERVAL

This figure shows the results of atrial pacing, electrodes in the right atrial appendage, on the EM coupling interval. Control rate was 180 beats per minute and the rate was increased to 200, 225 and 260 beats per minute. The black bars on the polygraph recordings (far left and far right of figure) indicate where the fast tracing (center two columns) were recorded from. See Figure 24 for further explanation.

180 beats per minute. As the pace rate was increased the EM coupling interval for the posterior segment fell 4 msec. The EM coupling for the anterior segment fell from 55 msec during control to 42 msec at a rate of 260 beats per minute. As will be shown later this was not a typical response of the anterior segment.

Norepinephrine (1 γ /Kg) was then injected. The response to this is seen in the bottom of Figure 26. The force of contraction increased in all segments. Along with the increased force, each segment also exhibited a decreased EM coupling interval. Calcium was also injected and the response to one-quarter of a gram of Ca^{++} is seen at the top of Figure 26. Contractile force increased as a result of injection of Ca^{++} . The EM coupling interval also shortened. The amount of shortening of the EM coupling interval was not as great with the Ca^{++} as it was with the NE.

Propranolol (0.5 to 1.0 mg/Kg) was then injected. The amount of propranolol was sufficient to block the response to stimulation of either stellate ganglion. Norepinephrine was again injected. As can be seen in Figure 27, 1 γ /Kg of NE did not elicit a response. The EM coupling interval did not change. Injection of calcium after propranolol did cause the force to increase and the EM coupling interval to shorten. However, the degree of shortening was not as great after the propranolol as it

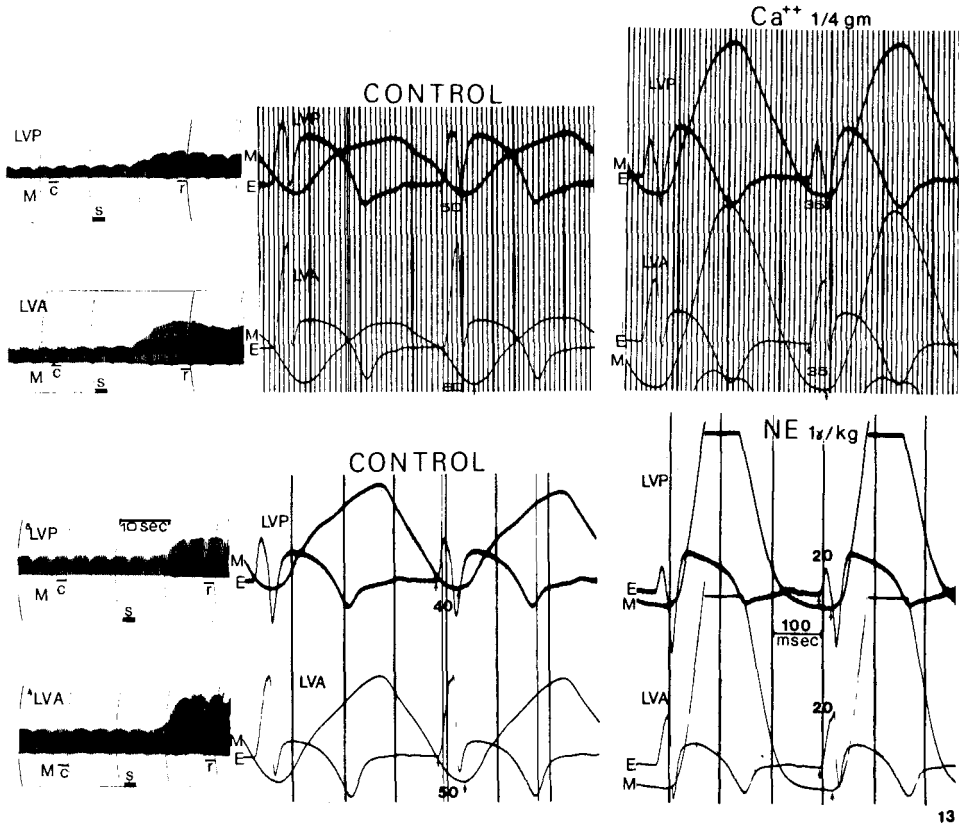


FIGURE 26

EFFECT OF CALCIUM AND NOREPINEPHRINE ON THE
ELECTROMECHANICAL COUPLING INTERVAL

This figure shows the results of calcium (Ca) and norepinephrine (NE) on the electromechanical coupling interval. See Figure 24 for further explanation.

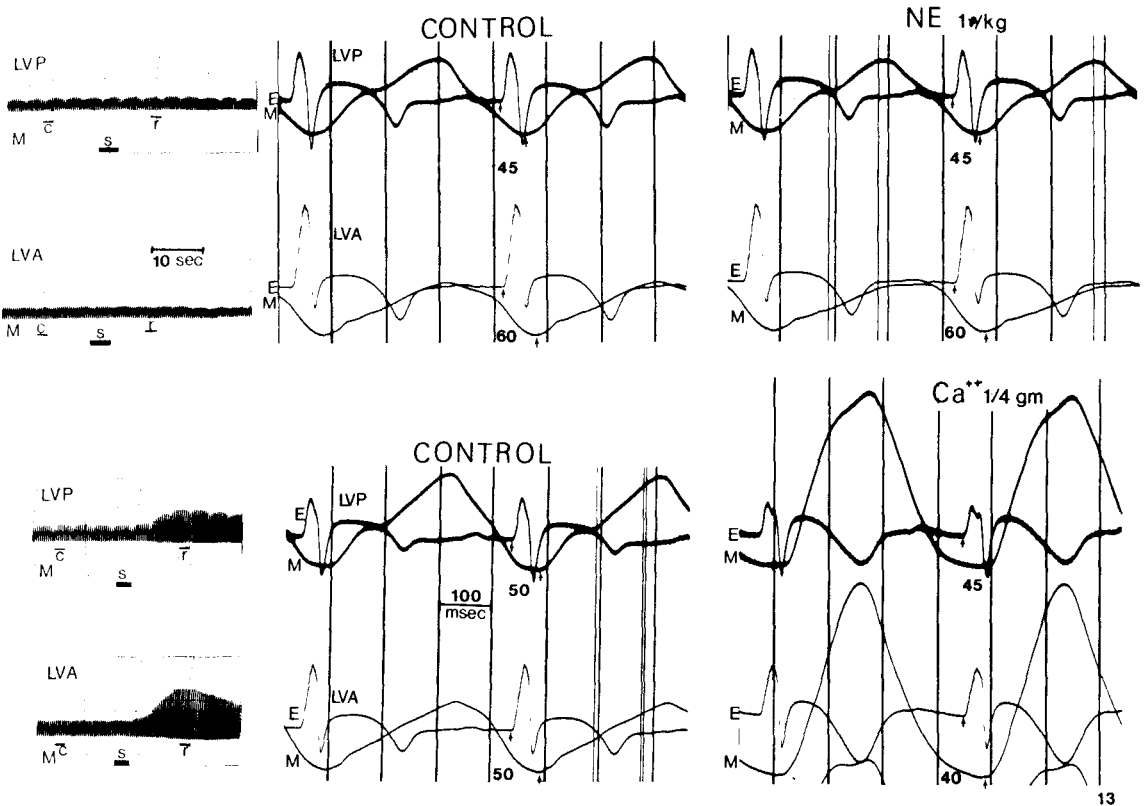


FIGURE 27

EFFECT OF CALCIUM AND NOREPINEPHRINE ON THE ELECTRO-
MECHANICAL COUPLING INTERVAL AFTER PROPRANOLOL

This figure shows the results of the same injections of calcium and norepinephrine as seen in the last figure, but after the injection of sufficient amounts of propranolol (0.5 to 1.0 mg/Kg) to block the response to stellate stimulation. See Figure 24 for further explanation.

was before. This may be due to the direct depressant effect of propranolol.

Figure 28 and Table VI show the statistical analysis of the atrial pace, NE and Ca data. The left ventricular epicardial segments studied in this series of experiments were the anterior (LVA), lateral base (LVL) and posterior (LVP). The right ventricular sinus (RVS) was also studied. In Figure 28, the control EM coupling interval is shown by the top of the white bar and the stimulation interval by the top of the black and white bar. The standard error for each interval is shown by the thin vertical black lines. The N value and the degree of significance between each control and response interval for each segment is shown in Table VI.

Both left (LSS) and right (RSS) stellate stimulation caused the EM coupling interval to shorten in all four muscle segments ($P < 0.001$ for all changes). The EM coupling intervals do not all change equivalent amounts. The lateral base EM interval changed 13.5 msec and the RVS changed 11.9 msec. The LVA interval shortened 10.9 msec and the posterior interval shortened only 8.4 msec. With RSS stimulation the lateral base shortened 13.7 msec, approximately the same as with LSS stimulation. The RVS and LVA EM interval shortened to the same degree, 10.3 and 10.4 msec respectively. The LVP again shortened the least, 6.4 msec.

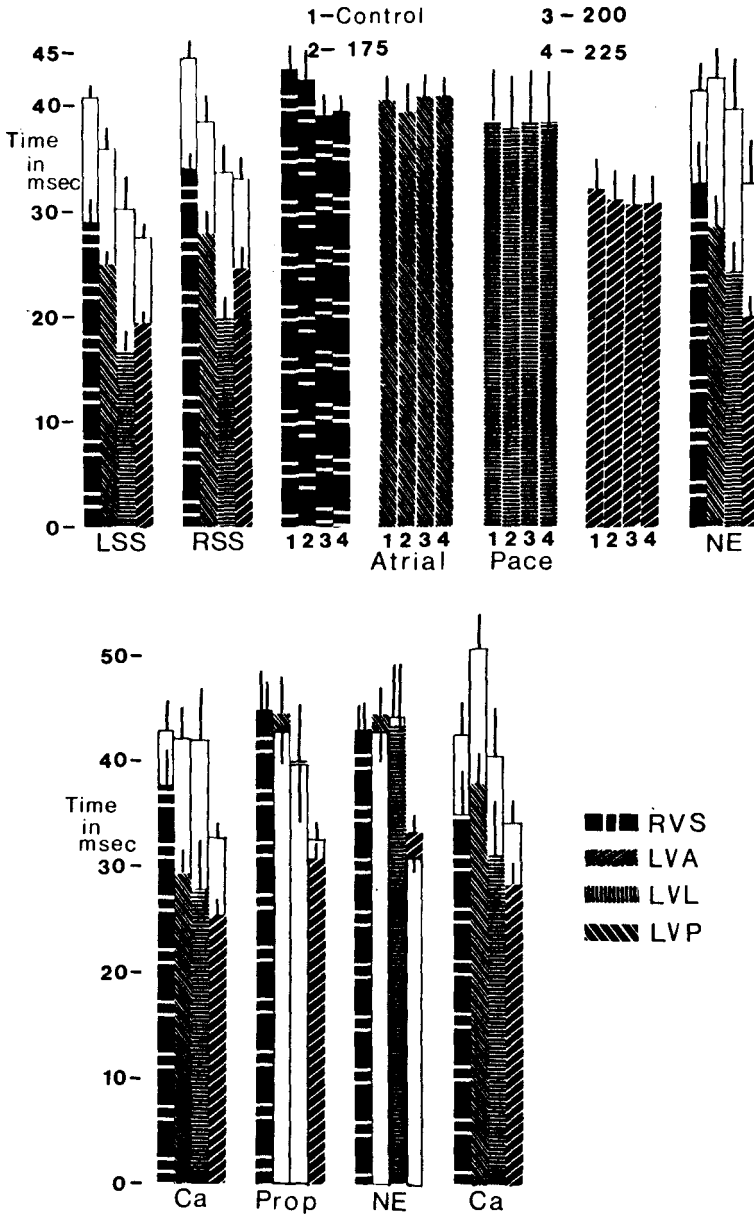


FIGURE 28

ANALYSIS OF ELECTROMECHANICAL COUPLING
INTERVAL CHANGES

FIGURE 28

LEGEND

Figure 28 is a series of histograms showing the analysis of the changes in electromechanical (EM) coupling interval to several different procedures. The control EM coupling interval for each segment is shown by the top of the open bar. The control interval was measured before each different procedure. The response EM coupling interval for each segment is shown by the different black bars. The standard error for each interval is shown by the thin vertical black bar.

The abbreviations are:

RVS	Right ventricular sinus
LVA	Left ventricular anterior
LVL	Left ventricular lateral base
LVP	Left ventricular posterior
LSS	Left stellate ganglion stimulation
RSS	Right stellate ganglion stimulation
NE	Norepinephrine (1 δ /Kg)
Ca	Calcium (1/4 gm)
Prop	Propranolol (0.5-1.0 mg/Kg)

The data for the atrial pace has been shown separately for each muscle segment. The rates are 1-control, 2-175 beats per minute, 3-200 beats per minute and 4-225 beats per minute. See also Table VI.

TABLE VI
 STATISTICAL ANALYSIS OF THE ELECTROMECHANICAL COUPLING
 INTERVAL CHANGES CAUSED BY STELLATE STIMULATION,
 NOREPINEPHRINE, CALCIUM AND ATRIAL PACING

	Atrial Pace									
	Control	LSS	Control	RSS	Control	175	200	225	Control	NE
LVA	35.9 [†] 1.96 [°] 15 [♠] 0.001	25.0 1.23	38.4 2.34	28.0 1.99	40.4 2.23	39.5 2.52	40.7 2.12	40.7 1.83	42.3 2.81	28.5 2.6 11 0.001
LVLB	30.2 3.33 14 0.001	16.7 2.02	33.6 2.72	19.9 1.97	38.7 4.44	37.9 4.79	38.3 4.76	38.3 4.74	39.4 4.76	24.0 3.1 9 0.01
LVP	27.7 1.28 12 0.001	19.3 1.06	32.9 2.00	24.5 1.96	32.0 2.68	31.1 2.73	30.2 2.77	30.5 2.69	32.5 3.28	19.9 1.76 8 0.01
RVS	40.7 2.37 11 0.001	28.8 1.84	44.3 1.59	34.0 1.45	43.4 [*] 2.12	42.0 1.81	39.7 [*] 1.72	39.5 [*] 1.25	41.2 2.46	32.5 3.66 8 0.01

[†]mean time in msec.

[°] standard error of the mean

[♠] number of observations

[~] degree of significance

Propranolol								
	<u>Control</u>	<u>CA⁺⁺</u>	<u>Control</u>	<u>INI</u>	<u>Control</u>	<u>NE</u>	<u>Control</u>	<u>CA⁺⁺</u>
LVA	41.9 3.30	29.3 2.43	42.9 2.74	44.6 3.54	43.2 3.47	44.4 2.75	50.6 3.16	37.9 2.86
	9 0.01		9 N.S.		10 N.S.		9 0.01	
LVLB	42.0 4.94	27.8 5.02	39.3 5.54	39.8 5.32	44.1 5.30	43.4 5.76	40.0 4.88	31.1 4.99
	9 0.01		6 N.S.		9 N.S.		7 0.01	
LVP	32.8 1.49	25.4 1.60	32.5 1.70	30.8 1.53	30.7 1.30	33.3 1.64	34.2 2.00	28.3 2.10
	7 0.05		6 N.S.		7 N.S.		6 N.S.	
RVS	42.9 2.86	37.9 3.42	45.0 3.62	45.0 2.67	43.1 2.31	43.1 2.67	42.5 3.09	35.0 3.87
	7 N.S.		7 N.S.		8 N.S.		6 0.1	

TABLE VI

LEGEND

Table VI shows the analysis of the data presented in Figure 32. See the legend of Figure 32 for an explanation of the abbreviations. The asterisk (*) indicates that the right ventricular sinus (RVS) EM coupling intervals at atrial pace rates of 200 and 225 beats per minute were significantly different from control at the 0.01 level. The data was analyzed using the paired t-test.

Pacing the atria resulted in no change in the EM coupling interval for any of the left ventricular segments but it did cause a change in the EM coupling interval of the RVS. The EM intervals at 200 and 225 beats per minute were significantly different from control at the 0.01 level.

Injection of NE (1 γ /Kg) caused the EM intervals in all segments to decrease. The largest decrease was in the LB (15.4 msec) with the anterior (13.8 msec) and posterior (12.6 msec) showing only slightly smaller decreases. The RVS interval decreased the smallest amount (8.7 msec). The calcium (1/4 gm) injection caused the lateral base EM interval to again shorten the most (15.8 msec) with the anterior interval decreasing almost as much (12.6 msec). The decrease in the EM interval for the posterior segment was less (7.4 msec) than that seen with the NE injection. The RVS decrease was not a significant decrease ($P > 0.1$).

Injection of an adrenergic blocking dose of propranolol (0.5-1.0 mg/Kg) caused no significant change in the EM coupling interval for any of the muscle segments. After propranolol, norepinephrine had no effect on the EM coupling interval for any muscle segment. The LVA and RVS intervals did not change at all. The lateral base interval shortened and the posterior interval lengthened slightly, but these changes were not significant ($P > 0.01$). The

calcium injection (1/4 gm) after atropine was used as a test to make sure that the lack of response to the NE was due to a blockage of the beta receptors and not a direct depressant action of propranolol. The lateral base and posterior segments both showed significant decreases ($P < 0.01$) in their respective EM coupling intervals. The change in the posterior and RV sinus were not significant ($P > 0.05$). Also the control and response times for EM coupling after propranolol were significantly greater ($P < 0.05$) than before the propranolol. This difference in the anterior segment and the lack of significance between the control and response intervals for the posterior area may be the result of direct myocardial depression of the propranolol.

3. Electromechanical Coupling Interval--Autonomic Nerve Stimulation

Figures 29 and 30 show typical changes in the electromechanical (EM) coupling interval seen with autonomic stimulation. Figure 29 shows changes in contractile force and heart rate during stimulation of the left side cardiac nerves. The ventrolateral cervical cardiac nerve (VLCN) is a predominantly sympathetic nerve. In this experiment VLCN stimulation did not change heart rate but did cause contractile force to increase in the lateral base (LVLB) and posterior (LVP) muscle segments. The

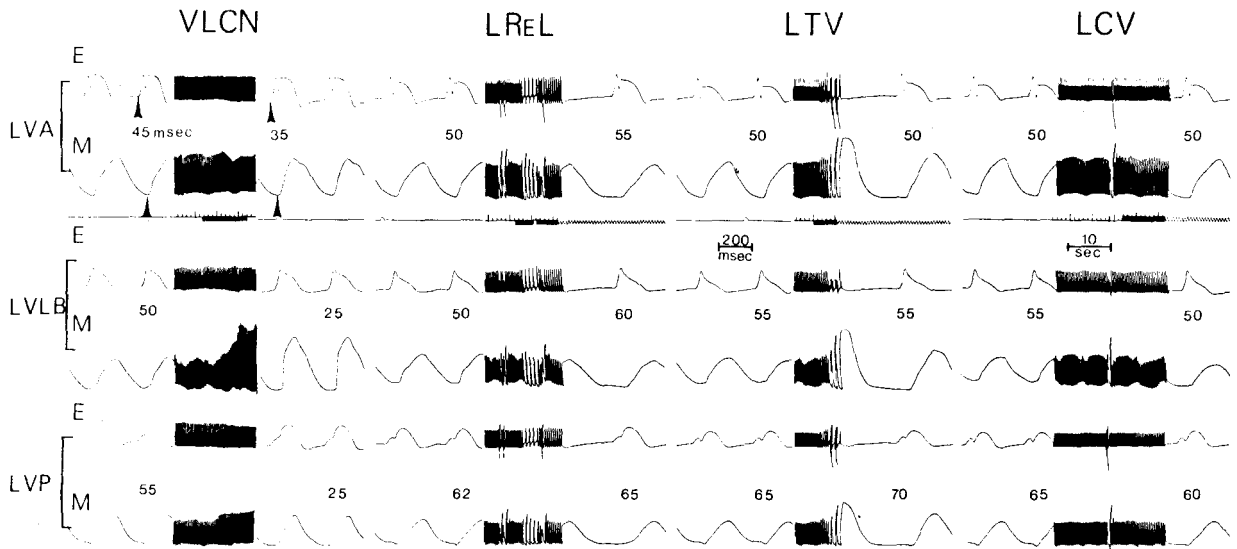


FIGURE 29
ELECTROMECHANICAL COUPLING INTERVAL CHANGES,
LEFT SIDE CARDIAC NERVES

FIGURE 29

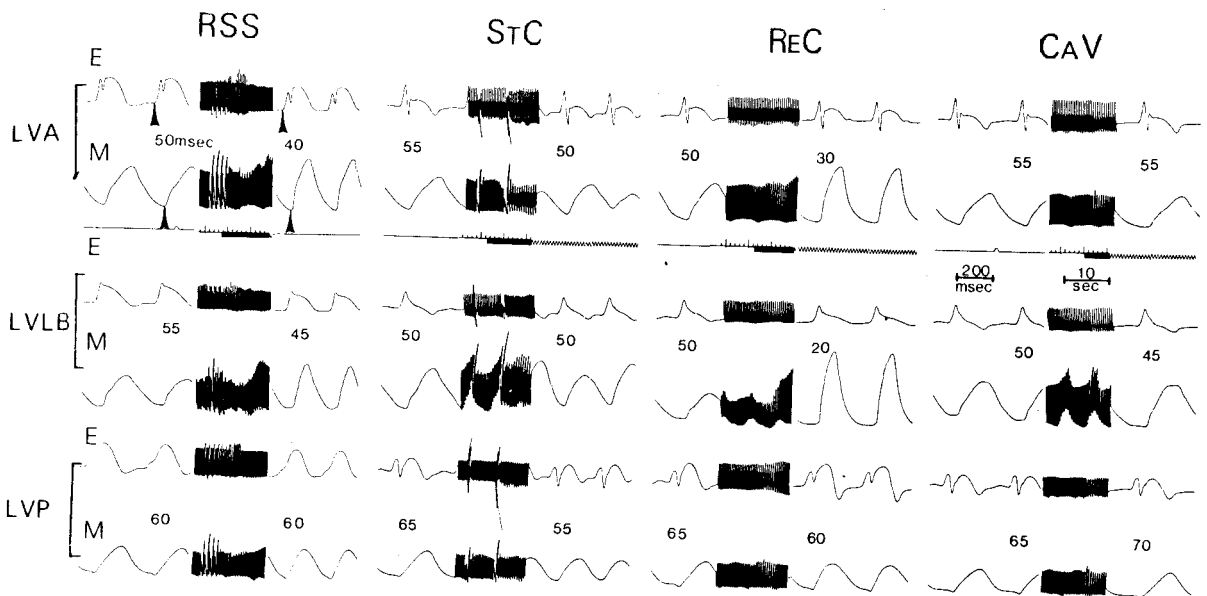
LEGEND

Figure 29 shows the results of stimulation of four left side cardiac nerves on the electromechanical coupling interval for the anterior (LVA), lateral base (LVLB) and posterior (LVP) epicardial muscle segments. The electromechanical coupling interval is the time between the first positive deflection in the local electrogram (E) to the onset of mechanical activity (M) in that muscle segment. The EM coupling interval time is shown between the electrical and mechanical tracings for each muscle segment. The nerves stimulated were the:

VLCN Ventrolateral cervical cardiac nerve
LReL Left recurrent laryngeal nerve
LTV Left thoracic vagus
LCV Left cervical vagus

anterior segment (LVA) exhibited a slight decrease in contractile force. In all three muscle segments, EM coupling intervals decreased. In the two segments in which contractile force increased the EM coupling interval shortened the most. The anterior segment also had a shorter EM coupling interval but it did not shorten as much as the LVLB and LVP. Stimulation of the left recurrent laryngeal (LReL) caused heart rate to decrease. Also in all three of the muscle segments studied the EM coupling interval lengthened. The LVLB interval lengthened the most (10 msec) with anterior (5 msec) and posterior (3 msec) segments exhibiting only minor changes in their respective coupling intervals. Left thoracic vagal (LTV) stimulation caused rate to decrease but for the exception of a slight prolongation in the posterior segment (5 msec), there was no change in the EM coupling interval. Left cervical vagus (LCV) stimulation caused only a slight drop in heart rate and no changes in contractile force. Still the LVLB and LVP EM coupling intervals decreased by 5 msec.

Figure 30 shows typical responses to stimulation of selected right side cardiac nerves. Right stellate (RSS) ganglion stimulation shortened the EM coupling interval in both the anterior and lateral base areas but did not change the interval in the posterior segment. RSS stimulation also caused heart rate and contractile force to increase in all areas studied. The stellate cardiac (St C) nerve



24

FIGURE 30
ELECTROMECHANICAL COUPLING INTERVAL CHANGES,
RIGHT SIDE CARDIAC NERVES

FIGURE 30

LEGEND

Figure 30 shows the results of stimulation of four right side cardiac nerves on the electromechanical coupling interval. The nerves stimulated were:

RSS Right stellate ganglion
StC Stellate cardiac nerve
ReC Recurrent cardiac nerve
CaV Caudal vagus

See Figure 29 for further explanation.

is primarily a heart rate regulating nerve. This is shown by the St C stimulation in this figure. Heart rate increased 80 beats per minute but contractile force did not change in any of the areas studied. The EM coupling interval did not change in the lateral base but did change in the anterior (5 msec) and posterior (10 msec). Recurrent cardiac (ReC) stimulation caused a mixed response. Rate decreased slightly at the beginning of the stimulation. Then the rate returned to normal and force increased in the anterior and lateral base segments. The contractile force in the posterior segment did not change. The EM coupling interval, which was measured at the peak of the force increase, decreased in all three muscle segments. The decrease in the posterior segment was small (5 msec) compared to the decreases in the anterior (20 msec) and lateral base (30 msec). Caudal vagal (CaV) stimulation caused heart rate to decrease concurrently with mixed but small EM coupling interval changes. The anterior interval remained unchanged, the lateral base interval decreased by 5 msec, and the posterior interval increased 5 msec.

Figures 31 and 32 show the results of the data analyses of the electromechanical coupling interval changes caused by cardiac nerve stimulation. The control coupling interval is shown by the top of the open bar. The coupling interval resulting from the nerve stimulation is shown by the top of the black bar. The standard error and number

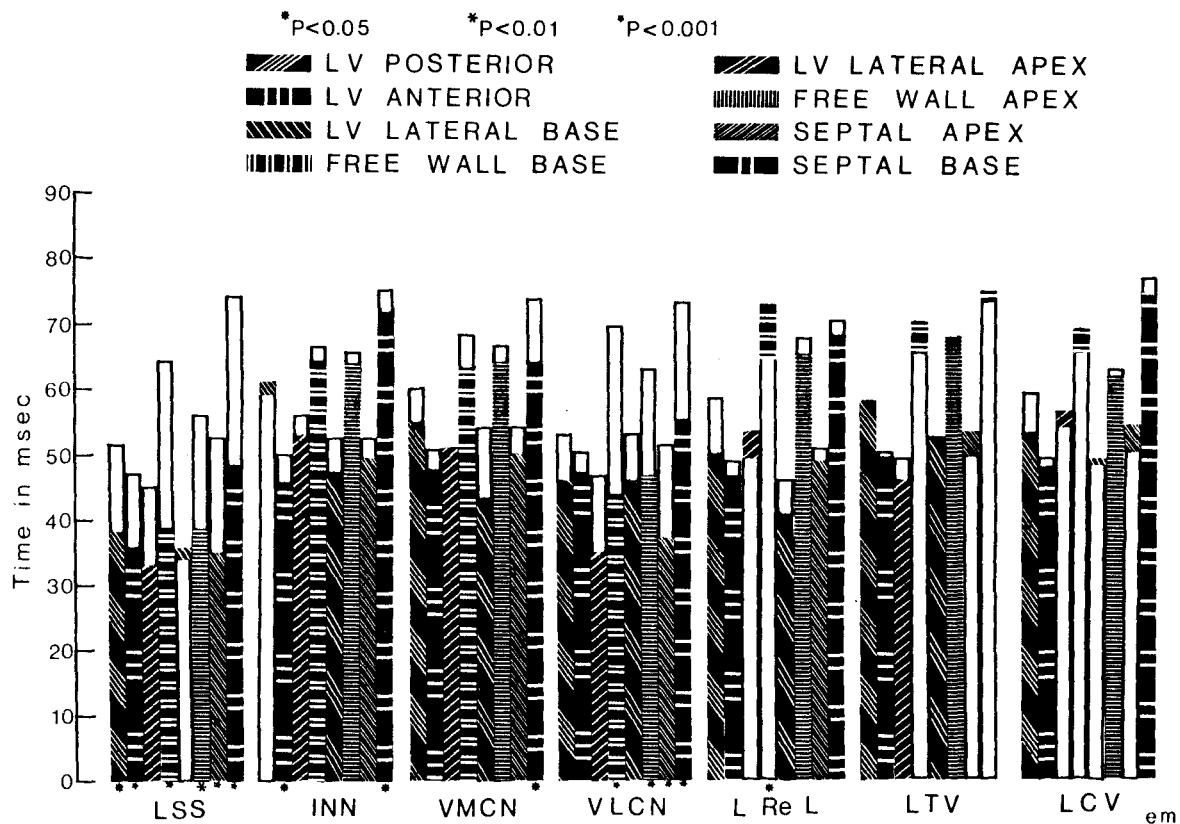


FIGURE 31

STATISTICAL ANALYSIS OF ELECTROMECHANICAL COUPLING
INTERVAL CHANGES, LEFT SIDE CARDIAC NERVES

FIGURE 31

LEGEND

Figure 31 is a histogram showing the statistical analyses of the electromechanical coupling interval changes. The data are also presented in Tables A-11 through A-18 in the appendix. The control EM interval is shown by the top of the open bar. The stimulation interval is shown by the top of the black and white bars. The degree of significance between control and stimulation, as calculated by the paired t-test, is shown at the bottom of each column. The abbreviations are as follows:

LSS	Left stellate ganglion
INN	Innominate nerve
VMCN	Ventromedial cervical cardiac nerve
VLCN	Ventrolateral cervical cardiac nerve
LReL	Left recurrent laryngeal nerve
LTV	Left thoracic vagus
LCV	Left cervical vagus

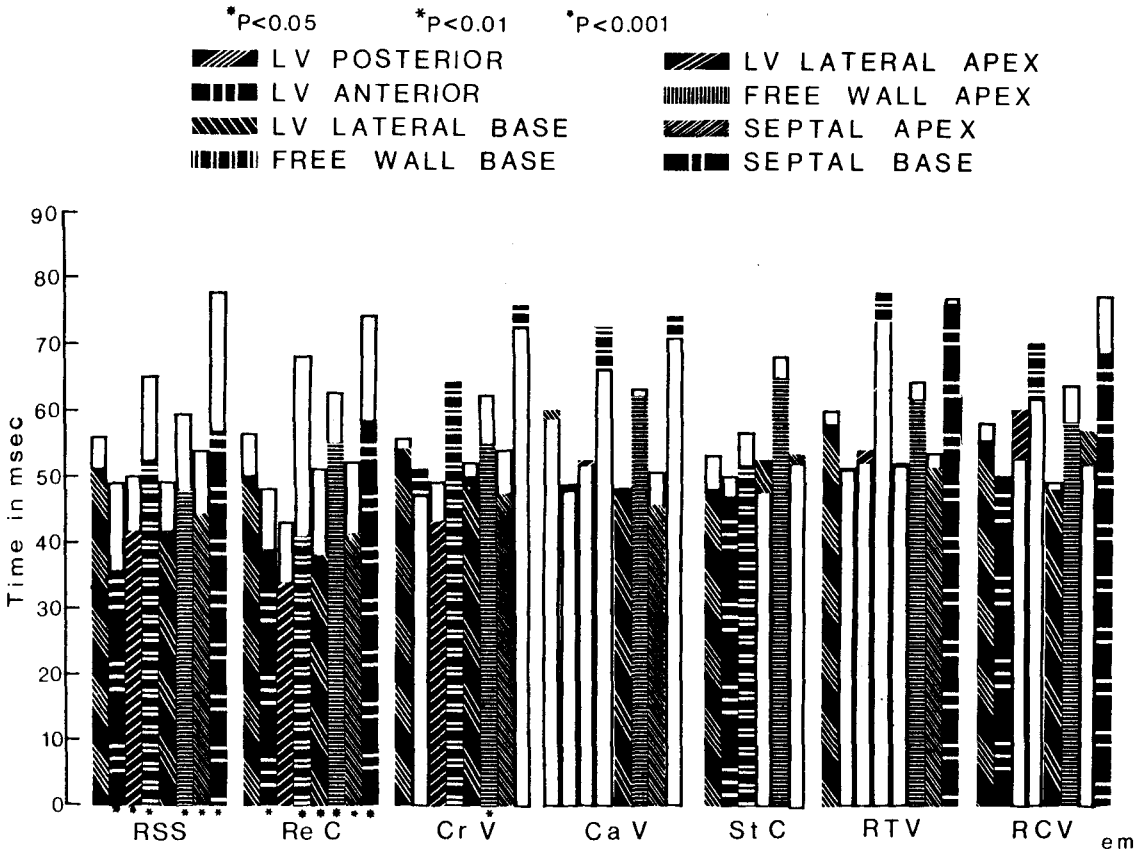


FIGURE 32

STATISTICAL ANALYSIS OF ELECTROMECHANICAL COUPLING
 INTERVAL CHANGES, RIGHT SIDE CARDIAC NERVES

FIGURE 32

LEGEND

Figure 32 is a histogram showing the statistical analysis of the electromechanical coupling interval changes. The data are also presented in Tables A-11 through A-18 in the Appendix. The abbreviations are as follows:

RSS	Right stellate ganglion
ReC	Recurrent cardiac nerve
CrV	Cranial vagus
CaV	Caudal vagus
StC	Stellate cardiac
RTV	Right thoracic vagus
RCV	Right cervical vagus

See Figure 35 for further explanations.

of observations for each column is presented in Tables A-11 through A-18 in the Appendix. The paired t-test was used to determine the degree of significance between the control and stimulation EM coupling intervals. The degree of significance is shown at the bottom of each column.

The results of stimulation of the left thoracic cardiac nerves are shown in Figure 31. Left stellate (LSS) stimulation caused all muscle segments except the epicardial lateral apex to have shorter EM coupling intervals than control. Innominate (INN) stimulation resulted in slightly shorter EM intervals for all segments except the posterior which showed a prolongation of the interval. Only the changes in the anterior and septal base were significant ($P < 0.05$ for both). With VMCN stimulation only the septal base's EM interval shortened significantly ($P < 0.05$). In contrast, with VLCN stimulation the EM intervals for all segments shortened. However, only the four endocardial segments exhibited significant shortening ($P < 0.001$ for all) of their EM intervals. The LReL stimulation caused a mixed response. While six segments exhibited shortened EM coupling intervals, the intervals in the basal free wall segments, both epicardial and endocardial, were slightly longer with stimulation. The longer interval in the endocardial segment was significantly different ($P < 0.05$) from control. Both left cervical and thoracic vagal stimulations caused a mixed response in EM

intervals, none proving to be statistically significant.

Figure 32 shows the results of statistical analysis of these responses to right side cardiac nerve stimulation. RSS stimulation, similar to LSS stimulation, caused all EM coupling intervals to shorten. However, the changes in the posterior and lateral apex epicardial segments were not significant. The remainder of the epicardial and all of the endocardial segments showed significant changes in their EM intervals. Recurrent cardiac (ReC) stimulation also caused all EM intervals to shorten but with a slight change from RSS stimulation. During ReC excitation, the posterior and free wall case EM interval changes were not significant. However, changes for the rest of the muscle segments did prove to be statistically significant. Electrical excitation of the remaining right side cardiac nerves induced mixed responses, some segments showing longer and some shorter EM intervals. Only the change in the free wall apex during cranial vagal stimulation proved significant ($P < 0.01$). The rest of the changes for the caudal vagal, stellate cardiac, thoracic vagal and cervical vagal stimulations were not significant.

CHAPTER V

DISCUSSION

A. Control Time Intervals

The sequence of contraction of the left ventricle has been thought to follow the sequence of activation (71, 91). The sequence of electrical activation has been well established as starting in the lower septum (43, 77). From there it spreads to the upper septum and free wall apex (38, 43, 77) followed by the free wall base. The activation spread from the endocardium outward to the epicardium (38, 77). This should result in a sequence of contraction that spreads out in the same direction.

Data concerning the sequence of contraction are sparse and not complete. Rushmer (71) felt that the first areas of the ventricle to contract were the papillary muscles and trabeculae carnae. Rushmer came to this conclusion on the basis of two factors: (1) the papillary muscles were activated early and (2) the initial length change in the ventricle is in the longitudinal axis.

Gross studies on the sequence of contraction were also reported by Hinds et al., (28), using length gauges and Tsakiris et al. (88) using dyes and fluoroscopy. The only addition these reports made was that the inflow tract contracted before the outflow tract. Priola et al. (48)

confirmed this concept by measuring pressures in the inflow and outflow tract of the left ventricle. They found that the first rise in pressure in 10 of 14 experiments occurred in the inflow tract followed by the outflow tract 4 to 18 msec later.

The sequence found in the present studies does not totally confirm the above results. The inflow tract (the free wall) contracts at the same time as the outflow tract. These differences may be due to the different means of measurement. The strain gauge measurement is a direct recording from a localized piece of tissue. The two studies (28, 88) above were both measuring changes in the entire wall of the ventricle.

Some data concerning the sequence of contraction using strain gauge arches have been reported, Cronin et al. (14) and Armour and Randall (6) both used strain gauge arches to measure force of contraction and onset of force in the anterior and posterior papillary muscles of the left ventricles. Both reports (6, 14) challenged the idea that the papillary muscles contracted early. Both groups of investigators found that the papillary muscles contracted after chamber pressure had begun to increase. This means that papillary muscle contraction must occur late in the sequence, not early as hypothesized by Rushmer (71).

Measurements of the sequence of contraction of

other areas of the heart were included in the Armour and Randall report (6) and in a later paper by Armour, Lippincott and Randall (3).

The first paper (6) reported that the anterior epicardium contracted 61.2 ± 4.1 S.E. msec, the posterior epicardium contracted 52.0 ± 4.3 S.E. msec and the basal epicardium contracted 58.0 ± 2.7 S.E. msec after the Q-wave. These all preceded the rise in ventricular pressure which began to increase 71.9 ± 6.0 S.E. msec after the Q-wave.

Some measurements of sequence were also made by Armour, Lippincott and Randall (3). They found the epicardium contracted before the septum. This differs from the results shown in this study. The septal apex contracts before the epicardium with the septal base following. The difference in these reports may be due to placement of the strain gauge arches. The lower the placement of the gauge on the septum the earlier the onset of contraction. The other three segments measured by Armour et al. (3) showed Q-wave to contraction intervals of 54.6 msec for the septal base, 40.4 msec for the anterior epicardium and 35.4 msec for the posterior epicardium. The intervals measured in these experiments were similar to those reported by Armour et al. (3).

It has been established (77, 79, 82) that excitation of the free wall of the left ventricle spreads from

endocardium to epicardium. If the assumption is made that the electromechanical coupling intervals for all the muscle segments are the same, then to explain the simultaneous contraction of the free wall endocardium and epicardium, the spread of excitation cannot be from endocardium to epicardium. If the excitation does spread from endocardium to epicardium then the electromechanical coupling intervals must be different in the various muscle segments. To determine whether or not the electromechanical coupling intervals were all identical or not, the electrical sequence was measured using the unipolar electrodes positioned in the leg of the strain gauge and the electromechanical coupling intervals were measured using the unipolar electrodes and strain gauge arches.

The electrical activation of the left ventricle, as shown in Figure 6, was first seen in the lower septum. This corresponds to the data presented by Myerburg, Nilsson and Gelband (43) using microelectrodes. They found that the earliest muscle activation was at the junction of the lower and middle thirds of the septum. Myerburg et al. (43) found that the free wall apex followed the septal apex with the activation spreading up to the free wall base. Scher and Young (77) using a different technique found similar results concerning the free wall. The results in the present report indicate that the endocardial free wall segments were activated simultaneously.

Both Myerburg et al. (43) and Scher and Young (77) also found that the last endocardial muscle segment to be activated was the septal base. This was confirmed in these studies.

As shown in Figure 6 the electrical activity broke through to the epicardium at the anterior and posterior muscle segments. The two lateral segments were activated later. This confirms the observations of Lewis and Rothschild (38), Harris (26) and Scher and Young (77). With the exception of Harris (26) the above reports (38, 77) indicated that the lateral apex was activated before the lateral base. Harris (26) did not show enough data to confirm or deny the above observations. It was found in the present experiments that the lateral apex and lateral base were electrically activated practically simultaneously.

Figure 7 and Table III show that the electromechanical coupling intervals were different for the different muscle segments. It can be seen that while both the lateral base (LB) and lateral apex (LA) were activated later they both had shorter electromechanical (EM) coupling intervals ($P < 0.01$) than their respective underlying endocardial segments. These differences in EM coupling intervals explain the sequence of contraction seen across the free wall as shown in Figure 5. The shorter EM coupling intervals combined with the late activation of the epicardial segments resulted in nearly

simultaneous contraction with the endocardial segments.

The septal base, which also contracted relatively late in the sequence in spite of the early electrical activation is explained by the long EM coupling interval. Those areas which contracted early (anterior, posterior and septal apex) and were activated early also had relatively short EM coupling intervals.

Osadjan and Randall (46) have the only report in the literature dealing with the electromechanical coupling times in the intact heart. They recorded the EM coupling intervals from the apex and base of the epicardium and the interventricular septum. The septum interval was measured by inserting a long-legged strain gauge arch into the muscular portion of the septum. They found EM coupling intervals of 25 msec in the septum, 30 msec in the apex and 34 msec in the base. These EM coupling intervals are all about 20 msec less than those found in the present experiments. The differences might be explained by the preparation and variability in animals. The EM coupling intervals in the present experiments were measured in animals which had undergone more extensive surgery than the animals used by Osadjan and Randall (46). The variability between animals can be seen in the ranges given in the Osadjan and Randall paper (46). For the septum they showed a range of 5 to 58 msec for the EM coupling intervals. Similar ranges were found for the apex and base.

Further evidence for disparity of activity between the endocardium and epicardium has been given by several investigators measuring the duration of the action potentials through-out the ventricular walls. van Dam and Durrer (15) measured the refractory periods in the endocardial, myocardial and epicardial layers of the ventricle. They found that the refractory periods were longer in the endocardium than in the epicardium. Burgess et al. (12) confirmed and expanded the van Dam and Durrer observations. In addition the refractory periods in the apex were longer than those in the base both in the septum and free wall. Burgess et al. (12) concluded that the variability in refractory periods may be a protective device. The earliest areas activated have long refractory periods, whereas the later activated areas have relatively short refractory periods. With this arrangement recovery would be complete throughout the ventricle at the same time. This would reduce the probability that a re-entrant arrhythmia may occur,

The disparity of EM coupling intervals along with the sequence of electrical activation provides for a mechanism whereby the entire heart can contract more or less synchronously. If the endocardium were to contract long before the epicardium it would have to pull against the epicardium reducing its effectiveness. With the epicardium contracting at the same time as the endocardium

the entire force of contraction can be transmitted to the interior of the chamber.

B. Chronotropic and Inotropic Changes during Autonomic Cardiac Nerve Stimulation

Stimulation of the thoracic cardiac nerves in these experiments usually resulted in a change in either or both heart rate or force of contraction.

The data in Figure 8 confirms the results on heart rate presented by Mizeres (41), Levy et al. (36) and Randall and co-workers (21, 33, 53, 62, 63, 66). Geis, Kaye and Randall (21) in a paper dealing with innervation to the two nodes and the atria found the following. Increased heart rate could be elicited by stimulation of the right stellate ganglion, left stellate ganglion, right stellate cardiac, recurrent cardiac, VMCN, VLCN, and innominate nerves. As can be seen in Figure 8 there are several differences between Geis et al. (21) and the present data. The VMCN and recurrent cardiac stimulations resulted in a reduction in heart rate. Geis et al. (21) reported that recurrent cardiac stimulation increased rate in 6 of 17 experiments whereas it decreased rate in 8 of 17 experiments. Similar results were seen with VMCN stimulations. The data in Figure 8 are an average for all of the stimulations whether rate went up or down.

The rest of the nerves stimulated caused decreases in heart rate. This was similar to the results given by

Geis et al. (21) and Randall and Armour (60).

Using degeneration-stimulation studies, Mizeres (41) found that cardioaccelerator fibers were carried in all of the thoracic cardiac nerves. Injection of atropine (2 mg/Kg), which blocks acetylcholine combination with the receptor, caused all nerves except the innominate, VMCN, left cervical vagus, and left and right ganglia to elicit significant increases in heart rate when stimulated. The left and right stellate ganglia did not exhibit significant increases after atropine because they were not stimulated.

Mizeres (41) found sympathetic nerve fibers mixed in with parasympathetic nerve fibers in the thoracic cardiac nerves. Injection of the atropine (2 mg/Kg) unmasks these sympathetic nerve fibers by blocking the action of the parasympathetic nerve fibers upon the sinoatrial node. The sympathetic component in these nerves was small. This can be seen in Figure 8. Stimulation of the intact nerves gave substantial decreases in heart rate but after the injection of atropine, the increases were small but significant ($P < 0.05$ or better).

The major emphasis of the discussion of the inotropic changes will be the endocardial responses. The epicardial force changes due to stimulation of the thoracic cardiac nerves have been well documented using both strain gauge arches (20, 33, 47, 53, 57, 58, 59, 60, 62, 64, 65,

84) and functional refractory periods (34).

The innervation patterns, as defined by force changes recorded by strain gauge arches, of both ventricles has been reviewed by Randall, Armour, Geis and Lippincott (62). Their descriptions were of the epicardial surfaces of both ventricles, the septum and papillary muscles within both ventricles. The figures used to illustrate the force changes were an artist's representation of the force changes. Arrows pointed to the various areas of the ventricles and the various widths of the arrows gave relative comparisons of force changes due to stimulation of the nerve in question.

Figures 33, 34 and 35 are an artist's representation of the relative force changes found in the present experiments. The relative widths of the arrows indicate the magnitude of inotropic change from control. All of the nerves in Figures 33 and 34, when stimulated caused the force to increase, the larger the force increase the greater the width of the arrow. The nerves illustrated in Figure 35, when stimulated, all caused the force of contraction to decrease. The wider arrowheads indicate the larger decreases in force of contraction.

Only six of the eight muscle segments studied (Table 4) are included in Figures 33, 34, and 35. The two areas not included are the anterior and posterior epicardial surfaces. Both the anterior and posterior epicardial

muscle segments exhibited increased force of contraction when either the left (LSS) or right (RSS) stellate ganglia were stimulated. With LSS stimulation the increase in the posterior segment was significantly greater than the anterior ($P < 0.05$) (Table 4 and Figure 12). The fibers from the left stellate ganglion reach the anterior surface through the innominate (INN), ventral medial cardiac nerve (VMCN), ventral lateral cardiac nerve (VLCN), and the left recurrent laryngeal (L Re L).

The last nerve listed (L Re L) was not discussed in any of the papers listed above concerning small nerve innervation of the ventricles (20, 33, 47, 53, 57, 58, 59, 60, 62, 64, 65, 84). This nerve is an important pathway for both sympathetic and parasympathetic fibers that reach the heart. As can be seen in Figure 8, stimulation of this nerve caused significant ($P < 0.001$) slowing of heart rate before atropine. Following atropine injection (1 mg/kg) heart rate increased significantly ($P < 0.01$) when the L Re L was stimulated. Stimulation of the L Re L also had an effect on force of contraction (Tables 5 and 6).

Randall et al. (62) found that the INN, VMCN, and VLCN all innervate the anterior segment with the stimulation of the INN giving the greatest force change. In these experiments stimulation of the VLCN resulted in the greatest force increase.

The primary pathways for fibers from the right

stellate ganglion were the recurrent cardiac (Re C) and stellate cardiac (St C) with the Re C being the major pathway (Table 4). This agrees with Randall et al. (62).

The posterior segment was innervated by both left and right stellate ganglia. The major pathways from the two ganglia were the VLCN and Re C respectively. The INN, L Re L and St C also supply fibers to the posterior muscle segment but to a lesser extent (Table 4). The extension of the recurrent cardiac (Re C) to the posterior surface was not reported by Randall et al. (62). They found that the Re C primarily innervated anterior surfaces of the left ventricle. They also found that the Re C stimulation primarily caused increased force in the anterior papillary muscle with little or no increase in the posterior papillary muscle (5, 62). In these experiments it was found that the Re C does innervate the posterior epicardial surface but to a lesser degree than it did the anterior surface (Table IV).

Figure 33 illustrates the left side innervation patterns of the remaining six areas studied, septal base (SB), septal apex (SA), free wall base (FWB), and free wall apex (FWA) of the endocardium and the lateral base (LB) and lateral apex (LA) of the epicardium. The left thoracic vagus when stimulated caused a decrease in force and is shown in Figure 35. The arrows in Figures 33, 34, 35, 36, and 37 are not intended to show how the nerves

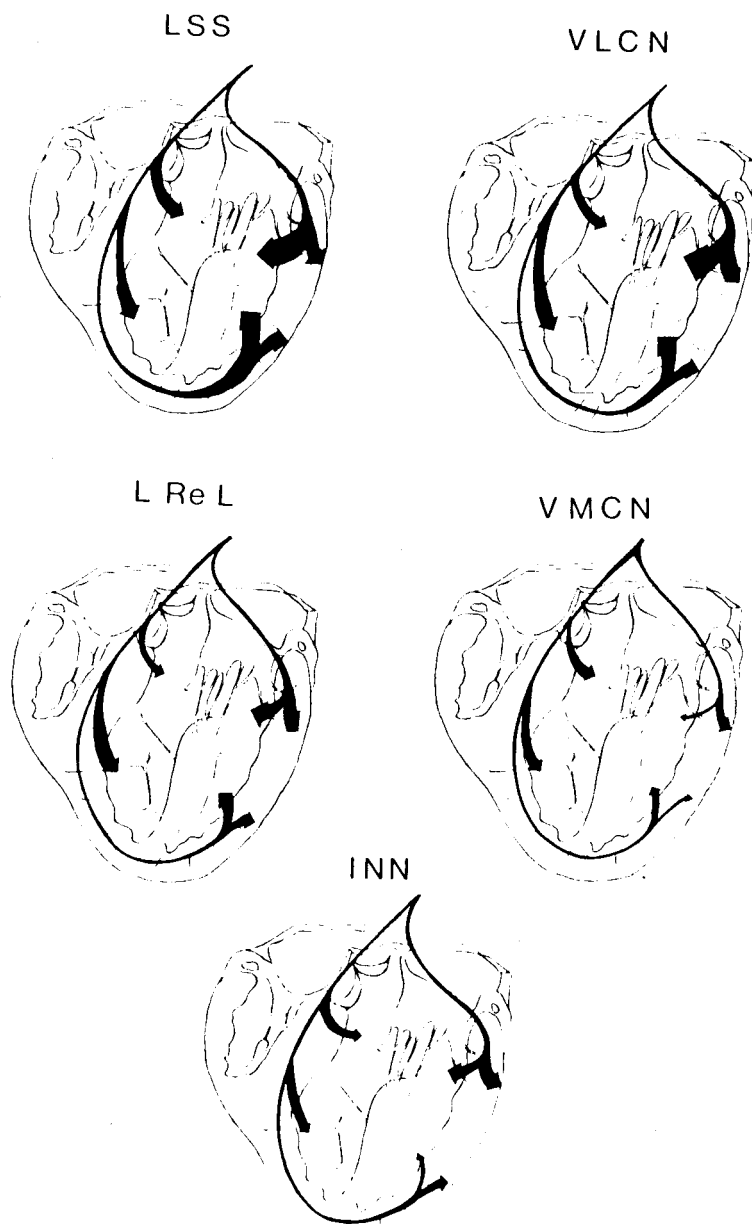


FIGURE 33
INNERVATION PATTERNS--POSITIVE INOTROPIC
LEFT SIDE NERVES

FIGURE 33

LEGEND

Figure 33 illustrates the relative force increases caused by stimulation of the left side cardiac nerves. The nerves illustrated are the left stellate ganglion (LSS), ventral lateral cervical cardiac nerve (VLCN), left recurrent laryngeal nerve (L Re L), ventral medial cervical cardiac nerve (VMCN) and innominate nerve (INN). The relative width of the arrowheads indicates the relative amount of force increase caused by stimulation of a given nerve. The arrows are not designed to illustrate the pathway of innervation. The arrows were drawn using the data shown in Table IV.

reach the heart or course through the heart. The relative size of the arrowhead indicates the relative increase or decrease in the magnitude of the force of contraction (Table IV and Figs. 12, 14, 16). Stimulation of all the nerves shown in Figure 33, except the VMCN, caused the force of contraction to increase in varying amounts in all six muscle segments studied. The VMCN stimulation caused force to increase in four of the six segments.

Stimulation of the left stellate ganglion (LSS) resulted in profound increases in force in all areas as was expected (36, 66). The significantly larger (see Fig. 12) increase in the free wall base and free wall apex was only partially expected. Armour and Randall (5) found that anterior and posterior papillary muscle forces were significantly larger than the respective overlying anterior and posterior epicardial muscles. No attempt was made to explain why the papillary muscles exerted more force than their respective overlying epicardial muscle segments.

The ventrolateral cardiac nerve (VLCN) which is known (62) to be the major pathway of the left side sympathetic fibers to the left ventricular epicardium was found to be the major supply to the left ventricular endocardium also (Table 4 and Fig. 33). Again as with the LSS, the free wall base and apex both had significantly higher force increases (Fig. 14). In contrast to the LSS

where both the free wall base and apex forces were significantly higher than their respective overlying epicardial force of contraction (Fig. 12A and B), only the free wall base force of contraction was significantly higher than the lateral base force of contraction (Fig. 14J) with VLCN stimulation. The free wall apex and lateral apex had similar increases with VLCN stimulation in both LV papillary muscles. Randall et al. (62) also show a larger force difference between the septal apex and septal base than was found in these experiments.

The left recurrent laryngeal (L Re L) stimulation augmented force in the septum to a similar degree as did the VLCN, but did not have as great an influence on the free wall either epicardially or endocardially. Augmentation of force across the free wall was approximately equal for the respective overlying-underlying muscle segments. The VMCN and INN both innervate the septum equally but the similarity ends there. The innominate stimulation had more effect on the basal portions of the free wall than the apical regions. Randall et al. (62) found that the innominate had profound influence on the papillary muscles with much less effect on the free wall segments. Kralios et al. (34) in measuring both T-wave and refractory period changes during INN stimulation found little change. In only 9 of 22 T-wave experiments and 7 of 23 refractory period experiments were any changes noted and these changes

were not consistent. They concluded the innominate had little effect on the left ventricle.

As Randall et al. (62) reported the VMCN fibers do not project to the free wall of the left ventricle in any appreciable numbers. The VMCN projects primarily to the interventricular septum. This observation was confirmed by Kralios et al. (34). They found that VMCN stimulation caused septal refractory periods to change in 13 of 15 experiments. However, the changes in free wall portions of the LV were inconsistent and not present in all animals.

Figure 34 demonstrates the nerve projections and relative force increases during stimulation of those right side nerves which increased force of contraction when stimulated before atropine (Table 4, Figs. 13, 15, 16). Stimulation of the right stellate ganglion resulted in large force increases in all muscle segments as expected (64). The force increase was approximately equal for both septal base and septal apex. The free wall base (FWB), as with LSS stimulation, had the largest increase in force with RSS stimulation (Fig. 13). The apical regions of the free wall, both epicardially and endocardially in contrast to the LSS stimulation had nearly identical increases in force of contraction. With LSS stimulation the free wall apex (FWA) force increased significantly more than the lateral apex (LA) ($P < 0.01$) (Fig. 12).

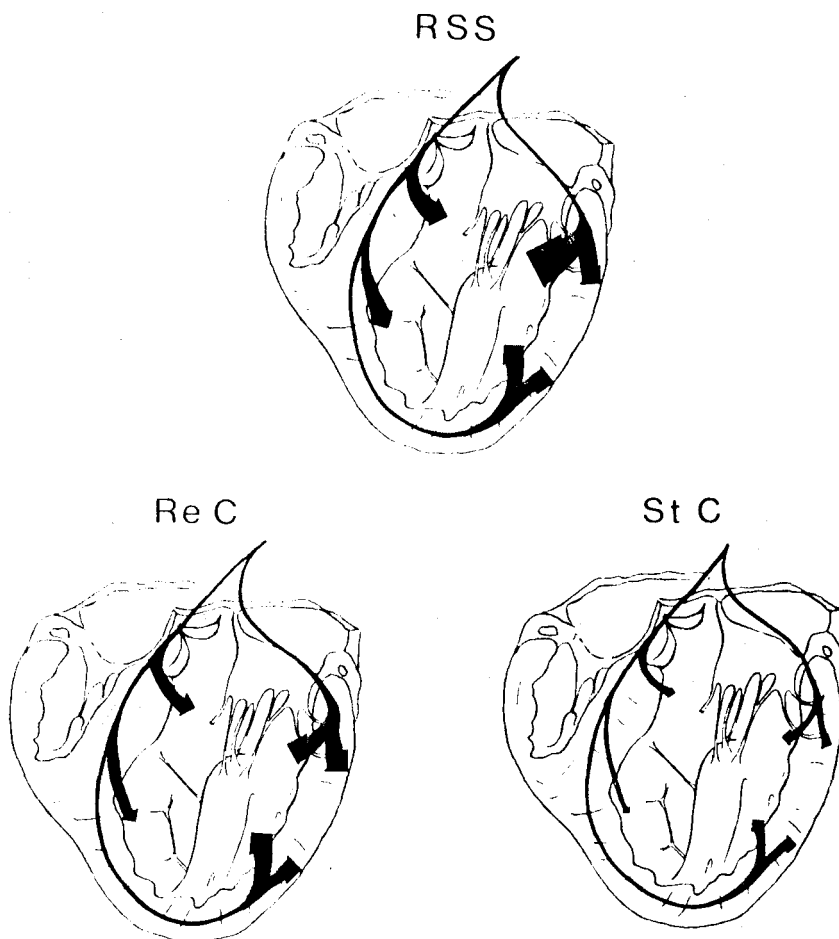


FIGURE 34
INNERVATION PATTERNS--POSITIVE INOTROPIC
RIGHT SIDE NERVES

FIGURE 34

LEGEND

Figure 34 illustrates the innervation patterns of the right side nerve stimulations that resulted in increased force of contraction. The nerves stimulated were the right stellate ganglion (RSS), recurrent cardiac nerve (Re C) and the stellate cardiac nerve (St C). See Figure 33 for further explanations.

The recurrent cardiac nerve was known to have its major projection to the right ventricle (62, 64) with fibers also reaching the anterior surface of the LV (62) and the LV anterior papillary muscle (5). The recurrent cardiac was also found to cause slightly larger changes in force in the septal apex than septal base (62). The above differs slightly from that found in these experiments. The septal base and septal apex exhibited nearly identical changes when the Re C was stimulated. The Re C when stimulated did cause the force in the epicardial and endocardial basal segments of the free wall to increase equally and significantly ($P < 0.05$) more than the septal forces (Fig. 15). Randall et al. (62) found that Re C actually had less effect on the free wall basal muscle segments than on the septum. The Re C also has fibers that reach the apical portions of the free wall with the endocardium exhibiting the same degree of force change as the basal portions with the epicardium displaying a smaller force increase (Table 4 and Fig. 15).

The stellate cardiac (St C) nerve is known to be primarily a rate nerve. It sends most of its fibers to the SA node to increase heart rate (21, 34, 62). It also has been demonstrated to have minor contractility influence (62). This was confirmed in the present study. Figure 8 shows that St C stimulation did cause a significant increase ($P < 0.01$) in heart rate both before and after

atropine. Figure 34 shows that while St C stimulation did cause all areas to exhibit increased force of contraction this increase was not very great.

Several of the cardiac nerves when stimulated not only decreased heart rate (Fig. 8) but also reduced the force of contraction of the muscle segments studied. These nerves are included in Fig. 35. The relative widths of the arrowheads indicate the relative magnitude of the force decrease. The wider the arrowhead, the greater the decrease in force of contraction. The force measurement was made following stimulation after heart rate had returned to normal (see Fig. 10 Ca V) (47, 60, 64). Right thoracic vagal (RTV) stimulation has been shown to cause decreased force of contraction both during pacing (47) and after heart rate has returned to normal (64). In these experiments the RTV stimulation decreased force in all muscle segments studied. The largest decrease occurred in the free wall base (FWB) with the smallest decrease in the free wall apex (FWA) (Table 4).

The craniovagal (Cr V) had a minor effect on force of contraction. In some animals Cr V stimulation resulted in an increase in force while in others force decreased. Randall et al. (62) reported that the caudovagal (Ca V) nerve stimulation did result in a slightly greater decrease in force in the anterior apex than in the basal portions of the left ventricle. It was found in these experiments

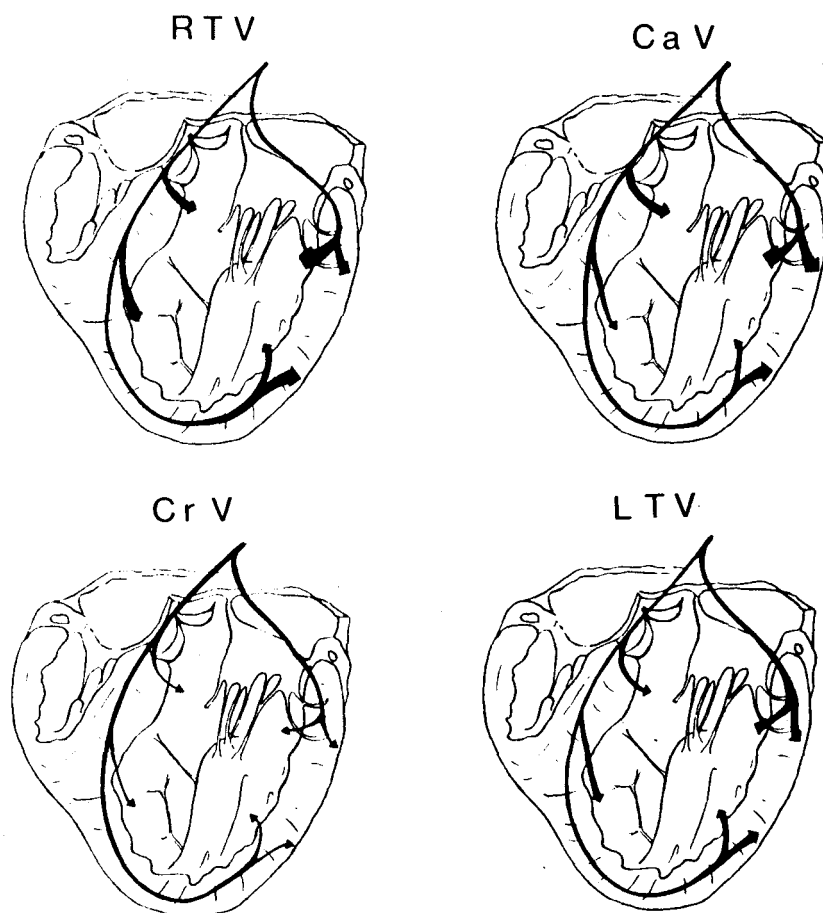


FIGURE 35
INNERVATION PATTERNS--NEGATIVE
INOTROPIC NERVES

FIGURE 35

LEGEND

Figure 35 illustrates the innervation patterns of those nerves that caused a force decrease when stimulated. The nerves stimulated were the right thoracic vagus (RTV), caudal vagus (Ca V), cranial vagus (Cr V) and left thoracic vagus (LTV). In this figure the size of the arrow indicates the relative decrease in force of contraction. The wider the arrow the greater the decrease in force. The data can be found in Table IV.

that the basal endocardium and epicardium and the apical epicardium of the free wall all decreased approximately equally. The free wall apex endocardium exhibited only a small decrease in force of contraction.

The left thoracic vagus (LTV) below the L Re L-LTV junction contained fibers that when stimulated caused slowing (Fig. 8) and a slight decrease in force in all muscle segments studied (Table IV, Fig. 35). The degree of decrease was similar in all muscle segments. Randall et al. (64) found that the apex and base epicardium of the LV had nearly identical decreases in force.

In order to study a pure response to sympathetic stimulation atropine (2 mg/kg) was injected. Following the atropine injection some, but not all, of the small cardiac nerves were restimulated. In attempts to keep the experiment as short as possible usually only the nerves which had caused cardiac slowing before atropine were restimulated following atropine injection. It was observed that some animals began to deteriorate after 2-3 hours of pump time. Fluid volume in the oxygenator would drop indicating a pooling of fluid in the dog.

Figure 36 diagrams the nerve projections and the relative magnitudes of force increases that occurred when the left side cardiac nerves were stimulated. The VLCN and INN diagrams do not include projections to either the septal base or the septal apex because insufficient data

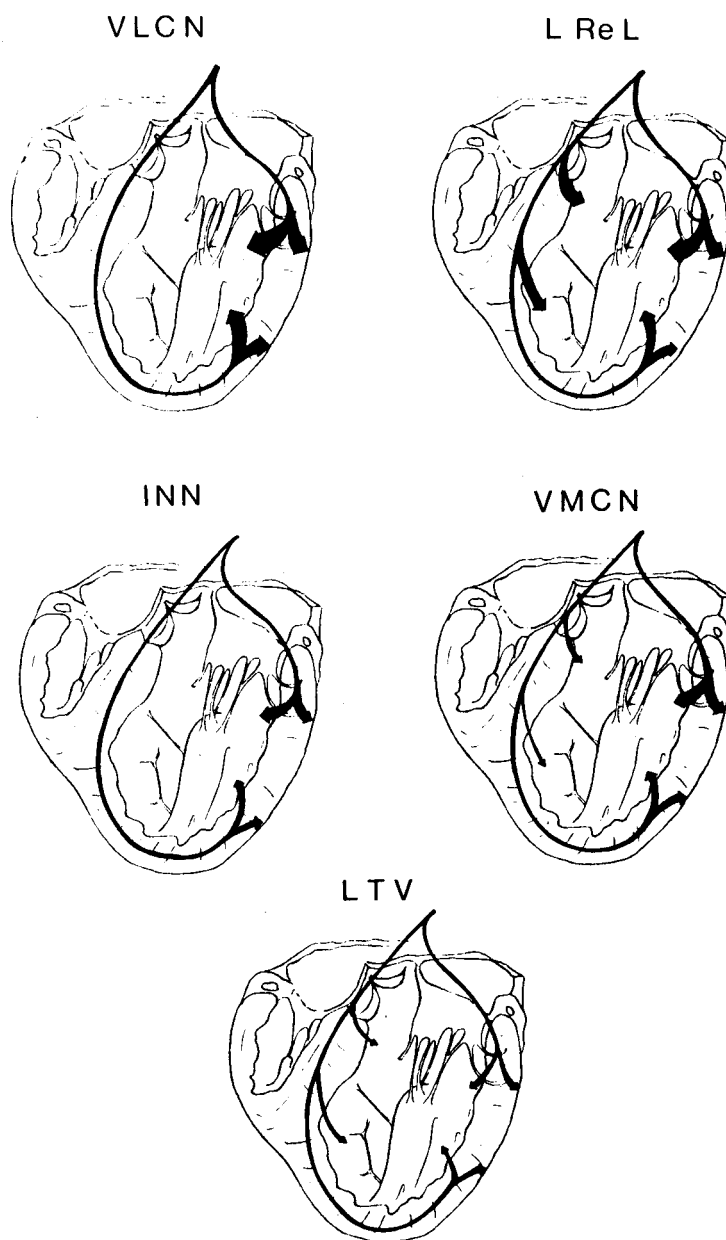


FIGURE 36
INNERVATION PATTERNS--LEFT SIDE
NERVES AFTER ATROPINE

FIGURE 36

LEGEND

Figure 36 illustrates the relative force changes that occurred with left side cardiac nerve stimulation. Atropine (2 mg/Kg) was injected prior to the stimulations. The relative widths of the arrowheads indicate the relative increases in force.

were collected to show projections to those segments. These figures are not intended to show a lack of projection to those areas.

The VLCN, presumed to be primarily a sympathetic nerve (62, 65, 34, 40, 41), gave nearly similar results when stimulated after atropine as it did before atropine. Any minor differences in the response before and after atropine (Tables IV and V) were due to the variability among animals and the fact that not all animals had their VLCN stimulated both before and after atropine.

Following atropine all muscle segments except the septal apex exhibited increased force of contraction with L Re L stimulation. It was shown earlier (Fig. 8) that the L Re L did carry parasympathetic fibers. The increase seen following atropine was probably the result of the removal of the depressing parasympathetic fibers stimulated in the intact nerve. The response to stimulation following atropine was the pure sympathetic response.

Both the INN and VMCN exhibited similar types of responses when stimulated. Following atropine both nerves caused similar patterns but slightly higher force responses. This may again be due to removal of parasympathetic suppression. The differences in response before and after atropine may also be due to animal variability.

The left thoracic vagal stimulation, in contrast to before atropine, now caused force to increase in all

muscle segments studied. The posterior and lateral epicardium exhibited the larger increases with the anterior epicardium and the septum increasing in force but to a lesser degree. This was similar to the results reported by Randall et al. (62) for the atropinized LTV stimulation.

With some minor differences, recurrent cardiac stimulation following atropine was nearly identical to that preceding atropine. The same was true for the stellate cardiac stimulation.

Following atropine the craniovagal (CrV), caudovagal (CaV), and right thoracic vagus (RTV) all caused force of contraction to increase when stimulated (Figure 37). Randall et al. (62) have shown that the RTV contained only a small number of sympathetic fibers. Stimulation of the RTV had more of an effect in the right ventricle with minimal force changes in the left ventricle. In these experiments force changed less than 10% with RTV stimulation. The caudovagal contains even fewer sympathetic fibers to the left ventricle (62). In these experiments the sympathetic component in the caudovagal was small. Force did not increase much with stimulation. The craniovagal in contrast did contain a significant amount of sympathetic fibers. Upon stimulation, force increased in all segments to varying degrees. The increase was slightly higher in the free wall than the septum with the increases across the free wall approximately similar. Randall et al.

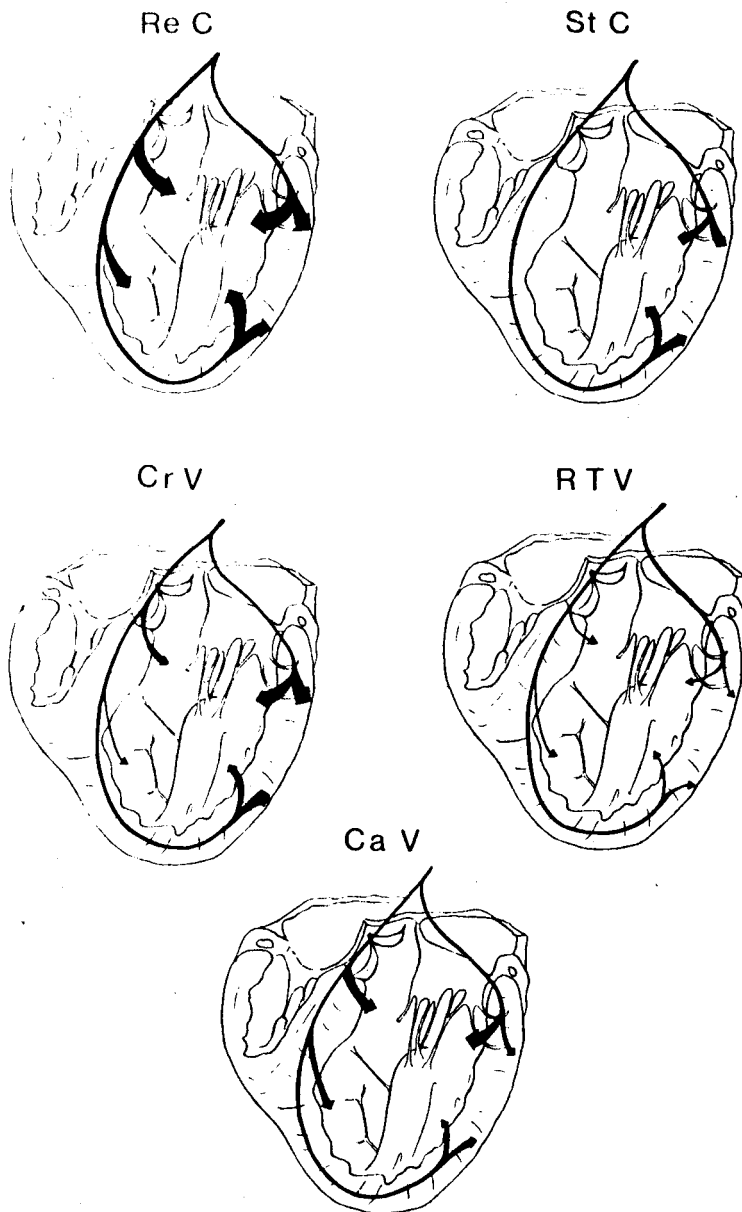


FIGURE 37
INNERVATION PATTERNS--RIGHT SIDE
NERVES AFTER ATROPINE

FIGURE 37

LEGEND

Figure 37 illustrates the relative force changes that occurred with right side cardiac nerve stimulation. Atropine (2 mg/Kg) was injected prior to the stimulations. The relative widths of the arrowheads indicate the relative increases in force.

found that the craniovagal when stimulated caused force changes across the anterior surface, the septum and both papillary muscles. They found that the increase was about equal in the free wall and septum.

Isoproterenol injection (1 γ /kg) at the end of each experiment elicited profound force increases in all muscle segments. The free wall base (FWB) and lateral base (LB) both had nearly identical force changes. These two areas had the highest increases but these were not significantly different from the changes in the rest of the left ventricle except the anterior and septal apex muscle segment (Fig. 19). The lateral apex (LA) and free wall apex (FWA) segments also had nearly identical force changes.

C. Time Interval Changes with Small Nerve Stimulation

Webster's New World Dictionary defines the term synchronous as "happening at the same time." It is well known that ventricular contraction is not synchronous (3, 6, 28, 73, 76, 88). However, a number of different authors have postulated a change in synchrony as a partial explanation as to the increase in force of contraction that occurs with sympathetic stimulation (46, 56, 75, 76, 91). Wiggers (92) introduced the term fractionate contraction to describe the contraction of the smallest imaginary units of muscle tissue. He applied this concept as follows.

The intraventricular pressure curve was the result of the summation of the cardiac muscle contractions, which occurred at differing times.

Thirty-eight years later Randall and Priola (56) postulated that with sympathetic stimulation these small muscle unit contractions occur more synchronously. They do not occur at exactly the same time but closer together in time. As a result the sum of the contractions is higher. In addition, each muscle unit generates more tension so that the sum is higher. This hypothesis was based on the use of three strain gauge arches in one series of experiments (46) and intraventricular pressure records from another series of experiments (56).

The data collected during the R-wave to mechanical onset time interval were analyzed in two ways. The mean time intervals before and after stimulation were analyzed using the t-test. The results were presented in Figures 22 and 23 and Table A-3 through A-10 in the Appendix. The values for the R-wave to mechanical onset time intervals before and after stimulation were compared by the analysis of variance and are tabulated in Appendix Tables A-19 and A-20. These tables indicate the degree of significance between each of the eight muscle segments before and after stimulation. Tables A-19, A-20, A-21 and A-22 show only whether or not there was a significant difference in the time intervals between one muscle segment and any of

the other muscle segments. The numbers that are being compared can be found in the respective Appendix tables A-3 through A-18. To the left of the hyphen is the control situation with the stimulation relationship shown to the right of the hyphen (see the Table legends for further explanations). As can be seen most of the pairs of time intervals were not significantly different. This is indicated by the zero. However, some of the pairs were significantly different before and after stimulation.

Left stellate ganglion stimulation had several effects on the muscle segments studied. It increased force in all areas as shown before. It caused all of the segments to have a shorter R-wave to mechanical onset time intervals with six of those changes being significant (Fig. 22). Also LSS stimulation caused fewer of the time intervals to be different by the analysis of variance (Table A-19). Before stimulation twelve of the pairs of intervals were significantly different. After stimulation only seven pairs were different. While the left stellate stimulation was causing all of the intervals to change some of the intervals were changing more than others. The septal base and free wall apex, both endocardial segments, each had shorter time intervals such that they were no longer significantly different from the rest of the time intervals. The anterior epicardium and the septal apex continued to contract first but following stimulation the

rest of the segments contracted nearly simultaneously, indicating a more synchronous contraction. Osadjan and Randall (46) described similar results using only three gauges. With LSS stimulation the three segments studied, basal and apical epicardium and septum all began to contract more simultaneously than they had before stimulation.

Right stellate (RSS) stimulation also elicited changes in the R-wave to mechanical onset time intervals. Only the two lateral apical muscle segments did not have significantly different intervals after stimulation (Fig. 23). The rest of the muscle segments' time intervals were significantly shorter following stimulation. As with LSS stimulation the number of pairs of intervals that were different decreased. The posterior segments' time interval did not shorten to the degree of the free wall apex, free wall base and septal base. As a result these time intervals were not different after stimulation, whereas they had been different during control. The septal apex also began to contract nearly simultaneously with the free wall apex and septal base during stimulation. As can be seen from Table A-20, other than the anterior segment, the rest of the segments contract more synchronously after stimulation.

As can be seen in Figures 22 and 23 stimulation of the small thoracic cardiac nerves did not have the same effect as either of the stellate stimulations. This was

expected. Mizeres (40, 41), Hirsch (29) and Wechsler et al. (90) all have reported that the major sympathetic outflow to the heart is through the stellate ganglia. This outflow then divides into five or six different small thoracic cardiac nerves on both sides. None of these small nerves could have the effect that the stellate would have when stimulated.

Neither the innominate (INN) nor the ventromedial cardiac (VMCN) nerves when stimulated had much effect on the time intervals. With INN stimulation only the anterior segment exhibited significant shortening ($P < 0.05$) and the number of pairs of intervals that were significantly different decreased slightly (Fig. 22 and Table A-19). The VMCN stimulation resulted in intervals that were unchanged (Fig. 22) while the analysis of variance showed that more pairs of numbers were significantly different compared to those before stimulation. Force was increased slightly in all areas but the time intervals were unchanged.

Stimulation of the left thoracic vagus (LTV) elicited similar results. No time intervals changed with stimulation. Also there was no change in the number of intervals that were significantly different (Table A-19).

Left recurrent laryngeal (LReL) stimulation resulted in a mixture of shortening and lengthening of the R-wave to mechanical onset time intervals. However, only one of these changes, the septal apex ($P < 0.05$) was

significant. When the control and stimulation values were compared by the analysis of variance, the total number of pairs that were significantly different decreased (Fig. A-19) suggesting a more synchronous contraction. However, due to the large increases in the free wall apex and free wall basal time intervals some pairs of segments were different after stimulation which were not different before (Fig. A-19).

Of the left side thoracic cardiac nerves the ventro-lateral cardiac nerve when stimulated caused the most muscle segments to have shorter time intervals. These muscle segments were the free wall apex and the septal apex and base. Analysis of variance of the data from the VLCN stimulation showed that the number of pairs of different intervals was smaller with stimulation. This indicates that the muscle segments were contracting more synchronously after stimulation.

Recurrent cardiac (ReC) stimulation resulted in the greatest disparity between the change in time intervals before and after stimulation and the number of pairs that were different before and after. With ReC stimulation not one muscle segment exhibited a time interval that was changed (Fig. 23). However, the number of pairs of times intervals that were significantly different decreased from nine before stimulation to two during stimulation. Of all the nerve stimulations studied it was the ReC that elicited

the greatest effect on the left ventricular R-wave-to-mechanical onset time intervals. This was not expected since it was found earlier in these experiments that the left side nerves had a larger effect on force changes.

Of the three vagal nerve stimulations on the right side the caudal vagal and right thoracic vagal stimulations resulted in some significant changes in the time intervals (Fig. 23). However, only the cranial vagal stimulation increased the synchrony of the LV contraction (Table A-20). The number of significantly different pairs decreased from 10 during control to 7 during stimulation. The caudal vagal (CaV) stimulation resulted in a mixture of responses with the end result being no change in the total number of pairs different before and after stimulation. The right thoracic vagus decreased the synchrony of contraction when stimulated.

The electrical-electrical time intervals were analyzed using the analysis of variance to compare all eight segments to each other before and after stimulation and paired t-test to compare each segment to itself before and after stimulation. No significant changes were found. Wallace and Sarnoff (89) reported that cardiac sympathetic nerve stimulation did not change conduction velocity in the Purkinje fibers and had only a minor effect on conduction through ventricular muscle. They also found that neither the pattern nor the sequence of ventricular

activation was altered by sympathetic stimulation. Thus the few changes seen above in the R-wave to mechanical onset time intervals cannot be explained by a change in the electrical activity of the ventricle. The electro-mechanical (EM) coupling time was studied before and after stimulation to see if it changed.

As described above, with left side stimulation the major changes in EM coupling intervals were found with the left stellate (LSS) ganglion and VLCN. The other left side cardiac nerves caused only minor changes in electro-mechanical coupling intervals. In comparing the muscle segments that had shown significant changes in R-wave to mechanical onset time intervals (Fig. 22) with LSS stimulation it can be seen in Fig. 31 these same muscle segments also exhibited significant changes in EM coupling intervals. The muscle segments all exhibited nearly identical EM coupling intervals following stimulation whereas during control there was a great deal of variability between the muscle segments' EM intervals (Table A-21). The largest changes in EM coupling intervals were exhibited by the four endocardial muscle segments. They all had long EM coupling intervals during control which shortened considerably with stimulation.

When the electrical-electrical time interval (Fig. 6) and the EM coupling interval were added together for each muscle segment, there existed a 30 msec spread

between the first and last muscle segments to contract. During stimulation this spread decreased to 19 msec. The contractions of the muscle segments were more synchronous during stimulation than during control.

When stimulated the ventrolateral cardiac nerve (VLCN) caused similar results to LSS stimulation. This was expected since the VLCN is the major pathway for fibers from the left stellate ganglion to the heart (40, 62). The VLCN stimulation did not cause any of the epicardial EM coupling intervals to shorten. All of the endocardial EM coupling intervals did shorten with stimulation (Fig. 31 and Tables A-15 through A-18). Fig. 22 shows that VLCN stimulation resulted in significant changes in the R-wave to mechanical onset in 3 of the 4 endocardial muscle segments with no change in the remaining five muscle segments. When the electrical-electrical time interval and the EM coupling interval are summed, the result is the time from LVA electrical activation to the onset of contraction in a muscle segment. This interval is similar to the R-wave to contraction interval. By using the difference in the total summed time interval for the fastest and slowest time a change in synchrony can be seen. If the difference is smaller after stimulation than during control it indicates that the synchrony of the muscle contractions has increased. VLCN stimulation caused the difference between the highest and lowest

summation to decrease from 27 msec during control to 20 msec.

Of the right side thoracic nerves that are known to change heart rate or force of contraction, only the right stellate ganglion and the recurrent cardiac nerve caused significant changes in EM coupling intervals. The right stellate ganglion stimulation shortened the EM coupling interval in all four endocardial muscle segments and the anterior and lateral basal portions of the epicardium. It was shown earlier that the RSS did not cause as large force changes in the posterior and lateral apical segments as it did in the other six segments. The RSS also did not cause changes in EM coupling intervals in those same two segments. Those segments which exhibited large decreases in R-wave to mechanical onset time intervals, primarily anterior and septal base, demonstrated large decreases in EM coupling interval. The septal base change was slightly greater than the anterior change. As a result the time spread between these two segments, which were the first and last respectively to contract, decreased from 26 to 19 msec with stimulation. This change was not as great as the change with LSS stimulation. Nevertheless, it still indicates a more synchronous contraction during RSS stimulation.

The recurrent cardiac nerve (ReC) stimulation differed from the previously discussed stimulations. ReC

stimulation resulted in force changes in all muscle segments (Table 5) and changes in EM coupling intervals in six of eight muscle segments (Fig. 32) but did not affect the R-wave to mechanical onset interval in any of the muscle segments.

It is clear from the above discussion that with cardiac nerve stimulation synchrony between the various muscle segments increased. The concept of increased synchrony with sympathetic stimulation has been advanced by other investigators (3, 22, 46, 49, 55, 71, 75, 76). Sarnoff and co-workers (76) felt that the external work and power were influenced by both the contraction of the individual myocardial fibers and the synchrony of their contractions. As the authors observed, if the sequence of ventricular contraction was prolonged so that some cells were contracting as others relaxed, no external work would be performed. They concluded that synchrony was involved with generation of force by the following experiments (22, 75): Hearts were paced from the atrium and chamber pressures were measured. The site of pacing was changed to the ventricle and again the chamber pressures were recorded. It was found that both cardiac output and LV stroke-work fell with ventricular pacing. Also the pulse contours exhibited a "less brisk initiation of ventricular systole" (22, 75). The authors felt that the lower rate of rise of pressure and the reduced stroke

work at any end-diastolic volume was indicative of a change in synchrony. With norepinephrine infusion at any end-diastolic volume, stroke work increased. This they felt was the result of both increased inotropy and synchrony.

D. Cardiac Neuromuscular Junctions

Randall, Armour, Geis and Lippincott (62) and Kralios, Martin, Burgess and Millar (34) postulated that the respective changes in force and repolarization times was a function of the distribution of the cardiac nerves. Both groups felt that a larger response by one muscle segment compared to another muscle segment was the result of the first area being more highly innervated than the second area.

With the advent of the electronmicroscope the motor end-plates were able to be described. In his book The Innervation of the Vertebrate Heart Edwin Hirsch (29) reviewed the early works concerning the innervation of the myocardium. The general consensus amongst the early workers such as Gerlach, Fischer, Retzius, Berkly and others was that the myocardium was richly innervated by nerves that had varicosities. These nerves lay between the muscle cells along the longitudinal axis of the cell. In some instances the nerves were thought to actually enter the cell. In no case was a motor end-plate described. Hirsch himself (30, 31) also described the canine

innervation patterns. He saw a rich innervation running parallel to the muscle fibers. These nerves finally formed perimysial plexi around muscle bundles. Hirsch felt that the neuromuscular relationships were synaptic but he could not see any neuromuscular junctions.

Akio Yamauchi (94) has reviewed the literature concerning the neuromuscular junctions between autonomic nerves and effector organs. In general these nerves consist of narrow portions (0.1-0.5 μ in diameter) separated by enlarged areas (1.0-1.5 μ). These enlarged areas of varicosities contain mitochondria and vesicles. These varicosities are usually uncovered by Schwann cells and their membranes lie close to that of the effector cell. It is thought that these enlarged areas are the neuromuscular junctions. The membrane to membrane distance has been measured between 60-200 \AA .

It has been established that the atria are more highly innervated than the ventricles (1, 17, 18). As a result much of the work concerning cardiac neuromuscular junctions has been conducted in the atria and nodes. Yamauchi and Burnstock (95) studied the trout SA node and found that all of the cells had at least one contact with a nerve. Some of the cells had up to eight contacts of less than 200 \AA distance. In some cases the nerves actually penetrated the cells. The cell made a tunnel of sarcolemma which contained the nerve.

J. C. Thaemert has studied and described the fine structure of the A-V node (87) and the fine structure of the neuromuscular junctions (85, 86) in the mouse heart. He was able to find close contact between the nerves and the muscle in all tissues studied except the ventricular apex. These contacts in some cases exhibited a gap of up to 775\AA between the nerve and myocardial cell. When the gap was smaller (160\AA) the nerve appeared to be "nestled" into a depression in the sarcolemma (85). Using serial sections Thaemert (86) was able to describe a small portion of the AV node. The portion he used consisted of two fascicles containing 68 and 87 cells respectively. Of the 68 cells in one fascicle 34 of them were seen to be in "intimate contact" with a nerve. Only 15 of the 87 cells in the second fascicle were in contact with a nerve. This means that only 50% and 17% respectively of the cells in the two fascicles were in contact with a nerve in an area that is considered to be highly innervated (94). Thaemert (86) however did feel that since his sections did not include an entire cell but at most one-third of a cell that it was possible that all the cells were in contact with one or more vasculated nerves. Using the serial sections Thaemert (86) was able to describe the three-dimensional structure of the nerves. They were as described by earlier workers (94), vesiculated with the expansions being of variable size. He also found that

many of the nerves lay in a sarcolemma-lined tunnel. In some cases the nerve would end in a blind cul-de-sac within a cell.

Thaemert (85) was able to find and describe neuromuscular junctions in the ventricular myocardium, that were similar to those he described in the AV node (86). He described a nerve that had a vesiculated enlargement that was approximately 260\AA from the muscle cell membrane. Another neuromuscular junction he described was a nerve process that fit into a "cup-shaped depression" in the sarcolemma. The membrane-to-membrane distance observed was 150\AA . Hadek and Talso (25) using the rat heart had some difficulty finding neuromuscular junctions. They were able to describe some neuromuscular junctions and some structures that looked like neuromuscular junctions. However they did not find very many junctions.

The low number of neuromuscular junctions in the ventricular myocardium supports the observations of Angelakos et al. (1), Ehinger et al. (82) and Friedman et al. (81). They observed that there are fewer nerve fibers, both adrenergic and cholinergic, in the ventricles than in the atria.

As a result of the above observations it can be concluded that: (1) in areas that are supposedly highly innervated (AV node) it is hard to demonstrate that all cells are in contact with nerves; and (2) the ventricles

have even fewer nerves and, therefore, it is probable that not all cells are innervated.

E. Synchrony Changes: Cellular Level

It has been shown in these experiments that stimulation of the autonomic nervous system will cause a change in either the R-wave to mechanical onset interval or the electromechanical coupling interval, but not in the electrical-electrical time interval. Those nerves that are known to be sympathetic (62) caused the electrical onset to mechanical onset time to shorten. To shorten that interval the cells must either be activated faster or contraction must occur faster. Wallace and Sarnoff (89) have shown that stimulation of the sympathetics does not change the speed of conduction through the Purkinje fibers. Therefore the muscles cannot be activated faster. This means that the contraction must occur faster.

The strain gauge measures the response of a large number of cells to the stimulation. Using the strain gauge it is not possible to separate whether all the cells are changing their contractile speed or only some are changing contractile speed. However, several factors are known that allow for speculation as to which of the above is probably happening.

Carl Wiggers (91) concluded that since different cells were activated at different times they must also contract at different times. He called this "fractionate

contraction." He felt that increased force was the result of an increased synchrony of contraction of the individual areas. Sarnoff and co-workers (22, 75, 76) and Randall and co-workers (46, 49, 56) also postulated synchrony changes leading to force increases.

If all of the cells are to increase their speed of contraction with stimulation of the sympathetics then all of the cells either must come in contact with a nerve or must be close enough for the transmitter to diffuse to the cell. As shown in the previous section all of the cells do not have close contact with a nerve. Bennett and Merrillees (7) found in smooth muscle that any membrane further away from the nerve than $1000\overset{\circ}{\text{Å}}$ would not be influenced by the transmitter released from the nerve. This implies that any cell more than $1000\overset{\circ}{\text{Å}}$ from the nerve will not change its speed of contraction during sympathetic stimulation.

As a result of the above observations the following hypothesis is presented. There are two populations of cells in the myocardium. One population is not innervated and therefore not influenced by stimulation of the sympathetics. A second population is innervated and controlled by the sympathetic nervous system. By altering the speed and maximum force of contraction of the second population of cells the total force and total speed of contraction of the entire muscle segment under a strain

gauge will be altered. For this hypothesis to be correct it must be assumed that the non-controlled population contracts with a maximum force and a speed that is faster than the controlled population. With an increased stimulation of the sympathetic nerves the controlled group of cells would then contract with more force and with a speed closer to that of the non-controlled group. The summation of the two groups would give the greater force and speed of contraction that has been observed in these experiments.

Figure 38 is a diagrammatic representation of a section of myocardium. It shows a number of cardiac muscle cells and two nerves (N) that have close contacts with only some of the cells. The nerves were drawn using the electronmicrographs taken by Thaemert (86) of neuromuscular functions in the AV node. It can be seen in the cell labelled T that in some instances the nerve actually tunnels through a cell. Thaemert (86) reported that this was a common occurrence in the AV node. When a nerve tunnels through a cell the transmitter released will only be able to control that particular cell. The transmitter will not be able to diffuse to other cells. Those cells that the nerves are in contact with are the cells of the controlled populations. These are labelled "C." Those cells labelled "F" are in the population of cells that are not influenced by the sympathetic nerves.

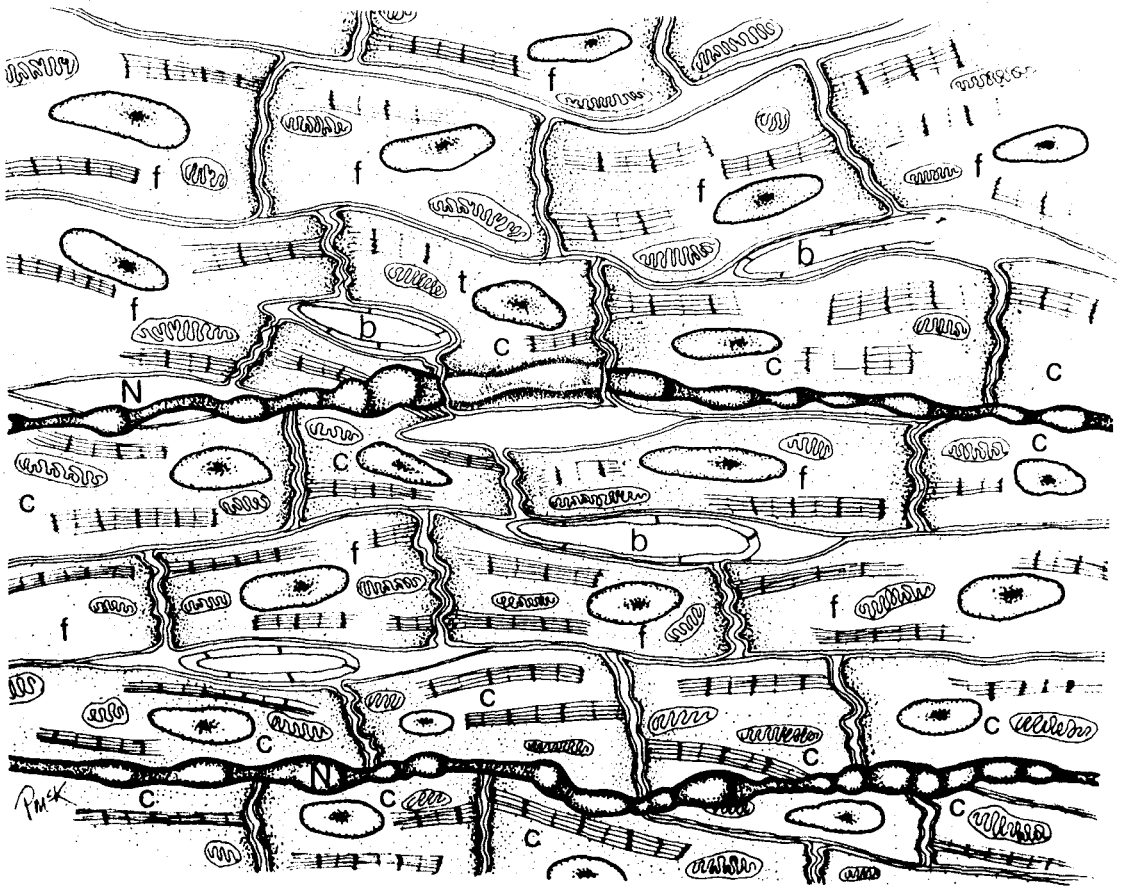


FIGURE 38
MYOCARDIAL CELLULAR STRUCTURE

FIGURE 38

LEGEND

Figure 38 is an artist's representation of the myocardial structure as shown by Thaemert (86). The diagram illustrates the relationships between sympathetic nerves and myocardial cells in the ventricles. Two nerves (N) are shown. The enlargements or varicosities are part of the neuromuscular junctions. One of the nerves is shown tunneling through a cell (T). Two populations of cells are shown: controlled cells (c) and non-controlled cells (F). Three blood vessels are shown (b). See text for further explanations.

It is postulated that the cells labelled "C" have their force and speed of contraction increased by sympathetic stimulation. The higher force and faster speed of the controlled cell's contraction is then closer to those of the non-controlled cells. As a result the total force is greater than normal and the speed of contraction is faster than normal.

This entire concept is based on the relative lack of nerves in the myocardium and the ability of the sympathetic nervous system to change the speed and force of contraction of a myocardial cell. The number of nerves and neuromuscular junctions in the myocardium have been discussed earlier. The ability of the sympathetics to change force and speed of contraction of a cell will be discussed now.

Catecholamines have many effects on the myocardial cell, all leading to an increased force and velocity of contraction. Grossman and Furchgott (24) in 1964 demonstrated that norepinephrine caused an increase in movement of Ca^{++} into the myocardial cell. This was associated with an increased inotropic state of the muscle.

Both epinephrine (70) and norepinephrine (35) have been shown to increase the cyclic adenosine 3',5'-monophosphate (C-AMP) activity inside the myocardial cell. La Raia and Sonnenblick (35) found that tension, adenyl cyclase and C-AMP all demonstrated parallel changes

following addition of norepinephrine to the tissue bath.

Nayler and Dunnet (44) reported that c-AMP stimulated the uptake of Ca^{++} by cardiac microsomal fractions. This microsomal fraction consisted of mitochondria and sarcoplasmic reticulum. They showed that the mitochondria were unable to bind enough Ca^{++} to reduce the intracellular concentration below that needed for relaxation. They also demonstrated that the sarcoplasmic reticulum can bind enough Ca^{++} to reduce the level below that needed for relaxation. With catecholamine induced increase in c-AMP there will be an increased accumulation of Ca^{++} in the sarcoplasmic reticulum. This additional Ca^{++} can then be released by the next action potential in the sarcolemma.

Brutsaert and Sonnenblick (10) demonstrated that addition of Ca^{++} to a tissue bath caused an increase in both the force of contraction and V_{max} of the muscle in the bath. The increase in V_{max} was associated with a change in velocity at any preload. Brutsaert and Sonnenblick felt that the Ca^{++} altered V_{max} was possibly due to one of two mechanisms. One mechanism was that the Ca^{++} was altering the crossbridge formation and breaking. The other possibility was that there is an unrecognized constant internal load. By having more crossbridges involved in contraction, as would be the case with more Ca^{++} available, the constant internal load would be

distributed to more force-generating sites and contraction could possibly take place faster. The other intracellular actions of c-AMP are reviewed by Braunwald, Ross and Sonnenblick (8).

To recapitulate not all cells of the myocardium have neuromuscular junctions with sympathetic nerves. Those that do are controlled by the nerve. The nerve releases norepinephrine which diffuses to the receptor on the muscle membrane. The combination of the norepinephrine and receptor causes an increase in the enzyme adenylyl cyclase which causes the conversion of ATP to c-AMP. The increased c-AMP causes the sarcoplasmic reticulum to bind the extra calcium that is moving across the membrane during the action potential. This calcium movement is also stimulated by the norepinephrine. When the myocardial action potential travels across the sarcolemma it causes the sarcoplasmic reticulum to release a larger amount of calcium than normal. This increased calcium results in a greater actin-crossbridge interaction leading to an increased force and a faster velocity of contraction. Those cells under this control then have a force and velocity approximating the uncontrolled cells. The summation of these two groups of cells now contracting faster and with more force will cause the strain gauge arch to record a faster onset of contraction and a greater force,

It would be expected from the above discussion that

calcium and norepinephrine would have similar effects to those seen during nerve stimulation. Figures 26, 27, 28 and Table 6 demonstrate that Ca^{++} (1/4 gm) and norepinephrine (1 γ /kg) did alter electromechanical (EM) coupling interval in the direction they should in accordance with this hypothesis. Calcium and norepinephrine both increased force and decreased EM-coupling interval. The injected norepinephrine stimulated the beta-receptor just as the nerve-released norepinephrine. The Ca^{++} diffused into the cell and increased the levels of intracellular Ca^{++} available for contraction. Injection of propranolol, a beta-blocker, abolished the norepinephrine response but did not alter the calcium response. Finally it would be expected that since force and time-to-onset are related the two should change together. This did happen and can be seen in Table 4 and Figures 31 and 32. Those muscle segments which exhibited a shorter electromechanical coupling interval during nerve stimulation also had a greater force of contraction. The converse was not always true. Some muscle segments that exhibited increased force with nerve stimulation did not statistically have a shorter EM coupling interval. An example of this is the VMCN stimulation. Most of the muscle segments had force increases (Table 4) but only the septal base had a significant change in EM coupling interval (Fig. 31). Probably the time change had occurred but it was not possible to

measure it using the strain gauge and polygraph.

CHAPTER VI

SUMMARY AND CONCLUSIONS

The effect of autonomic cardiac nerve stimulation upon the force and synchronicity of left ventricular contraction was studied in dogs maintained on total cardiopulmonary bypass. Strain gauge arches were sutured to the endocardium and epicardium of the left ventricle. These gauges were used to record force of contraction and the sequence of contraction, both during control and during stimulation of the small thoracic cardiac nerves.

A. Control Time Intervals

Using the upstroke of the Lead II ECG R-wave as the reference point, it was found that the muscle segments studied did not all contract simultaneously. The contraction sequence began in the septal apex, anterior and posterior muscle segments. The next segments to contract were the lateral base and lateral apex, both epicardial muscle segments. The endocardial free wall segments followed their respective overlying epicardial segments. It was confirmed in these studies that electrically the endocardium is activated before the epicardium.

Measurements of electromechanical (EM) coupling intervals disclosed that the epicardial muscle segments

had shorter EM coupling intervals than the endocardial segments. In conclusion those muscle areas that were electrically activated late had shorter EM coupling intervals which resulted in a sequence of contraction that started in the epicardium and progressed to the endocardium.

B. Force Alterations During Autonomic Nerve Stimulation

It was confirmed that the primary pathways for the sympathetics are the ventral lateral cervical cardiac nerve (VLCN) and left recurrent laryngeal nerve (L Re L) of the left side and recurrent cardiac (ReC) and stellate cardiac (St C) of the right side. The primary pathways for parasympathetic inotropic nerves are the left thoracic vagus and the right side vagal branches, cervical, caudal and thoracic.

It was demonstrated that while the sympathetic nerves innervate both the endocardium and epicardium of the free wall, the response to stimulation was different in the endocardium from the epicardium. The endocardial free wall segments exhibited larger force increases than their respective overlying epicardial segments with left stellate ganglion, VLCN, right stellate ganglion or recurrent cardiac stimulation.

C. Time Interval Changes

Several different time intervals were measured. The electrical-electrical time intervals, which were the

intervals from LV anterior electrical onset to the beginning of electrical activity in one of the other segments studied, were found to be unchanged with autonomic cardiac nerve stimulation. The R-wave to mechanical onset time intervals and the electromechanical coupling time intervals were altered by stimulation.

R-wave to mechanical onset time interval was found to shorten with stellate stimulation either right or left. As a result of greater time interval decreases in those segments that had longer time intervals during control the synchrony of contraction has increased. The major sympathetic pathways to the heart, VLCN and Re C, also caused shorter R-wave to mechanical onset time intervals when stimulated but many of these changes were not significant (see Discussion).

The electromechanical (EM) coupling interval was taken as the time between the first positive deflection in the local electrogram and the onset of mechanical activity in a localized muscle segment. Both right and left stellate ganglion stimulation shortened the EM coupling intervals in all four endocardial muscle segments and at least two of the epicardial segments. The muscle segments exhibiting the shorter EM coupling intervals also had shorter R-wave to mechanical onset time intervals. The VLCN and Re C stimulations resulted in similar EM coupling time interval changes as their respective stellate

ganglion.

D. Hypothesis

Finally an hypothesis was advanced as a possible explanation of the force and time changes that occurred with sympathetic cardiac nerve stimulation. The hypothesis also incorporated anatomical and intracellular data. It has been postulated that the ventricular myocardium consists of two populations of cells: One population is controlled by the sympathetic nerves and the other is not controlled. The non-controlled population contract with maximum possible force and rate of contraction. The sympathetically-controlled cells can have their force and rate of contraction altered. During sympathetic stimulation these cells increase their force and rate of contraction which causes them to contract in synchrony with the non-controlled cells. The summation of the two groups of cells results in the recorded activity of a muscle segment to exhibit increased force and a faster onset of contraction.

If one muscle segment, which normally contracts later than a second muscle segment, has a greater shortening of the time to onset of contraction than the second, then the two segments contract more synchronously.

BIBLIOGRAPHY

1. Angelakos, E. T., K. Fuxe and M. C. Torchiana. Chemical and histochemical evaluation of catecholamines in the rabbit and guinea pig hearts. Acta Physiol. Scand. 59: 184-192, 1963.
2. Anzola, J. and R. F. Rushmer. Cardiac responses to sympathetic stimulation. Circ. Res. 4: 302-307, 1956.
3. Armour, J. A., D. B. Lippincott and W. C. Randall. Functional anatomy of the interventricular septum. Cardiology 58: 65-79, 1973.
4. Armour, J. A., D. C. Randall, W. C. Randall, D. V. Priola, and W. J. Stekiel. Sympathoadrenal regulation of the cardiovascular system in the baboon. Am. J. Physiol. 222: 480-488, 1972.
5. Armour, J. A. and W. C. Randall. In vivo papillary muscle responses to cardiac nerve stimulation. Proc. Soc. Exp. Biol. and Med. 133: 948-952, 1970.
6. Armour, J. A. and W. C. Randall. Electrical and mechanical activity of papillary muscle. Am. J. Physiol. 218: 1710-1717, 1970.
7. Bennett, M. R. and N. C. R. Merrillees. An analysis of the transmission of excitation from autonomic nerves to smooth muscle. J. Physiol. 185: 520-535, 1966.
8. Braunwald, E., J. Ross, Jr., and E. H. Sonnenblick. Mechanisms of Contraction of the Normal and Failing Heart. Little, Brown and Company: Boston, 1976.
9. Brusca, A. and E. Rosettani. Activation of the human fetal heart. Am. Heart J. 86: 79-87, 1973.
10. Brutsaert, D. L. and E. H. Sonnenblick. Cardiac muscle mechanics in the evaluation of myocardial contractility and pump function: problems, concepts and directions. Prog. Cardiovasc. Dis. 16: 337-361, 1973.

11. Burchell, H. B., H. E. Essex, and R. D. Pruitt. Studies on the spread of excitation through the ventricular myocardium. II. The ventricular septum. Circ. 6: 161-171, 1952.
12. Burgess, M. J., L. S. Green, K. Millar, R. Wyatt, and J. A. Abildskov. The sequence of normal ventricular recovery. Am. Heart J. 84:660-669, 1972.
13. Cotten, M. DeV. and E. Bay. Direct measurement of changes in cardiac contractile force: relationship of such measurements to stroke work, isometric pressure gradient and other parameters of cardiac function. Am. J. Physiol. 187: 122-134, 1956.
14. Cronin, R., J. A. Armour, and W. C. Randall. Function of the in-situ papillary muscle in the canine left ventricle. Circ. Res. 25: 67-75, 1969.
15. van Dam, R. T. and D. Durrer. Experimental study on the intramural distribution of the excitability cycle and on the form of the epicardial T wave in the dog heart in situ. Am. Heart J. 61: 537-542, 1961.
16. Durrer, D., R. T. van Dam, G. E. Freud, M. J. Janse, F. L. Meyler, and R. C. Arzbacher. Total excitation of the isolated human heart. Circ. 41: 899-912, 1970.
17. Ehinger, B., B. Falck, H. Persson, and B. Sporrang. Adrenergic and cholinesterase-containing neurons of the heart. Histochemie 16: 197-205, 1968.
18. Friedman, W. F., P. E. Pool, D. Jacobowitz, S. C. Seagren, and E. Braunwald. Sympathetic innervation of the developing rabbit heart. Circ. Res. 23: 25-32, 1968.
19. Gaskell, W. H. On the structure, distribution and function of the nerves which innervate the visceral and vascular systems. J. Physiol. 7: 1-80, 1886.
20. Geis, W. P. and M. P. Kaye. Distribution of sympathetic fibers in the left ventricular epicardial plexus of the dog. Circ. Res. 23: 165-170, 1968.

21. Geis, W. P., M. P. Kaye, and W. C. Randall. Major autonomic pathways to the atria and S-A and A-V nodes of the canine heart. Am. J. Physiol. 224: 202-208, 1973.
22. Gilmore, J. P., S. J. Sarnoff, J. H. Mitchell, and R. J. Linden. Synchronicity of ventricular contraction: observations comparing hemodynamic effects of atrial and ventricular pacing. British Heart J. 25: 299-307, 1963.
23. Gregg, D. E. and R. E. Shipley. Changes in right and left coronary artery inflow with cardiac nerve stimulation. Am. J. Physiol. 141: 382-388, 1944.
24. Grossman, A. and R. F. Furchgott. The effects of various drugs on calcium exchange in the isolated guinea-pig left auricle. J. Pharm. and Exp. Thera 145: 162-172, 1964.
25. Hadek, R. and P. J. Talso. A study of nonmyelinated nerves in the rat and rabbit heart. J. Ultra-structure Res. 17: 257-265, 1967.
26. Harris, A. S. The spread of excitation in turtle, dog, cat and monkey ventricles. Am. J. Physiol. 134: 319-332, 1941.
27. Hawthorne, E. W. Introduction: dynamic geometry of the left ventricle. Federation Proceedings 28: 1323, 1969.
28. Hinds, J. E., E. W. Hawthorne, C. B. Mullins, and J. H. Mitchell. Instantaneous changes in the left ventricular length occurring in dogs during the cardiac cycle. Federation Proceedings 28: 1351-1357, 1969.
29. Hirsch, E. F. General review of the structure and the distribution of the nerves in the vertebrate heart. In The Innervation of the Vertebrate Heart. Ed. by E. F. Hirsch. Charles C. Thomas: Springfield, Illinois, 1970, pp. 3-24.
30. Hirsch, E. F., G. C. Kaiser and T. Cooper. The innervation of the canine heart. In The Innervation of the Vertebrate Heart. Ed. by E. F. Hirsch. Charles C. Thomas: Springfield, Illinois, 1970, pp. 80-124.

31. Hirsch, E. F., V. L. Willman, M. Jellinek, and T. Cooper. The terminal innervation of the heart. Archives of Pathology 76: 677-692, 1963.
32. Hunt, R. Direct and reflex acceleration of the mammalian heart with some observations on the relations of the inhibitory and accelerator nerves. Am. J. Physiol. 2: 396-470, 1899.
33. Kaye, M. P., J. M. Geesbreght, and W. C. Randall. Distribution of autonomic nerves to the canine heart. Am. J. Physiol. 218: 1025-1029, 1970.
34. Kralios, F. A., L. Martin, M. J. Burgess, and K. Miller. Local ventricular repolarization changes due to sympathetic nerve-branch stimulation. Am. J. Physiol. 228: 1621-1626, 1975.
35. LaRaia, P. J. and E. H. Sonnenblick. Autonomic control of cardiac c-AMP. Circ. Res. 28: 377-384, 1971.
36. Levy, M. N., M. L. Ng, and H. Zieske. Functional distribution of the peripheral cardiac sympathetic pathways. Circ. Res. 19: 650-661, 1966.
37. Lewis, T. and A. M. Master. Observations upon conduction in the mammalian heart, A-V conduction. Heart 12: 209-269, 1925-26.
38. Lewis, T. and M. A. Rothschild. IV. The excitatory process in the dog's heart. Part II. The ventricles. Phil. Trans. of Royal Society of London. 206: 181-226, 1915.
39. Mitchell, J. H., R. J. Linden, and S. J. Sarnoff. Influence of cardiac sympathetic and vagal nerve stimulation on the relation between left ventricular diastolic pressure and myocardial segment length. Circ. Res. 8: 1100-1107, 1960.
40. Mizeres, N. J. The anatomy of the autonomic nervous system in the dog. Am. J. Anat. 96: 285-318, 1955.
41. Mizeres, N. J. The origin and course of the cardio-accelerator fibers in the dog. Anat. Rec. 132: 261-279.
42. Mizeres, N. J. The cardiac plexus in man. Am. J. Anat. 112: 141-151, 1963.

43. Myerburg, R. J., K. Nilsson, and H. Gelband.
Physiology of canine intraventricular conduction and endocardial excitation. Circ. Res. 30: 217-243, 1972.
44. Nayler, W. G. and J. Dennett. Regulation of myocardial contraction. Adv. Cardiol. 12: 45-58, 1974.
45. Nonidez, J. F. Studies on the innervation of the heart. Am. J. Anat. 65: 361-413, 1939.
46. Osadjan, C. E. and W. C. Randall. Effects of left stellate ganglion stimulation on left ventricular synchrony in dogs. Am. J. Physiol. 207: 181-186, 1964.
47. Pace, J. B., W. C. Randall, J. S. Wechsler, and D. V. Priola. Alterations in ventricular dynamics induced by stimulation of the cervical vagosympathetic trunk. Am. J. Physiol. 214: 1213-1218, 1968.
48. Priola, D. V., C. E. Osadjan, and W. C. Randall. Functional characteristics of the left ventricular inflow and outflow tracts. Circ. Res. 17: 123-129, 1965.
49. Priola, D. V. and W. C. Randall. Alterations in cardiac synchrony induced by the cardiac sympathetic nerves. Circ. Res. 15: 463-472, 1964.
50. Pruitt, R. D., H. E. Essex, and H. B. Burchell. Studies on the spread of excitation through the ventricular myocardium. Circ. 3: 418-432, 1951.
51. Randall, D. C., J. A. Armour, and W. C. Randall. Dynamic responses to cardiac nerve stimulation in the baboon. Am. J. Physiol. 220: 526-533, 1971.
52. Randall, D. C., J. A. Armour, and W. C. Randall. Dynamic behavior of endocardial structures in the baboon heart. Proc. Soc. Exp. Biol. and Med. 140: 278-284, 1972.
53. Randall, W. C. New insights into the sympathetic innervation of the heart. From Cardiovascular Regulation in Health and Disease. Ed. by C. Bartorelli and A. Zanchetti. Cardiovascular Research Institute: Milan, 1971.

54. Randall, W. C. and A. F. Kelso. Dynamic basis for sympathetic cardiac augmentation. Am. J. Physiol. 198: 971-974, 1960.
55. Randall, W. C. and D. V. Priola. Influence of the cardiac sympathetics on synchrony of ventricular contraction. Proc. Soc. Exp. Biol. and Med. 115: 46-48, 1964.
56. Randall, W. C. and D. V. Priola. Sympathetic influences on synchrony of myocardial contraction. In Nervous Control of the Heart. Ed. by W. C. Randall. Williams and Wilkins Co.: Baltimore, 1965.
57. Randall, W. C., D. V. Priola, J. B. Pace, and J. S. Wechsler. Ventricular augmentor fibers in the cervical vagosympathetic trunk. Proc. Soc. Exp. Biol. and Med. 124: 1254-1257, 1967.
58. Randall, W. C., D. V. Priola, and R. H. Ulmer. A functional study of distribution of cardiac sympathetic nerves. Am. J. Physiol. 205: 1227-1231, 1963.
59. Randall, W. C. and J. A. Armour. Complex cardiovascular responses to vago-sympathetic stimulation. Proc. Soc. Exp. Biol. and Med. 145: 493-499, 1974.
60. Randall, W. C. and J. A. Armour. Regional vagosympathetic control of the heart. Am. J. Physiol. 227: 444-452, 1974.
61. Randall, W. C., J. A. Armour, D. C. Randall, and O. A. Smith. Functional anatomy of the cardiac nerves in the baboon. Anat. Rec. 170: 183-198, 1971.
62. Randall, W. C., J. A. Armour, W. P. Geis, and D. B. Lippincott. Regional cardiac distribution of the sympathetic nerves. Federation Proc. 31: 1199-1208, 1972.
63. Randall, W. C., J. B. Pace, J. S. Wechsler, and K. S. Kim. Cardiac responses to separate stimulation of sympathetic and parasympathetic components of the vagosympathetic trunk in the dog. Cardiologia 54: 104-118, 1969.

64. Randall, W. C., J. S. Wechsler, J. B. Pace, and M. Szentivanyi. Alterations in myocardial contractility during stimulation of the cardiac nerves. Am. J. Physiol. 214: 1205-1212, 1968.
65. Randall, W. C., M. Szentivanyi, J. B. Pace, J. S. Wechsler, and M. P. Kaye. Patterns of sympathetic nerve projections onto the canine heart. Circ. Res. 22: 315-323, 1968.
66. Randall, W. C. and W. B. Rohse. The augmentor action of the sympathetic cardiac nerves. Circ. Res. 4: 470-475, 1956.
67. Reeves, T. J. and L. L. Hefner. Isometric contraction and contractility in the intact mammalian ventricle. Am. Heart J. 64: 525-538, 1962.
68. Reeves, T. J., L. L. Hefner, W. B. Jones, C. Coghlan, G. Prieto, and J. Carroll. The hemodynamic determinants of the rate of change in pressure in the left ventricle during isometric contraction. Am. Heart J. 60: 745-761, 1960.
69. Robb, J. S. and R. C. Robb. The excitatory process in the mammalian ventricle. Am. J. Physiol. 115: 43-52, 1936.
70. Robison, G. A., R. W. Butcher, I. Øye, H. E. Morgan, and E. W. Sutherland. The effect of epinephrine on adenosine 3',5'-phosphate levels in the isolated perfused rat heart. Molec. Pharmacol. 1: 168-177, 1965.
71. Rushmer, R. F. Initial phase of ventricular systole: asynchronous contraction. Am. J. Physiol. 184: 188-194, 1956.
72. Rushmer, R. F. Pressure-circumference relations of the left ventricle. Am. J. Physiol. 186: 115-121, 1956.
73. Rushmer, R. F. and N. Thal. The mechanics of ventricular contraction: a cinefluorographic study. Circulation 4: 219-228, 1951.
74. Sano, T., M. Ono and T. Shimamoto. Intrinsic deflections, local excitation and transmembrane action potentials. Circ. Res. 4: 444-449, 1956.

75. Sarnoff, S. J., J. P. Gilmore, and A. G. Wallace. The influence of autonomic nerve activity on adaptive mechanisms in the heart. In Nervous Control of the Heart. Ed. by W. C. Randall. Williams and Wilkins Co.: Baltimore, 1965.
76. Sarnoff, S. J., S. K. Brockman, J. P. Gilmore, R. J. Linden, and J. H. Mitchell. Regulation of ventricular contraction: influence of cardiac sympathetic and vagal nerve stimulation on atrial and ventricular dynamics. Circ. Res. 8: 1108-1122, 1960.
77. Scher, A. M. and A. C. Young. The pathway of ventricular depolarization in the dog. Circ. Res. 4: 461-469, 1956.
78. Scher, A. M., A. C. Young, A. L. Malmgren, and R. V. Erickson. Activation of the interventricular septum. Circ. Res. 3: 56-64, 1955.
79. Scher, A. M., A. C. Young, A. L. Malmgren, and R. R. Paton. Spread of electrical activity through the wall of the ventricle. Circ. Res. 1: 539-547, 1953.
80. Shimosato, S., G. E. Herpfer, and B. E. Etsten. Static and dynamic performance of Walton strain-gauge arches. J. Appl. Physiol. 21: 1892-1896, 1966.
81. Shipley, R. E. and D. E. Gregg. The cardiac response to stimulation of the stellate ganglia and cardiac nerves. Am. J. Physiol. 143: 396-401, 1945.
82. Sodi-Pallares, D., A. Bisteni, G. A. Medrano, and F. Cisneros. The activation of the free left ventricular wall in the dog's heart. Am. Heart J. 49: 587-602, 1955.
83. Sodi-Pallares, D., E. Barbato, and A. Delmar. Relationship between the intrinsic deflection and subepicardial activation. Am. Heart J. 39: 387-396, 1950.
84. Szentivanyi, M., J. B. Pace, J. S. Wechsler, and W. C. Randall. Localized myocardial responses to stimulation of cardiac sympathetic nerves. Circ. Res. 21: 691-702, 1967.

85. Thaemert, J. C. Fine structure of neuromuscular relationships in mouse heart. Anat. Rec. 163: 575-586, 1969.
86. Thaemert, J. C. Atrioventricular node innervation in ultrastructural three dimensions. Am. J. Anat. 128: 239-264, 1970.
87. Thaemert, J. C. Fine structure of the atrioventricular node as viewed in serial sections. Am. J. Anat. 136: 43-66, 1973.
88. Tsakiris, A. G., D. E. Donald, R. E. Sturm, and E. H. Wood. Volume, ejection fraction, and internal dimensions of left ventricle determined by biplane videometry. Federation Proceedings 28: 1358-1367, 1969.
89. Wallace, A. G. and S. J. Sarnoff. Effects on cardiac sympathetic nerve stimulation on conduction in the heart. Circ. Res. 14: 86-92, 1964.
90. Wechsler, J. S., J. B. Pace, J. M. Goldberg, and W. C. Randall. Location of synaptic connections in canine sympathetic cardiac innervation. Am. J. Physiol. 217: 1789-1794, 1969.
91. Wiggers, C. J. The interpretation of the intraventricular pressure curve on the basis of rapidly summated fractionate contractions. Am. J. Physiol. 80: 1-11, 1927.
92. Wiggers, C. J. The physiology of the mammalian auricle. I. The auricular myogram and auricular systole. Am. J. Physiol. 40: 218-229, 1916.
93. Woollard, H. H. The innervation of the heart. J. Anat. and Physiol. 60: 345-373, 1926.
94. Yamauchi, A. Innervation of the vertebrate heart as studied with the electron microscope. Arch. Hist. Jap. 31: 83-117, 1969.
95. Yamaushi, A. and G. Burnstock. An electron microscopic study on the innervation of the trout heart. J. Comp. Neur. 132: 567-588, 1968.

96. Yanowitz, F., J. B. Preston, and J. A. Abildskov.
Functional distribution of right and left stellate innervation to the ventricles: production of neurogenic electro-cardiographic changes by unilateral alteration of sympathetic tone. Circ. Res. 18: 416-428, 1966.

APPENDIX

TABLE A-1
HEART RATE--BEFORE ATROPINE

		HEART RATE BEFORE ATROPINE						
		LSS (26)	INN (24)	VMCN (25)	VLCN (26)	L Re L (21)	LTV (25)	LCV (6)
Control		*135.3	128.5	128.8	131.8	124.8	128.9	130.8
		3.74	3.74	3.81	3.54	3.21	3.68	8.51
Stim		157.1	130.6	110.0	139.1	73.8	85.0	61.8
		3.77	3.64	6.19	3.60	7.26	7.47	12.53
		0.001	0.05	0.05	0.001	0.001	0.001	0.01
		RSS (26)	Re C (25)	St C	Cr V (23)	Ca V (21)	RTV (18)	RCV (8)
Control		133.3	120.0	119.1	120.8	120.8	121.9	132.1
		3.39	3.44	3.60	3.59	4.28	4.44	8.23
Stim		184.1	111.1	153.9	75.5	74.3	61.1	60.6
		2.77	6.33	4.89	5.75	7.02	4.77	10.15
		0.001	0.1	0.001	0.001	0.001	0.001	0.01

(*Mean)
(± SE)

TABLE A-2
HEART RATE--AFTER ATROPINE

HEART RATE
AFTER ATROPINE

	INN (11)	VMCN (16)	VLCN (10)	L Re L (15)	LTV (18)	LCV (6)	
Control	*126.1	123.8	122.5	123.6	125.1	124.3	
	5.04	4.38	5.49	3.63	3.75	4.06	
Stim	130.6	126.2	140.7	139.7	135.4	128.8	
	5.97	4.49	8.14	4.67	4.40	6.00	
	0.1	N.S.	0.05	0.01	0.05	N.S.	
	Re L (17)	St C (9)	Cr V (17)	Ca V (16)	RTV (16)	RCV (7)	ISO (6)
Control	119.3	125.9	121.5	121.6	122.2	125.6	124.2
	3.36	5.45	4.67	4.92	3.38	4.95	5.54
Stim	140.2	161.9	142.2	138.3	136.9	142.4	165.0
	4.64	6.82	4.98	6.10	2.07	4.90	7.19
	0.001	0.001	0.001	0.05	0.001	0.05	0.001

(*Mean)
(± SE)

TABLES A-1 AND A-2

LEGEND

Tables A-1 and A-2 show the heart rates before (control) and during stimulation (STIM) of the thoracic cardiac nerves. Table A-1 shows the heart rates before atropine and Table A-2 shows the rates after atropine. In each column from top to bottom are: (1) the nerve stimulated, (2) the number of observations, (3) the control heart rate, (4) standard error of the control value, (5) the stimulation heart rate, (6) standard error of the stimulation value, and (7) the degree of significance by the paired t-test.

The nerves stimulated are the

LSS	Left stellate ganglion
INN	Innominate
VMCN	Ventral medial cervical cardiac
VLCN	Ventral lateral cervical cardiac
L Re L	Left recurrent laryngeal
LTV	Left thoracic vagus
LCV	Left cervical vagus
RSS	Right stellate ganglion
Re C	Recurrent cardiac
St C	Stellate cardiac
Cr V	Cranial vagus
Ca V	Caudal vagus
RTV	Right thoracic vagus
RCV	Right cervical vagus

TABLE A-3
LEFT VENTRICULAR ANTERIOR R-WAVE

		LEFT VENTRICULAR ANTERIOR R-WAVE					
	LSS (12)	INN (12)	VMCN (12)	VLCN (13)	L Re L (11)	LTV (11)	
Control	*36.7	39.2	35.8	36.9	38.2	39.5	
	3.30	3.05	3.58	3.55	3.92	4.14	
Stim	25.8	35.0	37.1	36.9	43.2	48.2	
	3.00	3.54	2.67	4.20	5.90	4.42	
	0.001	0.05	N.S.	N.S.	N.S.	N.S.	
	RSS (13)	Re C (13)	St C (4)	Cr V (12)	Ca V (11)	RTV (12)	ISO (6)
Control	35.8	40.4	43.8	37.9	35.8	34.2	36.7
	3.21	4.12	8.17	3.70	3.67	3.81	2.55
Stim	19.6	32.7	45.0	40.4	45.2	50.8	33.3
	2.95	2.86	7.71	5.32	4.36	4.44	3.66
	0.001	0.1	N.S.	N.S.	0.05	0.05	N.S.

(*Mean)
(± SE)

Tables A-3 through A-10 show the R-wave to mechanical onset time intervals for the eight muscle segments studied. See Tables A-1, A-2 for an explanation of the table format on abbreviations. ISO = isoproterenol; N.S. = not significant.

TABLE A-4
LEFT VENTRICULAR LATERAL APEX R-WAVE

LEFT VENTRICULAR LATERAL APEX							
R-WAVE							
	LSS (6)	INN (5)	VMCN (6)	VLCN (6)	L Re L (4)	LTV (5)	
Control	*51.7	59.0	52.5	52.5	60.0	58.0	
	4.77	5.10	6.55	6.16	6.12	5.83	
Stim	40.8	57.0	54.2	45.0	56.2	56.0	
	4.52	4.64	4.90	6.95	4.38	8.86	
	0.1	N.S.	N.S.	0.05	N.S.	N.S.	
	RSS (6)	Re C (6)	St C	Cr V (6)	Ca V (6)	RTV (6)	ISO (3)
Control	52.5	56.7	---	55.0	57.5	53.3	53.3
	3.59	5.72	---	7.07	8.83	9.10	8.34
Stim	44.2	46.7	---	65.8	61.7	62.5	65.0
	7.00	6.79	---	10.6	9.89	4.42	18.0
	N.S.	0.1	---	N.S.	N.S.	N.S.	N.S.

(*Mean)
± SE

See Table A-3.

TABLE A-5
LEFT VENTRICULAR LATERAL BASE R-WAVE

LEFT VENTRICULAR LATERAL BASE							
R-WAVE							
	LSS (12)	INN (12)	VMCN (11)	VLCN (13)	L Re L (11)	LTV (11)	
Control	*48.3	51.7	47.3	51.9	52.3	52.3	
	2.52	2.85	3.66	3.67	4.23	5.16	
Stim	40.0	48.8	47.3	48.1	46.4	66.4	
	3.12	3.96	3.24	4.73	6.10	5.96	
	0.01	N.S.	N.S.	0.1	N.S.	0.05	
	RSS (13)	Re C (13)	St C (5)	Cr V (12)	Ca V (12)	RTV (12)	ISO (6)
Control	47.3	54.2	52.0	53.3	51.7	49.6	47.5
	3.42	5.46	6.42	4.62	5.05	5.96	3.06
Stim	35.0	44.6	56.0	54.2	63.6	65.4	42.5
	3.44	3.71	6.07	6.87	7.32	6.30	5.86
	0.001	N.S.	0.05	N.S.	N.S.	0.05	N.S.

(*Mean)
± SE

See Table A-3.

TABLE A-6

LEFT VENTRICULAR POSTERIOR R-WAVE

LEFT VENTRICULAR POSTERIOR

	LSS (5)	INN (6)	VMCN (6)	VLCN (6)	L Re L (5)	LTV (6)	
Control	*40.0	36.7	37.5	35.0	33.0	35.8	
	6.32	7.49	7.28	8.16	10.44	7.24	
Stim	31.0	33.3	42.5	30.0	36.0	43.3	
	8.85	8.33	7.16	8.85	10.77	7.26	
	0.1	N.S.	N.S.	0.1	N.S.	N.S.	
	RSS (6)	Re C (6)	St C	Cr V (6)	Ca V (6)	RTV (6)	ISO (4)
Control	37.3	35.8	---	38.3	37.5	33.3	40.0
	7.95	7.68	---	6.67	7.04	6.79	4.56
Stim	29.2	40.0	---	36.7	38.3	42.5	32.5
	7.24	7.19	---	7.15	5.58	3.59	7.77
	0.05	N.S.	---	N.S.	N.S.	N.S.	0.1

(*Mean)
± SE

See Table A-3.

TABLE A-7
FREE WALL APEX R-WAVE

		LEFT VENTRICULAR					
		FREE WALL APEX R-WAVE					
	LSS (9)	INN (9)	VMCN (10)	VLCN (10)	L Re L (8)	LTV (9)	
Control	*55.6	58.3	53.5	58.5	60.6	58.9	
	4.20	6.62	4.95	5.43	6.44	7.30	
Stim	37.8	52.2	60.0	46.0	84.4	77.7	
	4.50	5.47	5.68	5.31	9.66	10.97	
	0.01	0.1	N.S.	0.01	0.1	N.S.	
	RSS (10)	Re C (10)	St C (3)	Cr V (9)	Ca V (9)	RTV (9)	ISO (5)
Control	56.0	64.5	63.3	66.1	66.7	62.2	65.0
	4.07	5.46	9.28	6.86	7.91	8.12	7.07
Stim	4.45	60.5	66.7	73.9	79.2	81.1	57.0
	7.58	7.36	10.10	9.31	13.30	10.99	9.16
	N.S.	N.S.	N.S.	N.S.	N.S.	N.S.	N.S.

(*Mean)
± SE

See Table A-3.

TABLE A-8
FREE WALL BASE R-WAVE

		LEFT VENTRICULAR					
		FREE WALL BASE R-WAVE					
	LSS (8)	INN (8)	VMCN (7)	VLCN (8)	L Re L (7)	LTV (7)	
Control	*52.5	49.4	52.1	51.9	54.3	50.7	
	4.33	6.8	7.23	7.00	7.60	7.90	
Stim	39.4	46.9	67.9	42.5	67.1	70.0	
	6.58	6.96	11.12	7.13	15.31	12.20	
	0.05	N.S.	N.S.	N.S.	N.S.	N.S.	
	RSS (8)	Re C (8)	St C	Cr V (7)	Ca V (6)	* RTV (7)	ISO (3)
Control	49.4	57.5	---	60.7	50.0	53.67	50.0
	5.46	7.13	---	6.94	7.64	7.30	11.55
Stim	35.0	43.1	---	70.0	72.5	75.0	30.0
	4.01	7.44	---	18.6	13.71	11.29	10.41
	0.05	N.S.	---	N.S.	0.1	0.1	0.05

(*Mean)
± SE

See Table A-3.

TABLE A-9
SEPTAL APEX R-WAVE

		LEFT VENTRICULAR					
		SEPTAL APEX					
		R-WAVE					
	LSS (8)	INN (8)	VMCN (9)	VLCN (9)	L Re L (6)	LTV (8)	
Control	*37.5	38.8	36.7	36.1	39.2	39.4	
	4.76	3.62	4.08	4.06	4.63	4.17	
Stim	23.8	37.5	41.1	26.1	26.7	46.2	
	3.40	4.24	5.43	4.31	5.74	12.05	
	0.01	N.S.	N.S.	0.05	0.05	N.S.	
	RSS (8)	Re C (9)	St C (3)	Cr V (9)	Ca V (9)	RTV (9)	ISO (5)
Control	33.8	37.2	38.3	37.2	35.6	35.0	39.0
	3.40	4.18	6.01	4.18	4.04	4.72	8.43
Stim	25.6	35.0	38.3	45.6	49.1	53.3	27.0
	2.86	7.99	4.41	9.70	10.70	5.95	5.38
	0.001	N.S.	N.S.	N.S.	N.S.	0.05	0.1

(*Mean)
± SE

See Table A-3.

TABLE A-10
SEPTAL BASE R-WAVE

LEFT VENTRICULAR							
SEPTAL BASE							
R-WAVE							
	LSS (10)	INN (10)	VMCN (12)	VLCN (11)	L Re L (8)	LTV (10)	
Control	*59.0	58.0	54.17	55.9	58.1	59.5	
	7.22	7.90	6.60	7.29	7.32	7.87	
Stim	37.0	53.5	52.9	47.7	51.2	73.0	
	4.67	7.78	6.70	6.23	14.57	10.81	
	0.001	N.S.	N.S.	0.05	N.S.	N.S.	
	RSS (11)	Re C (11)	St C (4)	Cr V (10)	Ca V (10)	RTV (10)	ISO (5)
Control	58.6	59.5	61.2	57.0	61.0	59.5	66.0
	5.92	7.60	12.47	8.47	8.52	9.47	8.86
Stim	37.3	50.5	61.2	74.0	70.8	79.6	52.0
	4.83	9.33	10.68	11.27	12.0	10.73	7.52
	0.001	N.S.	N.S.	N.S.	N.S.	0.1	0.05

(*Mean)
± SE

TABLE A-11
ELECTROMECHANICAL COUPLING ANTERIOR

ELECTRO-MECHANICAL COUPLING

ANTERIOR

	LSS (14)	INN (14)	VMCN (15)	VLCN (15)	L Re L (16)	LTV (13)	LCV (11)
Control	47.1*	50.0	50.7	50.3	48.9	50.0	49.1
	2.08	2.16	2.06	1.65	1.52	2.04	2.00
Stim	35.7	45.9	47.7	47.3	46.6	49.6	47.7
	2.15	2.34	1.88	2.43	3.19	2.50	2.89
	0.001	0.05	0.1	N.S.	N.S.	N.S.	N.S.
	RSS (15)	Re C (12)	Cr V (13)	Ca V (14)	St C (5)	RTV (14)	RCV (11)
Control	49.0	47.9	46.9	48.2	50	50.7	50.0
	1.77	2.08	1.65	1.93	2.58	2.21	1.91
Stim	35.7	38.8	51.5	48.9	47.0	51.4	50.2
	2.48	3.49	3.42	2.35	3.00	2.69	2.53
	0.001	0.01	0.1	N.S.	N.S.	N.S.	N.S.

*Time in msec
Mean \pm S. E.

Tables A-11 through A-18 show the electromechanical coupling intervals for the eight muscle segments studied. The electromechanical coupling interval is the time between the first positive deflection in the electrogram from the muscle segment and the onset of mechanical activity in the muscle segment. See Tables A-1, A-2 for an explanation of the table format and abbreviations.

TABLE A-12
ELECTROMECHANICAL COUPLING POSTERIOR

ELECTRO-MECHANICAL COUPLING

POSTERIOR

	LSS (6)	INN (5)	VMCN (5)	VLCN (6)	L Re L (5)	LTV (5)	LCV (5)
Control	51.7*	59.0	60.0	55.0	58.4	58.0	59.0
	3.33	2.92	1.58	1.83	1.435	2.55	3.67
Stim	38.3	61.0	55.0	46.7	50.0	58.0	53.0
	2.11	1.87	2.74	5.58	5.00	4.06	3.39
	0.05	N.S.	N.S.	N.S.	N.S.	N.S.	N.S.
	RSS (5)	Re C (4)	Cr V (6)	Ca V (7)	St C (3)	RTV (5)	RCV
Control	56.0	56.2	55.8	58.6	53.3	60.0	58.0
	1.87	5.91	3.52	2.83	7.27	2.74	3.39
Stim	51.4	50.0	54.2	60.0	48.3	58.0	56.0
	2.44	4.56	5.23	3.78	4.41	4.90	5.79
	N.S.	N.S.	N.S.	N.S.	N.S.	N.S.	N.S.

*Time in msec
Mean \pm S. E.

See Table A-11.

TABLE A-13
ELECTROMECHANICAL COUPLING LATERAL APEX

ELECTRO-MECHANICAL COUPLING

LATERAL APEX

	LSS (5)	INN (5)	VMCN (5)	VLCN (5)	L Re L (7)	LTV (4)	LCV (5)
Control	34.0**	52.4	54.0	53.0	45.7	52.5	48.0
	2.45	10.1	12.0	10.8	9.66	13.9	10.1
Stim	35.0	47.0	43.4	46.0	40.7	52.5	49.0
	9.13	13.7	9.98	12.4	7.59	11.3	11.0
	N.S.	N.S.	0.1	N.S.	N.S.	N.S.	N.S.
	RSS (5)	Re C (5)	Cr V (5)	Ca V (6)	St C (2)	RTV (5)	RCV
Control	49.0	51.0	52.0	48.3	47.5	51.4	49.0
	10.8	10.5	10.32'	8.72	7.5	10.4	11.0
Stim	41.6	38.0	50.0	48.3	52.5	52.0	48.0
	5.12	9.3	11.1	9.80	7.5	10.6	11.1
	0.1	0.05	N.S.	N.S.	N.S.	N.S.	N.S.

*Time in msec
Mean \pm S. E.

See Table A-11.

TABLE A-14
ELECTROMECHANICAL COUPLING LATERAL BASE

ELECTRO-MECHANICAL COUPLING							
LATERAL BASE							
	LSS (6)	INN (5)	VMCN (5)	VLCN (6)	L Re L (6)	LTV (6)	LCV (4)
Control	45.0*	56.0	51.0	46.7	49.2	49.2	53.7
	3.42	5.57	4.85	5.43	4.90	4.73	6.58
Stim	33.3	53.0	51.0	35.0	53.3	45.8	56.2
	3.57	4.64	4.3	5.63	4.01	3.74	8.51
	0.05	0.1	N.S.	0.1	N.S.	N.S.	N.S.
	RSS (6)	Re C (5)	Cr V (6)	Ca V (6)	St C	RTV (5)	RCV (4)
Control	50.0	43.0	49.2	51.7	--	52.0	52.5
	4.28	4.06	3.96	2.79	--	3.39	5.95
Stim	4.17	34.0	43.3	52.5	--	54.0	60.0
	3.80	7.31	3.33	4.61	--	4.00	5.40
	.001	N.S.	N.S.	N.S.	--	N.S.	0.1

*Time in msec
Mean \pm S. E.

See Table A-11.

TABLE A-15
ELECTROMECHANICAL COUPLING FREE WALL APEX

ELECTRO-MECHANICAL COUPLING							
FREE WALL APEX							
	LSS (8)	INN (8)	VMCN (10)	VLCN (9)	L Re L (10)	LTV (7)	LCV (8)
Control	55.6*	65.6	66.5	62.8	67.5	67.9	62.5
	5.38	8.58	7.07	7.87	6.92	9.31	6.12
Stim	39.4	64.4	64.0	46.7	65.0	67.9	61.5
	8.04	9.03	7.92	9.79	6.91	9.44	6.55
	0.01	N.S.	N.S.	0.001	N.S.	N.S.	N.S.
	RSS (9)	Re C (8)	Cr V (7)	Ca V (9)	St C (5)	RTV (8)	RCV (8)
Control	59.4	62.5	62.1	63.1	68.0	64.4	63.8
	8.44	4.72	6.80	5.51	4.06	6.08	5.65
Stim	47.8	55.0	55.0	62.2	65.0	61.9	58.1
	7.27	6.20	6.55	5.84	4.74	6.74	7.07
	0.01	0.05	0.01	N.S.	0.1	N.S.	N.S.

*Time in msec
Mean \pm S. E.

TABLE A-16
ELECTROMECHANICAL COUPLING FREE WALL BASE

ELECTRO-MECHANICAL COUPLING
FREE WALL BASE

	LSS (8)	INN (7)	VMCN (8)	VLCN (8)	L Re L (7)	LTV (7)	LCV (4)
Control	64.4*	66.4	68.1	69.4	64.3	65.0	65.0
	2.58	5.64	5.08	5.04	7.27	6.46	9.79
Stim	38.8	64.3	63.1	43.8	72.9	70.0	68.8
	2.79	6.77	7.84	6.26	8.92	9.06	10.9
	0.001	N.S.	N.S.	0.001	0.05	N.S.	0.1
	RSS (8)	Re C (5)	Cr V (6)	Ca V (6)	St C (3)	RTV (7)	RCV (4)
Control	65.0	68.0	64.2	65.8	56.7	73.6	61.2
	4.91	8.60	7.35	7.79	8.82	6.52	8.75
Stim	52.5	41.0	64.2	72.5	51.7	77.9	70.0
	4.82	4.58	7.90	9.01	7.27	11.5	12.2
	0.01	0.05	N.S.	N.S.	N.S.	N.S.	N.S.

*Time in msec
Mean \pm S. E.

See Table A-11.

TABLE A-17

ELECTROMECHANICAL COUPLING SEPTAL APEX

ELECTRO-MECHANICAL COUPLING							
SEPTAL APEX							
	LSS (8)	INN (7)	VMCN (7)	VLCN (8)	L Re L (8)	LTV	LCV
Control	52.5*	52.1	54.3	51.2	50.6	49.4	50.0
	4.63	3.25	3.69	2.95	3.83	3.59	6.06
Stim	35.0	49.3	50.7	37.1	48.7	53.1	54.2
	3.78	2.30	6.40	4.23	7.72	7.61	11.6
	0.001	N.S.	N.S.	0.001	N.S.	N.S.	N.S.
	RSS (8)	Re C (7)	Cr V (6)	Ca V (7)	St C (3)	RTV (7)	RCV (6)
Control	53.8	52.1	54.0	50.7	51.7	53.6	51.7
	2.95	3.43	3.52	3.35	1.67	4.59	4.22
Stim	44.4	41.4	47.5	45.7	53.3	51.4	56.7
	1.99	3.22	2.50	4.15	4.41	3.57	8.53
	0.01	0.001	0.1	N.S.	N.S.	N.S.	N.S.

*Time in msec
Mean \pm S. E.

See Table A-11.

TABLE A-18
ELECTROMECHANICAL COUPLING SEPTAL BASE

ELECTRO-MECHANICAL COUPLING
SEPTAL BASE

	LSS (10)	INN (9)	VMCN (11)	VLCN (10)	L Re L (11)	LTV (9)	LCV (7)
Control	74.5*	75.0	73.6	73.2	70.3	72.8	76.4
	3.98	3.82	3.17	4.42	4.01	3.02	3.73
Stim	48.5	71.7	64.1	55.2	68.1	74.4	74.3
	3.80	4.49	4.36	3.94	3.82	4.89	4.93
	0.001	0.05	0.05	0.001	N.S.	N.S.	N.S.
	RSS (9)	Re C (7)	Cr V (9)	Ca V (9)	St C	RTV (9)	RCV (7)
Control	77.8	74.3	72.2	70.6	--	76.7	77.1
	4.50	4.00	3.45	3.17	--	3.54	4.48
Stim	56.9	58.6	75.6	76.7	--	76.1	68.6
	5.32	5.64	4.45	5.89	--	5.82	5.09
	0.01	0.05	N.S.	0.1	--	N.S.	0.1

*Time in msec
Mean \pm S. E.

See Table A-11.

TABLE A-19

ANALYSES OF VARIANCE, R-WAVE LEFT SIDE NERVES

IIR R-WAVE ANALYSIS OF VARIANCE

	A	LB	LA	P	FVA	FVB	SB
LB	**						
LA	**	0-0					
P	0-0	0-0	0-0				
FVA	**	0-0	0-0	**			
FVB	**	0-0	0-0	0-0	0-0		
SB	**	0-0	0-0	**	0-0	0-0	
SA	0-0	**	**	0-0	**	**	**

* P<0.05 ** P<0.01

IIR R-WAVE ANALYSIS OF VARIANCE

	A	LB	LA	P	FVA	FVB	SB
LB	0-0						
LA	**	0-0					
P	0-0	0-0	**				
FVA	**	**	0-0	**			
FVB	0-0	0-0	0-0	**	0-0		
SB	0-0	0-0	0-0	**	0-*	0-0	
SA	0-0	0-0	0-0	0-0	**	0-*	0-0

* P<0.05 ** P<0.01

IIR R-WAVE ANALYSIS OF VARIANCE

	A	LB	LA	P	FVA	FVB	SB
LB	0-0						
LA	**	0-0					
P	0-0	0-0	**				
FVA	**	0-0	0-0	**			
FVB	0-0	0-0	0-0	0-0	0-0		
SB	**	0-0	0-0	**	0-0	0-0	
SA	0-0	0-0	**	0-0	**	0-*	**

* P<0.05 ** P<0.01

VLON R-WAVE ANALYSIS OF VARIANCE

	A	LB	LA	P	FVA	FVB	SB
LB	**						
LA	0-0	0-0					
P	0-0	0-*	0-0				
FVA	**	0-0	0-0	**			
FVB	0-0	0-0	0-0	0-0	0-0		
SB	**	0-0	0-0	**	0-0	0-0	
SA	0-0	**	0-*	0-0	**	0-*	**

* P<0.05 ** P<0.01

LTV R-WAVE ANALYSIS OF VARIANCE

	A	LB	LA	P	FVA	FVB	SB
LB	0-0						
LA	0-*	0-0					
P	0-0	0-0	0-*				
FVA	0-0	0-0	0-0	0-0			
FVB	**	0-0	0-0	**	0-0		
SB	0-0	0-0	0-0	0-0	0-0	0-0	
SA	0-0	0-0	0-*	0-0	0-0	**	0-0

* P<0.05 ** P<0.01

VMCN R-WAVE ANALYSIS OF VARIANCE

	A	LB	LA	P	FVA	FVB	SB
LB	0-**						
LA	**	0-0					
P	0-0	0-0	0-0				
FVA	**	0-0	0-0	0-0			
FVB	**	0-*	0-0	0-*	0-0		
SB	**	0-0	0-0	**	0-0	0-0	
SA	**	0-0	0-0	0-0	**	0-**	**

* P<0.05 ** P<0.01

TABLE A-20
ANALYSES OF VARIANCE, R-WAVE RIGHT SIDE NERVES

RSS R-WAVE ANALYSIS OF VARIANCE

	A	LB	LA	P	PWA	PWB	SB
LB	0-*						
LA	**	0-0					
P	0-0	0-0	0-0				
PWA	**	0-0	0-0	*-0			
PWB	**	0-0	0-0	*-0	0-0		
SB	**	0-0	0-0	**	0-0	0-0	
SA	0-0	0-0	0-*	0-0	**	0-0	**

* P<0.05 ** P<0.01

CR.V. R-WAVE ANALYSIS OF VARIANCE

	A	LB	LA	P	PWA	PWB	SB
LB	*-0						
LA	0-0	0-0					
P	0-0	0-0	0-0				
PWA	**	0-0	0-0	**			
PWB	**	0-0	0-0	*-*	0-0		
SB	**	0-0	0-0	*-*	0-0	0-0	
SA	0-0	0-0	0-0	**	**	**	**

* P<0.05 ** P<0.01

R.T.V. R-WAVE ANALYSIS OF VARIANCE

	A	LB	LA	P	PWA	PWB	SB
LB	0-0						
LA	0-0	0-0					
P	0-0	0-0	0-0				
PWA	**	0-0	0-0	**			
PWB	0-*	0-0	0-0	0-*	0-0		
SB	**	0-0	0-0	**	0-0	0-0	
SA	0-0	0-0	0-0	0-0	**	**	**

* P<0.05 ** P<0.01

Re. C. R-WAVE ANALYSIS OF VARIANCE

	A	LB	LA	P	PWA	PWB	SB
LB	0-0						
LA	0-0	0-0					
P	0-0	0-0	0-0				
PWA	**	0-0	0-0	**			
PWB	*-0	0-0	0-0	*-0	0-0		
SB	*-0	0-0	0-0	0-0	0-0	0-0	
SA	0-0	*-0	0-0	0-0	**	*-0	*-0

* P<0.05 ** P<0.01

CA.V. R-WAVE ANALYSIS OF VARIANCE

	A	LB	LA	P	PWA	PWB	SB
LB	0-0						
LA	*-0	0-0					
P	0-0	0-0	0-0				
PWA	**	0-0	0-0	**			
PWB	0-*	0-0	0-0	0-*	0-0		
SB	**	0-0	0-0	*-*	0-0	0-0	
SA	0-0	0-0	*-0	0-0	**	0-*	**

* P<0.05 ** P<0.01

TABLES A-19 AND A-20

LEGEND

Tables A-19 and A-20 show the analyses of variance of the R-wave referenced time intervals for the left and right side nerves respectively. The time intervals are shown in Tables A-3 through A-10. Tables A-19 and A-20 only show if a degree of significance exists between any two muscle segments during either control or stimulation. The muscle segments are the anterior (A), lateral base (LB), lateral apex (LA) and posterior (P) portions of the epicardium and the free wall apex (FWA), free wall base (FWB), septal base (SB) and septal apex (SA) of the endocardium. In the table the symbol to the left of the hyphen indicates the degree of significance between the control time intervals for the two muscle segments. A zero indicates no significant difference. The symbol to the right of the hyphen indicates the degree of significance between the time intervals of the two muscle segments during stimulation of the particular nerve. See Table A-3 for list of nerve abbreviations.

TABLE A-21
 ANALYSES OF VARIANCE, ELECTROMECHANICAL
 COUPLING--LEFT SIDE NERVES

IRS ELECTROMECHANICAL COUPLING
 ANALYSIS OF VARIANCE

VLOS ELECTROMECHANICAL COUPLING
 ANALYSIS OF VARIANCE

VMOE ELECTROMECHANICAL COUPLING
 ANALYSIS OF VARIANCE

	A	LB	LA	P	PWB	PWA	SA
LB	0-0						
LA	*-0	0-0					
P	0-0	0-0	**0				
PWB	**0	**0	**0	*-0			
PWA	0-0	0-0	**0	0-0	0-0		
SA	0-0	0-0	**0	0-0	*-0	0-0	
SB	**0	**0	**0	**0	*-0	**0	**0

* P<0.05 ** P<0.01

	A	LB	LA	P	FWB	PWA	SA
LB	0-0						
LA	0-0	0-0					
P	0-0	0-0	0-0				
PWB	**0	**0	*-0	0-0			
PWA	*-0	*-0	0-0	0-0	0-0		
SA	0-0	0-0	0-0	0-0	*-0	0-0	
SB	**0	**0	*-0	*-0	0-0	0-0	**0

* P<0.05 ** P<0.01

	A	LB	LA	P	FWB	PWA	SA
LB	0-0						
LA	0-0	0-0					
P	0-0	0-0	0-0				
PWB	**0	*-0	0-0	0-0			
PWA	**0	0-0	0-0	0-0	0-0		
SA	0-0	0-0	0-0	0-0	0-0	0-0	
SB	**0	**0	*-0	0-0	0-0	0-0	**0

* P<0.05 ** P<0.01

INN ELECTROMECHANICAL COUPLING
 ANALYSIS OF VARIANCE

L REL ELECTROMECHANICAL COUPLING
 ANALYSIS OF VARIANCE

LTV ELECTROMECHANICAL COUPLING
 ANALYSIS OF VARIANCE

	A	LB	LA	P	PWB	PWA	SA
LB	0-0						
LA	0-0	0-0					
P	0-0	0-0	0-0				
PWB	*-0	0-0	0-0	0-0			
PWA	*-0	0-0	0-0	0-0	0-0		
SA	0-0	0-0	0-0	0-0	0-0	0-0	
SB	**0	*-0	**0	0-0	0-0	0-0	**0

* P<0.05 ** P<0.01

	A	LB	LA	P	FWB	PWA	SA
LB	0-0						
LA	0-0	0-0					
P	0-0	0-0	0-0				
PWB	**0	0-0	**0	0-0			
PWA	**0	*-0	**0	0-0	0-0		
SA	0-0	0-0	0-0	0-0	0-0	*-0	
SB	**0	**0	**0	0-0	0-0	0-0	**0

* P<0.05 ** P<0.01

	A	LB	LA	P	FWB	PWA	SA
LB	0-0						
LA	0-0	0-0					
P	0-0	0-0	0-0				
PWB	*-0	0-0	0-0	0-0			
PWA	*-0	*-0	0-0	0-0	0-0		
SA	0-0	0-0	0-0	0-0	*-0	*-0	
SB	**0	**0	*-0	0-0	0-0	0-0	**0

* P<0.05 ** P<0.01

TABLE A-22
ANALYSES OF VARIANCE, ELECTROMECHANICAL
COUPLING--RIGHT SIDE NERVES

RSS ELECTROMECHANICAL COUPLING ANALYSIS OF VARIANCE								REC ELECTROMECHANICAL COUPLING ANALYSIS OF VARIANCE								R.V. ELECTROMECHANICAL COUPLING ANALYSIS OF VARIANCE							
A	LB	LA	P	FWB	FWA	SA		A	LB	LA	P	FWB	FWA	SA		A	LB	LA	P	FWB	FWA	SA	
LB	0-0							LB	0-0							LB	0-0						
LA	0-0	0-0						LA	0-0	0-0						LA	0-0	0-0	0-0				
P	0-*	0-0	0-0					P	0-0	0-0	0-0					P	0-0	0-0	0-0	0-0			
FWB	**	0-0	0-0	0-0				FWB	**	**	**	0-0				FWB	**	**	**	0-0	0-0		
FWA	0-*	0-0	0-0	0-0	0-0			FWA	**	**	0-*	0-0	0-0			FWA	**	0-0	0-0	0-0	0-0	0-0	
SA	0-0	0-0	0-0	0-0	0-0	0-0		SA	0-0	0-0	0-0	0-0	**	0-0		SA	0-0	0-0	0-0	0-0	0-0	0-0	
SB	**	**	**	**	0-0	**	**	SB	**	**	**	**	0-*	0-0	**	SB	**	**	**	**	**	**	**
	* P<0.05	** P<0.01							* P<0.05	** P<0.01							* P<0.05	** P<0.01					

C.A.V. ELECTROMECHANICAL COUPLING ANALYSIS OF VARIANCE								R.T.V. ELECTROMECHANICAL COUPLING ANALYSIS OF VARIANCE							
A	LB	LA	P	FWB	FWA	SA		A	LB	LA	P	FWB	FWA	SA	
LB	0-0							LB	0-0						
LA	0-0	0-0						LA	0-0	0-0					
P	0-0	0-0	0-0					P	0-0	0-0	0-0				
FWB	**	0-*	0-*	0-0				FWB	**	**	**	0-0			
FWA	**	0-0	0-0	0-0	0-0			FWA	**	0-0	0-0	0-0	0-0		
SA	0-0	0-0	0-0	0-0	**	0-*		SA	0-0	0-0	0-0	0-0	**	0-0	
SB	**	**	**	0-*	0-0	0-0	**	SB	**	**	**	0-0	0-0	0-0	**
	* P<0.05	** P<0.01							* P<0.05	** P<0.01					

TABLES A-21 AND A-22

LEGEND

Tables A-21 and A-22 show the results of the analyses of variance of the electromechanical coupling intervals before and during stimulation of the left and right side thoracic cardiac nerves. The time intervals are shown in Tables A-11 through A-18. Tables A-21 and A-22 only show the degree of significance between the EM time intervals from any two muscle segments during either control or stimulation of the respective nerve. See Tables A-19 and A-20 for further explanations.

APPROVAL SHEET

The dissertation submitted by David B. Lippincott has been read and approved by the following committee:

Dr. Walter C. Randall, Director
Professor, Physiology, Loyola

Dr. Clarence N. Peiss
Professor, Physiology and
Associate Dean, Graduate School, Loyola

Dr. George P. Pollack
Assistant Professor, Physiology, Loyola

Dr. Rolf M. Gunnar
Professor, Medicine, and
Chief, Section Cardiology, Loyola

Dr. Donald V. Priola
Professor, Physiology/Pharmacology
University of New Mexico

The final copies have been examined by the director of the dissertation and the signature which appears below verifies the fact that any necessary changes have been incorporated and that the dissertation is now given final approval by the Committee with reference to content and form.

The dissertation is therefore accepted in partial fulfillment of the requirements for the degree of Doctor of Philosophy.

Date

July 29, 1976

Director's Signature

Walter C. Randall